Chemistry–A European Journal

Supporting Information

Structure and Biosynthesis of Myxofacyclines: Unique Myxobacterial Polyketides Featuring Varing and Rare Heterocycles[]

Alexander Popoff, Joachim J. Hug, Sebastian Walesch, Ronald Garcia, Lena Keller, and Rolf Müller*

Table of Contents

1. General materials and methods

1.1 Applied software, sequence analysis and bioinformatics methods

Geneious prime (Biomatters Ltd., Auckland, New Zealand) was used to design primers for PCR and sequencing, to create plasmid maps and to find open reading frames (ORF). Furthermore all pairwise and multiple alignments of nucleotide or amino acid sequences where performed with the plugin software from Geneious by using the MUSCLE (Multiple Sequence Comparison by Log-Expectation) alignment (3.8.425 by Robert C. Edgar) since it claims to achieve higher average accuracy and to be faster than ClustalW2 or the T-Coffee algorithm[1]. In order to find homologous genes or proteins, either the nucleotide or amino acid sequence of interest was aligned with the basic local alignment search tool (BLAST) against the in-house genome database or the publicly available nucleotide database. Raw data from alignments for *in silico* evaluation of the *iso* biosynthetic gene clusters (BGCs) are stored on the in-house server. The functional prediction of ORFs was performed by either using protein blast and/or blastx program (https://blast.ncbi.nlm.nih.gov/Blast.cgi) and Pfam (http://pfam.xfam.org)[2]. To obtain further information concerning the catalytic function of identified biosynthetic proteins, the amino acid sequences were evaluated by the *in silico* protein homology analogy recognition engine 2 (Phyre2)[3]. The in-house standard extract database embedded in the software bundle Mxbase Explorer 3.2.27 was used for the search of alternative producers of myxofacyclines. The molecular formula and experimentally determined retention times of ions typically observed from the myxofacyclines were used as data input. The BGC sequences of alternative confirmed producers of myxofacyclines deriving from our in-house database have been deposited in GenBank and are accessible under the accession number as displayed in **Table S1**. In addition, the sequence of the myxofacycline biosynthetic gene cluster (BGC) originating from *Myxococcus xanthus* Mx x48 will be deposited in the Minimum Information about a Biosynthetic Gene cluster (MIBiG) database.

Table S1. In-house genome sequence analysis of myxobacterial strains

Myxofacyclines producing strains	**Reference**	**Accession number BGC**
M. xanthus Mx x48 (MCy8278)	[4]	MT513750
Stigmatella aurantiaca Sg a32 DSM No. 53785	This study	MT513751
Stigmatella erecta MCy6787 (Pd e42)	This study	MT513752

1.2 Maintenance of bacterial cultures, molecular cloning and construction of plasmids[5–7]

Routine handling of nucleic acids, such as isolation of plasmid DNA, restriction endonuclease digestions, DNA ligations, and other DNA manipulations, was performed according standard procedures[5]. *Escherichia coli* HS996 (Invitrogen) was used as host for standard cloning experiments and *E. coli* SCS110 (Stratagene) for preparation of plasmid DNA free of Dam or Dcm methylation. *E. coli* strains were cultured in LB liquid medium or on LB agar (1% tryptone, 0.5% yeast extract, 0.5% NaCl, (1.5% agar) at 30–37 °C and 200 rpm) overnight. Antibiotics were used at the following final concentrations: 100 µg/mL ampicillin, 50 µg/mL kanamycin and 25 µg/mL chloramphenicol. Transformation of *E. coli* strains was achieved via electroporation in 0.1 cm wide cuvettes at 1250 V, a resistance of 200 Ω, and a capacity of 25 µF. Plasmids (**Table S4)** were purified either by standard alkaline lysis[5] or by using the GeneJet Plasmid Miniprep Kit (Thermo Fisher Scientific) or the NucleoBond PC100 kit (Macherey-Nagel). Restriction endonucleases, alkaline phosphatase (FastAP) and T4 DNA ligase were purchased from Thermo Fisher Scientific. Oligonucleotides used for PCR and sequencing were acquired from Sigma-Aldrich and are listed in **Table S2** and **Table S3** PCRs were carried out in a Mastercycler® pro (Eppendorf) using Phusion™ High-Fidelity according to the manufacturer's protocol. Temperature and duration setting for each thermocycling step for PCRs using Phusion™ High-Fidelity polymerase were performed as follows: Initial denaturation (30 s, 98 °C); 33 cycles of denaturation (15 s, 98 °C), annealing (15 s, 53–72 °C, depending on the melting temperature of primers) and elongation (based on PCR product length 30 s/1 kb, 72 °C); and final extension (10 min, 72 °C). PCR products or DNA fragments from restriction digestions were purified by agarose gel electrophoresis and isolated using the PCR clean-up gel extraction kit using Nucleo Spin® (Macherey-Nagel). After selection with suitable antibiotics, clones harboring correct ligation constructs were identified by plasmid isolation and restriction analysis with a set of different restriction endonucleases. In addition to restriction analysis, integrity of the constructs for genetic disruption experiments and induced gene expression was verified by sequencing.

Table S2. List of oligonucleotides used in this study.

No.	Primer name	Primer sequence 5'–3'
1	JHuFw_Mxx48_iso1_KO	ATATAAGCTTACTCCACGCCCTGCTGATTG
2	JHuRv_ Mxx48_iso1_KO	ATATACTAGTTCACGGATGACCTTCGCGGT
3	JHuFw_Mxx48_iso2_KO	ATATAAGCTTGCAGCATCGTCCACAACAAC
4	JHuRv_ Mxx48_iso2_KO	ATATACTAGTTCGATGACGAACGAGTTCAGC

5	JHuFw_Mxx48_iso3_KO	ATATAAGCTTGCAGCTCTCGCTCTACCTGTTT
6	JHuRv_ Mxx48_iso3_KO	ATATACTAGTAGTTGTAGAAGCGCCCCGTG
7	JHuFw_Mxx48_iso4_KO	ATATAAGCTTAGATTTCCCGCCGCATCGTG
8	JHuRv_ Mxx48_iso4_KO	ATATACTAGTTGGGCCGTAGTAGGGGATGA
9	JHuFw_Mxx48_iso5_KO	ATATAAGCTTAGATTGACATGGCCATCGTC
10	JHuRv_ Mxx48_iso5_KO	ATATACTAGTTACTCTAACGCGAACAGGGA
11	JHuFw_Mxx48_iso6_KO	ATATAAGCTTCAACACGTACCTCGACTTCA
12	JHuRv_ Mxx48_iso6_KO	ATATACTAGTAATACCAGAGGGCTTCCTGG
13	JHuFw_Mxx48_iso8_KO	ATATAAGCTTCCTGGTCGCGGAGGGACTTC
14	JHuRv_ Mxx48_iso8_KO	ATATACTAGTGCCAGGATGCGCACCGAGAC
15	JHuFw_Mxx48_iso9_KO	ATATAAGCTTTCATCTCGAACGTGACAGGC
16	JHuRv_ Mxx48_iso9_KO	ATATACTAGTAGAGCTTGTCCTTCCAGGTG
17	JHuFw_Mxx48_activate_iso2	ATATCATATGAGTCTCGAAGGGGTCATGACGG
18	JHuRv_Mxx48_activate_iso2	ATATGAATTCATGCCCACCAGCGTCTGCAC
19	JHu_Fw_kanR_P_{Van}_iso1	GTTACCCATTGTGTAACTATAACGGTCCTAAGGTAGCGAAAGATCTGTTTCATATGTCAGAAGAACTCGTCAAGAAGG
20	JHu_Rv_kanR_P_{Van}_iso1	GGTGCTTCATTGAACTGGGCAATCAAGAATGCATGGAGTGGGTTCGACATATGCGTTTCCTCGCATCG
21	JHu_Fw_kanR_P_{Van}_iso2	GTTACCCATTGTGTAACTATAACGGTCCTAAGGTAGCGAAAGATCTGTTTCATATGTCAGAAGAACTCGTCAAGAAGG
22	JHu_Rv_kanR_P_{Van}_iso2	ACTCCATGTGGGGCGGCGCTGCCGCCGCACCCGTAGGGGCGCGGCGGCATATGCGTTTCCTCGCATCG
23	JHuFw_pBR322_ampR	CGTCCAGTTCCAGCCACAGGCTGCATCAGTTGATGGTGCAGGTCAGGGTGTATACCTAGGGAGACGTCGG
24	JHuRv_iso_pBR322_ampR	TCCAATTCTTGGAGTGGTGAATCCGTTAGCGAGGTGCCGCCGGCTTCCATAGTGGGTCTTAAGCATGCTT

Table S3. List of oligonucleotides used as sequencing primers.

No.	Primer name	Primer sequence 5'–3'
1	Test_Fw1_Mxx48_iso1_KO	CGCGACAATAAACATACGCAA
2	Test_Rv2_Mxx48_iso1_KO	TCCACCTTCTCGATGCAGAT
3	Test_Rv3_Mxx48_iso1_KO	CTATCGCCATGTAAGCCCACT
4	Test_Fw4_Mxx48_iso1_KO	CCGATTCATTAATGCAGCTGG
5	Test_Fw1_ Mxx48_iso2_KO	CCTTCCTCCAGTACACGTCCGGTTC
6	Test_Rv2_ Mxx48_iso2_KO	GAGCAGCTCCATCACCCGCAG
7	Test_Rv3_ Mxx48_iso2_KO	GCGATGGCCCACTACGTGAACC
8	Test_Fw4_ Mxx48_iso2_KO	GTGATGCTCGTCAGGGGGGC
9	Test_Fw1_ Mxx48_iso3_KO	CTTCTGGGAAGGTTGAACAAG
10	Test_Rv2_ Mxx48_iso3_KO	GTGGATGCTGTGATAGCCAT
11	Test_Rv3_ Mxx48_iso3_KO	GTCTAGCTATCGCCATGTAAG
12	Test_Fw4_ Mxx48_iso3_KO	CCGATTCATTAATGCAGCTGG
13	Test_Fw1_Mxx48_iso4_KO	CTGAAGCGACGAAGCATGAC
14	Test_Rv2_Mxx48_iso4_KO	AGTTGCCGATGCCGAAGTAG
15	Test_Rv3_Mxx48_iso4_KO	CTATCGCCATGTAAGCCCACT
16	Test_Fw4_Mxx48_iso4_KO	CCGATTCATTAATGCAGCTGGC
17	Test_Fw1_Mxx48_iso5_KO	ACTCACCGCGCTGCACTTCG
18	Test_Rv2_Mxx48_iso5_KO	GGAGTGAAAGGCATGGCGTGTCC
19	Test_Rv3_Mxx48_iso5_KO	GCGATGGCCCACTACGTGAACC
20	Test_Fw4_Mxx48_iso5_KO	GTGATGCTCGTCAGGGGGGC
21	Test_Fw1_Mxx48_iso6_KO	GTGTTTCCCATCGTCGCGGAGC
22	Test_Rv2_Mxx48_iso6_KO	CGTTGTAGAGGGCCGCGATGC
23	Test_Rv3_Mxx48_iso6_KO	GCGATGGCCCACTACGTGAACC
24	Test_Fw4_Mxx48_iso6_KO	GTGATGCTCGTCAGGGGGGC
25	Test_Fw1_Mxx48_iso8_KO	CTGACGAAGTACGACCTCTG
26	Test_Rv2_Mxx48_iso8_KO	ACCGTCCTGATCATCTTGAAG
27	Test_Rv3_Mxx48_iso8_KO	AGTCTAGCTATCGCCATGTAAG
28	Test_Fw4_Mxx48_iso8_KO	CCGATTCATTAATGCAGCTGG
29	Test_Fw1_Mxx48_iso9_KO	CACTCGGAGCTGATGCGGCC
30	Test_Rv2_Mxx48_iso9_KO	GCTGGCGTGTCGGGCATCTC
31	Test_Rv3_Mxx48_iso9_KO	GCGATGGCCCACTACGTGAACC
32	Test_Fw4_Mxx48_iso9_KO	GTGATGCTCGTCAGGGGGGC
33	Test_Fw1_ Mxx48_iso2_KO_activate	CTTCCAGACCTTTCCTCGTC
34	Test_Rv2_ Mxx48_iso2_KO_activate	TGCTCGTCTTGGGAATCATC

35	Test_Rv3_ Mxx48_iso2_KO_activate	CTGATTCTGTGGATAACCGTATTAC
36	Test_Fw4_ Mxx48_iso2_KO_activate	GACTCTAGCCGACCGACTGA
37	Test_Fw_pCos	GATCTCCATCGACTAAACGT
38	Test_Rv_pCos	GTTAACTGCGGTCAAGATAT
39	Mx8-attB-up2	GCGCACTGGACCATCACGTC
40	Mx8-attP-down	GGCTTGTGCCAGTCAACTGCG
41	Mx8-attP-up2	CGACGGTGCCGACAAATAC
42	Mx8-attB-down	CGGATAGCTCAGCGGTAGAG

Table S4. **List of plasmids used in this study**

No.	Plasmid name/ characteristic	Size [kb]	Function	Reference
1	pCR2.1-TOPO (EcoRI, religated)	3.931	Used as template to PCR-amplify *tn5_kanR* gene	TOPO®TA Cloning® Kit Thermo Fisher Scientific
2	pFP_{Van}_*pcyA*	6.181	pCR2.1-TOPO derivative used as vector to ligate PCR products for subsequent vanillate-induced gene expression in *M. xanthus* DK1622; also used as template for the generation of PCR-amplified construct No.10	[8]
3	pCos15AtetMx8-For-31/37	7.663	Vector backbone for the generation of cosmid library of *S. aurantiaca* Sg a32	Explogen LLC (EXG)
4	pCos15AtetMx8-For-31/37_E06_9184	40.186	Vector backbone harboring the myxofacycline BGC with additional five	Explogen LLC (EXG)

			genes upstream and two genes downstream	
5	pBR322-amp-tetR-tetO-hyg-ccdB	4.454	Used as template to PCR-amplify the pBR322 origin of replication and *ampR*	[9]
6	pMycoMar	----	Used as control to investigate pleiotropic effects regarding the production of myxofacyclines after mutagenesis in *M. xanthus* Mx x48	[10,11]

Table S5. List of PCR-amplified constructs

No.	**PCR product name / characteristic**	**Size [bp]**	**Template**	**Primer used**
1	Mxx48_*iso1*_ homology	317	gDNA from *M. xanthus* Mx x48	primer No. 1 primer No. 2
2	Mxx48_*iso2*_ homology	1269	gDNA from *M. xanthus* Mx x48	primer No. 3 primer No. 4
3	Mxx48_*iso3*_ homology	598	gDNA from *M. xanthus* Mx x48	primer No. 5 primer No. 6
4	Mxx48_*iso4*_ homology	583	gDNA from *M. xanthus* Mx x48	primer No. 7 primer No. 8
5	Mxx48_*iso5*_ homology	1230	gDNA from *M. xanthus* Mx x48	primer No. 9 primer No. 10
6	Mxx48_*iso6*_ homology	1357	gDNA from *M. xanthus* Mx x48	primer No. 11 primer No. 12
7	Mxx48_*iso8*_ homology	938	gDNA from *M. xanthus* Mx x48	primer No. 13 primer No. 14
8	Mxx48_*iso9*_ homology	1373	gDNA from *M. xanthus* Mx x48	primer No. 15 primer No. 16

9	Mxx48_*iso2*_activate	1117	gDNA from *M. xanthus* Mx x48	primer No. 17 primer No. 18
10	P_{van}-*iso1_kanR*	2986	pFP_{Van}_*pcyA*	primer No. 19 primer No. 20
11	P_{van}-*iso2_kanR*	2986	pFP_{Van}_*pcyA*	primer No. 21 primer No. 22
12	pBR322-amp-tetR-tetO-hyg-ccdB extraction	2064	pBR322-amp-tetR-tetO-hyg-ccdB	primer No. 23 primer No. 24

Table S6. List of genetic constructs generated in this study

No.	Plasmid name	Construction details/ characteristic
1	pCR2.1-TOPO_ Mxx48_*iso1*_KO	Construct obtained by conventional restriction ligation of plasmid pCR2.1-TOPO and PCR product No. 1
2	pCR2.1-TOPO_ Mxx48_*iso2*_KO	Construct obtained by conventional restriction ligation of plasmid pCR2.1-TOPO and PCR product No. 2
3	pCR2.1-TOPO_ Mxx48_*iso3*_KO	Construct obtained by conventional restriction ligation of plasmid pCR2.1-TOPO and PCR product No. 3
4	pCR2.1-TOPO_ Mxx48_*iso4*_KO	Construct obtained by conventional restriction ligation of plasmid pCR2.1-TOPO and PCR product No. 4
5	pCR2.1-TOPO_ Mxx48_*iso5*_KO	Construct obtained by conventional restriction ligation of plasmid pCR2.1-TOPO and PCR product No. 5
6	pCR2.1-TOPO_ Mxx48_*iso6*_KO	Construct obtained by conventional restriction ligation of plasmid pCR2.1-TOPO and PCR product No. 6
7	pCR2.1-TOPO_ Mxx48_*iso8*_KO	Construct obtained by conventional restriction ligation of plasmid pCR2.1-TOPO and PCR product No. 7
8	pCR2.1-TOPO_ Mxx48_*iso9*_KO	Construct obtained by conventional restriction ligation of plasmid pCR2.1-TOPO and PCR product No. 8

9	pFP$_{Van}$_*iso2*_precursor_activate	Construct obtained by conventional restriction ligation of plasmid pFP$_{Van}$_*pcyA* and PCR product No. 9
10	pCos15AtetMx8-For-31/37_E06_9184_P$_{van}$-*iso1_kanR*	Construct obtained by Red αβ recombineering of PCR product No.10 with plasmid pCos15AtetMx8-For-31/37_E06_9184
11	pCos15AtetMx8-For-31/37_E06_9184_P$_{van}$-*iso2_kanR*	Construct obtained by Red αβ recombineering of PCR product No.11 with plasmid pCos15AtetMx8-For-31/37_E06_9184
12	pCos_pBR322_ampR_Mx8-For-31/37_E06_9184_P$_{van}$-*iso1_kanR*	Construct obtained by Red αβ recombineering of PCR product No.13 with construct pCos15AtetMx8-For-31/37_E06_9184_P$_{van}$-*iso1_kanR*
13	pCos_pBR322_ampR_Mx8-For-31/37_E06_9184_P$_{van}$-*iso2_kanR*	Construct obtained by Red αβ recombineering of PCR product No.13 with construct pCos15AtetMx8-For-31/37_E06_9184_P$_{van}$-*iso2_kanR*

Bacterial cultures and preparation of cryogenic long-term stocks

In our ongoing screening for novel secondary metabolites from myxobacteria, we isolated *Corallococcus* sp. strain MCy9072 from a Chinese soil sample taken in 1980 from the HZI soil collection (formerly called German Center for Biotechnology (GBF)). The myxobacterial strain *Corallococcus* sp. MCy9072 was recognized for its swarming and fruiting body formation in the standard *Escherichia coli* bacterial baiting method[12]. Repeated transfer of the swarm edge onto fresh VY/2 agar led to the isolation of the strain (**Figure S1**). Cultivation and maintenance was kept at VY/2 agar for 3–4 weeks at 30 °C.

Long-term storage of *Corallococcus* sp. MCy9072, *Myxococcus xanthus* Mx x48 (wild type and mutants), *Stigmatella aurantiaca* Sg a32 and *Stigmatella erecta* MCy6787 (Pd e42) was achieved by cryogenic preservation at -80 °C as tenfold concentrated glycerol stocks. Ten mL of well-grown liquid culture was transferred to a 50-mL Falcon tube and centrifuged for 5 min at 8000 rpm (Eppendorf Centrifuge 5804R). Nine mL of the supernatant was discarded, leaving 1.0 mL supernatant in the Falcon tube. The cell pellet was re-suspended by pipetting up and down and then mixed with 1.0 mL glycerol (50%). The myxobacterial glycerol sample (25% glycerol) was transferred into a cryogenic vial and maintained at -80 °C.

Figure S1. Orange scattered fruiting bodies of *Corallococcus* sp. MCy9072 on VY/2 agar with typical ridge and hump-shaped morphologies.

Bacterial strains for the experiments of this work, their relevant characteristics and sources are listed in the **Table S7**.

Table S7. Bacterial strains used in this study.

Strain	**Function**	**Origin**
E. coli HS996	Standard cloning host	Invitrogen
E. coli GB05-*red*	Host for Red α,β-based recombineering of circular plasmids	[13]
Corallococcus sp. MCy9072	Producer of myxofacyclines: Identification and isolation of myxofacycline A	This study
Myxococcus xanthus Mx x48	Producer of myxofacyclines: Identification and isolation of myxofacyclines B–G, genetic characterization	MINS lab
Stigmatella aurantiaca Sg a32	Producer of myxofacyclines: Alternative producer with available genome and metabolome data ; used BGC for heterologous expression in *M. xanthus* DK1622	MINS lab

Stigmatella erecta MCy6787 (Pd e42)	Producer of myxofacyclines: Alternative producer with available genome and metabolome data	MINS lab
Myxococcus xanthus DK1622	Host for the heterologous expression of the myxofacycline BGC from Sg a32; establishment of heterologous production platform for the myxofacyclines.	MINS lab

Cultivation media

The pH of all cultivation media was adjusted before autoclaving. Autoclaving was conducted at 121°C for 20 min.

CTT-medium

Ingredient	Concentration
Casitone	10 g/L
TRIS	10 mM
KH_2PO_4	1 mM
$MgSO_4$ x $6H_2O$	8 mM

pH 7.6 with KOH_{aq}

VY/2-medium

Ingredient	Concentration
Baker's yeast	5 g/L
$CaCl_2$ x $2H_2O$	1 g/L

pH 7.2 with $KOH_{aq,}$ after autoclaving medium was supplemented with 0.5 mg/L vitamin B_{12}.

LB-medium

Ingredient	Concentration
Yeast extract	5 g/L
Tryptone	10 g/L
NaCl	5 g/L

pH 7.2 with KOH_{aq}

M7/s4-medium

Ingredient	Concentration
Soy flour	5 g/L
Corn starch	5 g/L
Glucose	2 g/L
Yeast extract	1 g/L
$MgSO_4$ x $6H_2O$	1 g/L
$CaCl_2$ x $2H_2O$	1 g/L
HEPES	10 g/L

pH 7.4 with $NaOH_{aq}$, after autoclaving medium was supplemented with 0.1 mg/L vitamin B_{12}.

CyH-medium

Ingredient	Concentration
Casiton (Difco)	1.5 g/L
Yeast extract (Difco)	1.5 g/L
Soluble starch (Roth)	4.0 g/L
Soy flour, defatted (Hensel)	1.0 g/L
D-glucose	1 g/L
$MgSO_4$ x $6H_2O$	0.5 g/L
$CaCl_2$ x $2H_2O$	1 g/L
HEPES	11.9 g/L

pH 7.4 with KOH_{aq}, after autoclaving medium was supplemented with 0.05 mg/L vitamin B_{12} and 0.8 mg/L Fe-EDTA.

Crude extract preparation for analysis of secondary metabolism

The initial screening for *Coralloccccus* sp. MCy9072 secondary metabolites was performed in CyH medium supplemented with 2% (v/v) amberlite resin XAD-16 and cultivated for 10 d at 30 °C, 180 rpm.

M. xanthus Mx x48, *M. xanthus* DK1622 and mutant strains thereof were grown on CTT agar plates for 3–5 days at 30 °C. For the preparation of liquid pre-cultures, a suitable portion of overgrown agar was transferred to inoculate 20 mL of CTT medium in an Erlenmeyer flask (100 mL) and incubated at 30 °C and 180 rpm for 2–4 days. 3 mL of the pre-culture was used to inoculate 50 mL of M7/s4 or CTT medium containing appropriate antibiotic selection and 2% amberlite resin XAD-16 (Sigma Aldrich) (after one day of incubation at 30 °C and 200 rpm).

For mutant strains of *M. xanthus* Mx x48 or *M. xanthus* DK1622 harboring the vanillate-inducible promoter in front of *iso1* or *iso2* (Mx x48: native iso-BGC, DK1622: iso-BGC from Sg a32 mobilized on a plasmid and integrated into the Mx8 phage attachment site of DK1622), mutant samples were chemically induced with 2 mM vanillate 1–2 days after inoculation (depending on bacterial growth). One day after chemical induction XAD-16 was added to the respective culture; negative samples were treated similarly, except for omitting vanillate supplementation. In order to obtain statistically significant results, three independent transformants of each recombinant strain were selected and fermentations were performed at least in triplicates.

After eight days of fermentation at 30 °C and 200 rpm, the culture broths were harvested and lyophilized. Afterwards the residual material was extracted by stirring with 25 mL MeOH and 25 mL acetone for 2 h, filtered through filter paper (folded filters grade: 3hw from Sartorius) into a round bottom flask. The solvent of the filtered extracts was removed under vacuum (BÜCHI Rotavapor R–210) and the extracts re-dissolved in 1.5 mL MeOH and stored at -20 °C. The re-dissolved extracts were diluted with MeOH (1:3 (extract/MeOH (v:v)) centrifuged at 13000 g for 10 min (VWR centrifuge ECN521-3601, Hitachi Koki Co., Ltd) and 1 µL of the supernatant was subjected to HPLC-MS analysis as described further below.

Feeding experiments with stable isotope-labeled precursors

0.5 mL of myxobacterial pre-culture was used to inoculate 10 mL of CTT or M7/s4 medium and for three consecutive days, two times a day, 10 µL (in total 60 µL) of a 0.1 M solution of either L-glutamine $^{15}N_2{}^{13}C_6$, L-asparagine $^{15}N_2$ $^{13}C_5$, L-glutamic acid ^{15}N, L-valine d8, glycine ^{15}N $^{13}C_1$, acetate $^{13}C_2$ in H_2O_{dd} + MeOH [1:1 vol.] was added. Additionally, one sample without feeding was prepared used as control. 12 h after the last supplementation with the respective stable isotope-labeled precursor, the culture broths were complemented with 2% amberlite resin XAD-16 (Sigma). After 10 days of incubation at 30 °C and 200 rpm, the culture broths were harvested by centrifugation at 8000 rpm for 10 min, the supernatant was discarded, and the residual material was extracted first with 25 mL MeOH, stirred for 1 h, filtered through filter paper into a round bottom flask and afterwards this procedure was repeated with 25 mL acetone. Filtered extracts were evaporated and subsequently re-dissolved in 2 mL MeOH. For metabolic analysis the re-dissolved sample was centrifuged and analyzed by a Dionex HPLC coupled to the TOF mass spectrometer maXis 4G as described further below.

Analysis of secondary metabolites in broth extracts

The secondary metabolism of broth extracts was analyzed by HPLC-HRESI-DAD-MS on a Bruker maXis 4G mass spectrometer coupled with a Dionex Ultimate 3000 RSLC system using a BEH C18 column (100 × 2.1 mm, 1.7 µm, Waters, Germany) with a gradient of 5–95% acetonitrile (ACN) + 0.1% formic acid (FA) in H_2O + 0.1% FA at 0.6 mL/min and 45 °C over 9 or 18 min with UV detection by a diode array detector at 200–600 nm. Mass spectra were acquired from 150 to 2000 m/z at 2 Hz. The detection was performed in the positive MS mode. The plugin for Chromeleon Xpress (Dionex) was used for operation of UltiMate 3000 LC System. HyStar (Bruker Daltonic) was used to operate on maXis 4G speed MS system. HPLC-MS mass spectra were analyzed with DataAnalysis 4.2 (Bruker Daltonic).

Large-scale fermentation *of Myxococcus xanthus* Mx x48

M. xanthus Mx x48 was grown on CTT agar plates for 3–5 days at 30 °C. For the preparation of liquid pre-cultures, a suitable portion of overgrown agar was transferred to inoculate 50 mL of CTT medium in an Erlenmeyer flask (300 mL) and incubated at 30 °C and 200 rpm for 2–4 days. 8 x 5 mL of the pre-culture was used to inoculate 8 x 250 mL of M7/s4 medium (1 L shake flask with baffles) and incubated at 30 °C and 200 rpm for 2–4 days. Afterwards 12 x 150 mL of pre-culture was used to inoculate 12 x 1.25 L M7/s4 medium (5 L shake flask with baffles) and incubated at 30 °C and 160 rpm for nine days. After two days of incubation, each shake flask was supplemented with 2% amberlite resin XAD-16 (Sigma Aldrich). The fermentation was terminated through centrifugation of the whole cell broth; the supernatant was discarded, whereas the cell pellet and amberlite resin XAD-16 was lyophilized. The lyophilized cell pellet with XAD-16 was used to prepare a crude extract (see below).

1.3 Compound isolation

Analysis during purification of the myxofacyclines

All measurements to analyze the mass of myxofacyclines during purification were performed on a Dionex Ultimate 3000 RSLC system coupled to the amaZon iontrap MS using a BEH C18, 100 x 2.1mm, 1.7 µm dp column equipped with a C_{18} precolumn (Waters). Samples of 1 µL were separated by a gradient from (**A**) H_2O + 0.1% formic acid (FA) to (**B**) ACN + 0.1% FA at a flow rate of 0.6 mL/min and 45 °C. The gradient was initiated by a 0.5 min isocratic step at 5% **B**, followed by linear increase to 95% **B** in 18 min. After a 2 min step at 95% **B** the system was re-equilibrated to the initial conditions (5% **B**). UV-spectra were recorded by a DAD in the range from 200–600 nm. The detection was performed in the positive ESI MS/MS positive mode

Myxofacycline A

Semi-preparative HPLC chromatography – Initial Isolation of Myxofacycline A

A 2.5 L culture of MCy9072 (25 x 100 ml in 300 mL flasks) in CyH medium was harvested by pouring the culture through a 100 µm sieve to separate the medium from cells and the absorber resin XAD-16. The cells and the XAD-16 were lyophilized for two days and extracted three times with 150 mL acetone/MeOH 1:1. The solvents were poured through a funnel with glass wool and the solvent was evaporated. The dried extract was re-dissolved in 100 mL hexane and 100 ml MeOH and transferred into a separatory funnel. The layers were separated, and the liquid/liquid extraction was repeated with 100 mL hexane. The MeOH layer was dried and re-dissolved in 300 mL H2O and 150 mL CHCl3. The layers were separated in a separatory funnel and the aqueous layer was re-extracted with 150 mL $CHCl_3$. After extraction with $CHCl_3$ the liquid/liquid extraction was repeated twice with 150 mL ethyl acetate. During extraction with ethyl acetate the aqueous layer was acidified with 1 N HCl. The layers were dried, dissolved in MeOH and united. For further purification a size exclusion chromatography was performed using Sephadex LH-20 resin and MeOH as eluent. A flow rate of 1 drop/sec was applied and 500 drops were collected for each fraction. An aliquot of each fraction was taken and measured by LC-MS to screen for the myxofacycline A. The fractions containing myxofacycline A were pooled and the solvent was evaporated. For further purification HPLC was used.

Following setup was used for HPLC: Dionex Ultimate 3000 coupled with Bruker High capacity trap mass spectrometer (HCT); Column: Luna 250 x 10 mm, 5 µm , flowrate 6 mL/min and column temperature 40 °C with H_2O + 0.1% FA as eluent **A** and ACN + 0.1% FA as eluent **B**.

The following gradient was applied 0–35 min linear increase of eluent B to 95%; 30–34 min 95% eluent **B**; 34–34.5 min linear decrease of eluent **B** to 5%; 34.5–46 min re-equilibration with 5% eluent B. Myxofacycline A was collected from 23.75–24 min. The collected fraction was dried and dissolved in 4 mL MeOH.

Myxofacycline A–C

Semi-preparative HPLC chromatography – Isolation of Myxofacycline A–C

A 5 L culture of vanillate-induced *M. xanthus* Mx x48 harboring a vanillate-inducible promoter in front of *iso2* (100 x 50 mL in 300 mL flasks) was cultivated in M7/s4 medium for 10 days in the presence of XAD-16 adsorber resin. The culture and resin were separated from the supernatant by centrifugation and freeze-dried. The resin and cells were extracted three times with 600 ml 1:1 acetone/MeOH. The solvent was poured through a filter and dried *in vacuo*. The dried extract was re-dissolved in 500 ml MeOH with 10% H_2O and defatted with twice 400 mL n-hexane. The MeOH extract was dried and re-dissolved in 400 mL H_2O followed by liquid/liquid extraction with 2 x 400 mL DCM and 2 x 400 mL ethyl acetate in a sequential manner. Myxofacycline A–C were present in the DCM layer. The DCM layer was dried and fractionated by normal phase flash chromatography. The following setups were used:

Biotage Isolera One with a 25 g Snapfit column, Silica 60 Å, 70–230 mesh, 63–200 µm, Solvent System: **A**= Hexane + 0.1% FA; **B**= EE + 0.1% FA; **C**= MeOH 0.1% FA; A flow rate of 25 mL/min was used and 45 mL were collected per fraction. The column was equilibrated with with 3 column volumes (CV) 90% **A**: 10% **B**. The sample was loaded on the column using iSolute beads. Following gradient was used: 3 CV 90% **A**: 10% **B**; 17 CV linear increase from 10–100% **B**; 5 CV 100% **B**; 12 CV linear increase from 0–50% **C**; 5 CV 50% **B**, 50% **C**. The collected fractions were screened for thy myxofacyclines by LC-MS. Myxofacyclines A–C were found in fraction 7. This fraction was dried and the myxofacyclines were further purified by semi-preparative HPLC.

The following setup was used for HPLC: Dionex Ultimate 3000; Column: Waters Xbridge Peptide BEH 250 x 10 mm, 5 µm, 130 A, flowrate 5 ml/min and column temperature 45 °C with H_2O + 0.1 % FA as eluent A and ACN + 0.1% FA as eluent B. The following gradient was applied: 0-2 min 5 % eluent B; 2-4 min linear increase of eluent B to 55 %; 4-19 min linear increase of eluent B to 59 %; 19-20 min linear increase of eluent B to 95 %; 20-22 min 95 % eluent B; 22-23 min linear decrease of eluent B to 5 %; 23-26 min re-equilibration with 5 % eluent B. The collected myxofacyclines were dried *in vacuo*.

Myxofacycline D–G

Semi-preparative HPLC chromatography – Isolation of Myxofacycline D–G

A 2.5 L culture of vanillate-induced *M. xanthus* Mx x48 harboring a vanillate-inducible promoter in front of *iso2* (50 x 50 mL in 300 mL flasks) was cultivated in M7/s4 medium for 10 days in the presence of XAD-16 adsorber resin to yield myxofacyclines D–G. The culture and resin were separated from the supernatant by centrifugation and freeze-dried. The resin and cells were extracted three times with 700 mL 1:1 acetone/MeOH. The solvent was poured through a filter and dried *in vacuo*. The dried extract was re-dissolved in 500 mL MeOH with 10% H_2O and defatted with twice with 500 mL n-hexane. The MeOH extract was dried and re-dissolved in 500 ml H_2O and followed by liquid/liquid extraction with 2 x 500 mL DCM and 2 x 500 mL ethyl acetate in a sequential manner. Before the liquid/liquid partitioning with EE, the aqueous layer was adjusted to pH 4 using 10% HCl. The DCM and EE layers were dried and an aliquot of each layer was screened for the presence of myxofacyclines by LC-MS. Myxofacycline D was found in the DCM layer, while myxofacyclines E–G were present in the EE layer.

For the isolation of myxofacyclines E–G the EE layer was further fractionated by normal phase flash chromatography. The following setups were used:

Biotage Isolera One with a 25 g Snapfit column, Silica Silica 60 Å, 70–230 mesh, 63–200 µm Solvent System: **A**= Hexane + 0.1% FA; **B**= EE + 0.1% FA; **C**= MeOH. A flow rate of 25 mL/min was used and 45 mL were collected per fraction. The column was equilibrated with 3 CV 50% **A**: 50% **B**. The sample was loaded on the column using iSolute beads. Eighteen CV linear increase from 50–100% **B**; 5 CV 100% **B**; 18 CV linear increase from 0–50% **C**; 5 CV 50% **C**. The collected fractions were screened for thy myxofacyclines by LC-MS. Myxofacycline G was mostly present in fractions 20 and 21, while the myxofacyclines E and F were found in fractions 16–19. Myxofacycline G was purified by semi-preparative HPLC.

Following setup was used for HPLC: Dionex Ultimate 3000; Column: Waters Xbridge BEH 250 x 10 mm, 5 µm, 130 Å flowrate 5 mL/min and column temperature 40 °C with H_2O + 0.1 % FA as eluent **A** and ACN + 0.1% FA as eluent **B**. The following gradient was applied: 0–2 min 5% **B**; 2–4 min linear increase of **B** to 35%; 4–19 min linear increase of **B** to 38%; 19–20 min linear increase of **B** to 95%; 20–22 min 95% **B**; 22–23 min linear decrease of **B** to 5%; 23–26 min re-equilibration with 5% **B**. Collected Myxofacycline G was dried *in vacuo*. Myxofacyclines E and F were isolated with the same setup and method.

For isolation of Myxofacycline D the DCM layer was fractionated by flash chromatography. The following setup was used: Biotage Isolera One with a 25 g Snapfit column, Silica Silica 60 Å, 70–230 mesh, 63–200 µm Solvent System: **A**= Hexane + 0.1% FA; **B**= EE + 0.1% FA; **C**=

MeOH 0.1% FA; A flow rate of 25 mL/min was used and 45 mL were collected per fraction. The column was equilibrated with 3 CV 90% **A**: 10% **B**. The sample was loaded on the column using iSolute beads. Following gradient was used: 3 CV 90% **A**: 10% **B**; 17 CV linear increase from 10-100 **B**; 5 CV 100% **B**; 12 CV linear increase from 0–50% **C**; 5 CV 50% **C**. The collected fractions were screened for myxofacycline D by LC-MS. Myxofacycline D was found in the fractions 10 and 11. These fractions were dried and myxofacycline D was further purified by semi–preparative HPLC. Following setup was used:

Following setup was used for HPLC: Dionex Ultimate 3000; Column: Waters Xbridge Peptide BEH 250 x 10 mm, 5 µm, 130 Å, flowrate 5 mL/min and column temperature 45 °C with H_2O + 0.1% FA as eluent **A** and ACN + 0.1% FA as eluent **B**. The following gradient was applied: 0–2 min 5% eluent B; 2–4 min linear increase of **B** to 55%; 4–19 min linear increase of **B** to 59%; 19–20 min linear increase of **B** to 95%; 20–22 min 95% **B**; 22–23 min linear decrease of **B** to 5%; 23–26 min re-equilibration with 5% **B**. The collected myxofacycline D was dried *in vacuo*.

1.3 NMR-based structure elucidation and IR spectroscopy

The chemical structure of the myxofacyclines were determined via multidimensional NMR analysis. The 1D and 2D NMR data used for the structure elucidation of the myxofacyclines were acquired in DMSO-d_6 and MeOH-d_4 on a Bruker Ascend 700 spectrometer equipped with a TCI 5mm probe head (^{1}H at 700 MHz, ^{13}C at 175 MHz) and Bruker Ultra Shield 500 spectrometer equipped with a TCI 5mm probe head (^{1}H at 500 MHz, ^{13}C at 125 MHz). All observed chemical shift values (δ) are given in in ppm and coupling constant values (J) in Hz. Standard pulse programs were used for ^{1}H, ^{13}C, HMBC, HSQC, 1,1 ADEQUATE, ^{15}N-HMBC, gCOSY and DQF-COSY experiments. HMBC experiments were optimized for $^{2,3}J_{C\text{-}H}$ = 6 Hz and $^{2,3}J_{N\text{-}H}$ = 5 Hz. The spectra were recorded in DMSO-d_6 and chemical shifts of the solvent signals at δ^H 2.50 ppm and δ^C 39.5 ppm were used as reference signals for spectra calibration. To increase sensitivity, the measurements were conducted in a 5 mm Shigemi tube (Shigemi Inc., Allison Park, PA 15101, USA). The NMR signals are grouped in the tables below and correspond to the numbering in the schemes corresponding to every table.

The myxofacyclines were re-dissolved in MeOH (approx. 8 mg/mL) and 2 µL samples were measured on the Spectrum™ 100 FT-IR Spectrometer (PerkinElmer) equipped with an UATR accessory (Diamond/ZnSe). Pure methanol was used as a blank for background subtraction. Absorbance spectra were collected between 400 cm^{-1} and 4000 cm^{-1} at a spectral resolution of 4 cm^{-1} and 64 scans were co-added and averaged.

2. Results

2.1 Structure elucidation of the myxofacyclines

Myxofacycline A (**1**)

The ^{1}H spectrum of myxofacycline A (1) in DMSO d_6 exhibited one signal at $\delta_{H\text{-}10}$ 6.15, characteristic for a proton of an sp^2 hybridized methine group. Furthermore, six methylene proton signals were found in the spectrum at $\delta_{H2\text{-}8}$ 2.68, $\delta_{H2\text{-}14}$ 2.57, $\delta_{H2\text{-}16}$ 2.24, $\delta_{H2\text{-}15}$ 1.79, $\delta_{H2\text{-}7}$ 1.60 and $\delta_{H2\text{-}4}$ 1.13 with resonances typical to be found in alkyl chains. In addition, one methine group at $\delta_{H\text{-}2}$ 1.49 was found and one intense signal at $\delta_{H3\text{-}1/3}$ 0.84 implies presence of two methyl groups. Examination of the HSQC spectrum revealed presence of two additional methylene groups at ($\delta_{C\text{-}6}$ 29.7, $\delta_{H2\text{-}6}$ 1.32) and ($\delta_{C\text{-}5}$ 27.5, $\delta_{H2\text{-}5}$ 1.31). Examination of COSY cross peaks indicates that both methyl groups, H_3-1 and H_3-3 are linked via the methine group at position two. Further COSY correlations from H-2 imply presence of an *iso*-branched alkyl chain, consisting of the two methyl groups, the methine group and five additional methylene groups (H_2-4 – H_2-8). Further analysis of the COSY spectrum revealed a butyric acid chain, which is comprised of three methylene groups (H_2-12, H_2-13 and H_2-14) and a terminal carboxyl group as indicated by HMBC correlations from $\delta_{H2\text{-}15}$ 1.79 and $\delta_{H2\text{-}16}$ 2.24 to a characteristic carbon resonance at $\delta_{C\text{–}17}$ 174.1. In order to establish connectivity between alkyl chain and butyric acid chain, the HMBC spectrum was examined. The methylene group at $\delta_{H2\text{-}8}$ 2.68 shows HMBC correlations to a carbon resonance at $\delta_{C\text{-}9}$ 173.0 and to the corresponding carbon of a sp^2 hybridized methine resonance at $\delta_{C\text{–}10}$ 100.7. Outgoing from this methine proton at $\delta_{H\text{-}10}$ 6.15, HMBC correlations to carbon resonance at $\delta_{C\text{-}11}$ 163.0 and $\delta_{C\text{-}9}$ 173.0. In addition, from $\delta_{H2\text{-}14}$ 2.57 HMBC correlations can be observed to the same carbon resonance at $\delta_{C\text{-}11}$ 163.0 and the carbon resonance of the sp^2 hybridized methine group, suggesting both alkyl chains are connected by a heteroaromatic system. The shift values of $\delta_{C\text{-}9}$ 173.0, $\delta_{C\text{–}10}$ 100.7 and $\delta_{C\text{-}11}$ 163.0 are typical for an isoxazole type heterocycle[14]. Also the determined ^{15}N resonance of $\delta_{\square\text{-}12}$ 361in MeOD is exemplarily for an isoxazole type heterocycle with reported resonances between δ_N 377–388[15] . Also observed correlations in an 1,1 ADEUQUATE NMR experiment from H-10 to $\delta_{C\text{-}9}$ 173.0 and $\delta_{C\text{-}11}$ 163.0 are in agreement with the carbon-carbon connectivity of an isoxazole ring.

Myxofacycline B (**2**)

The proton spectrum of Myxofacycline B (**2**) strongly resembled the one of **1**. The only difference to be found was multiplet at δ_{H3-1} 0.86 with correlations in the COSY spectrum to methylene protons at δ_{H2-2} 1.26, which is part of the alkyl chain. In combinations with the sum formula of $C_{14}H_{24}NO_3$ we suggest, that **2** contains a linear alkyl chain, instead of a linear chain.

Myxofacycline C (**3**)

Comparison of spectral data of Myxofacycline C (**3**) with **1** and **2** clearly shows that this molecule contains an *iso*-branched alkyl chain and an identical butyric chain. One ^{15}N resonance of δ_{N-12} 378 also suggest an isoxazole heterocycle. But the sum formula of $C_{15}H_{24}NO_4$ shows an additional oxygenation. Examination of the HMBC spectrum revealed correlations from δ_{H2-7} 2.94 and the isoxazole sp^2 hybridized methine proton at δ_{H1-10} 7.29 to a fully substituted carbon resonance at δ_{C-8} 189.3, which is indicative for carbonyl groups. Since HMBC correlations to this carbon resonance can be only observed from the *iso*-branched alkyl chain and the methine proton of the ring and since a correlation to δ_{C-8} 189.3 was only observed from δ_{H2-7} 2.94 in an 1,1-ADEUQUATE NMR experiment, we deduce that the carbonyl group is located between the *iso*-branched alkyl chain and the isoxazole ring.

Myxofacycline D (**4**)

The proton spectra of Myxofacycline D (**4**) differed only in the shift of the triplet of δ_{H2-8} 2.68 from **1** into a douplet of a douplet at δ_{H2-8} 4.61. Considering the sum formula of $C_{15}H_{26}NO_4$ an additional hydroxylation analogous to **3** is implied. The HSQC spectrum shows an additional methine group (δ_{C-8} 65.2, δ_{H2-8} 4.61) with characteristic shift values of a hydroxylation. Since COSY crosspeaks from the methine proton to an alkyl chain methylene protons at δ_{H2-7}1.68 were observed and HMBC correlations from δ_{H-10} 6.23 to the carbon resonance of the methine group at δ_{C-8} 65.2 can be found, the position of hydroxylated methine group between alkyl chain and isoxazole ring is confirmed. An attempt to determine the absolute configuration of the hydroxyl group by Mosher ester derivatization according the procedure of Hoye et al. did not succeeded.[16]

Myxofacycline E (**5**)

The acquired proton spectrum of Myxofacycline E (**5**) resembled the spectra of **1**, but the proton resonance of the sp^2 hybridized methine group was slightly upfield shifted to δ_{H-11} 5.92. Inspection of the HMBC spectra showed correlations from H-11 to two carbon resonances at δ_{C-10} 162.2 and δ_{C-12} 167.1. In addition, from δ_{H2-7} 2.48 HMBC correlations to a third fully substituted resonance at δ_{C-8} 161.9 were found. The sum formula of $C_{15}H_{25}N_2O_3$ and two nitrogen resonance at δ_{N-9}175 and δ_{N-13} 242, observed in an N-HMBC experiment as correlations from δ_{H-11} 5.92, indicate a different heterocycle than found in **1**–**4**. In order to establish C-C connectivities, we performed an 1,1-ADEQUATE NMR experiment. By examination of the spectrum we observed correlations from the sp^2 hybridized methine proton δ_{H-11} 5.92 to carbon resonances at δ_{C-10} 162.2 and δ_{C-12} 167.1, which is linked to the butyric acid chain as seen by a correlation from δ_{H-11} 2.40 to C-12. In addition, we found a correlation from δ_{H2-7} 2.48 to the carbon resonance δ_{C-8} 161.9, demonstrating the third fully substituted carbon at δ_{C-8} 161.9 neighbors the *iso*-branched alkyl chain.Considering the determined connectivities and the chemical shift values we deduce a 4-pyriminidol heterocycle in between the *iso*-branched alkyl chain and butyric acid chain.

Myxofacycline F (**6**)

The sum formula of Myxofacycline F (**6**) ($C_{14}H_{23}N_2O_3$) and the proton as well as HSQC and HMBC spectra imply a 4-pyriminidol heterocycle, while the triplet at δ_{H3-1} 0.85 with COSY correlations to a methylene group clearly indicates a linear alkyl chain like in **2.**

Myxofacycline G (**7**)

As indicated by the proton spectrum Myxofacycline G (**7**) consists of an *iso*-branched alkyl chain and a butyric acid chain, like most of the other described myxofacyclines. Despite the sum formula of $C_{15}H_{26}NO_4$ being similar to the one of **4** and the presence of a sp^2 hybridized methine group as seen in the HSQC at (δ_{C-10} 93.0, δ_{H-10} 4.62), other NMR signals clearly opposed an isoxazole ring. In contrast to the other described molecules, a nitrogen proton at δ_{H12} 8.06 was observed in the proton spectrum. Outgoing from δ_{H12} 8.06, HMBC correlations to three fully substituted carbons at δ_{C-8} 87.5, δ_{C-9} 201.0, δ_{C-11} 179.8 and the sp^2 hybridized methine group at δ_{C-10} 93.0 were observed. The shift value of C-9 strongly implies this carbon to be a keto group while the shift value of C-8 is characteristic for carbons with one or more heteroatoms as substituents. Based on the shift value of C-11, this carbon shows properties of an enol or enamine. Since the same correlations could be observed from the methine proton at δ_{H-10} 4.62, we deduce that the methine group, the nitrogen and the three fully substituted carbon form a five membered heterocycle. The alkyl chain shows HMBC correlations to δ_{C-8}

87.5, δ_{C-9} 201.0, while the carboxylic acid chain shows HMBC correlations to δ_{C-11} 179.8 and the methine carbon at δ_{C-10} 93.0. Based on these observed correlations, we conclude a 1,2-dihydropyrrol-3-one type heterocycle. Although the Iso6-catalzyed cyclization is probably stereospecific, the hydroxyl group on **7** might be prone to dehydration to form a C=N double bond, which in turn is hydroxylated again to yield racemic **7**. This might provide an explanation, why an attempt to determine the absolute configuration of the hydroxyl group by Mosher ester derivatization according the protocol of Hoye et al. did not succeed[16].

2.3 HR-MS spectra and IR data of isolated myxofacyclines

Myxofacycline A (**1**)

Colorless amorphous solid, IR (film) ν_{max} 2957, 2931, 2856, 1599, 1567, 1419, 1358 cm^{-1}, UV (ACN/H_2O) λ_{max} 218 nm, HR-ESI-MS *m/z* 268.19057 $[M+H]^+$ (calc. 268.19072 Δ: 0.55 ppm $C_{15}H_{26}NO_3$)

Myxofacycline B (**2**)

Colorless solid, IR (film) ν_{max} 2954, 2928, 2852, 2857, 1709, 1602, 1456,1435, 1245, 1155 cm^{-1}, UV (ACN/H_2O) λ_{max} 216 nm, HR-ESI-MS *m/z* 254.17421 $[M+H]^+$ (calc. 254.17502 Δ: 3.38 ppm $C_{14}H_{24}NO_3$)

Myxofacycline C (**3**)

Colorless solid, IR (film) ν_{max} 3114, 2955, 2932, 2869, 1687, 1581, 1465, 1417, 1378, 1367, 1278, 1271, 1256, 1210, 1165, 1138, 1052, 1017, 961, 939 cm^{-1}, UV (ACN/H_2O) λ_{max} 240 nm, HR-ESI-MS *m/z* 282.16965 $[M+H]^+$ (calc. 282.16998 Δ:1.18 ppm $C_{15}H_{24}NO_4$)

Myxofacycline D (**4**)

Colorless solid, $[\alpha]_D^{20}$ -2.33 (in MeOH), IR (film) ν_{max} 2953, 2935, 2868, 1710, 1601, 1458, 1426, 1244, 1212, 1206 cm^{-1}, UV (ACN/H_2O) λ_{max} 216 nm, HR-ESI-MS *m/z* 284.18517 $[M+H]^+$ (calc. 284.18563 Δ: 1.65 ppm $C_{15}H_{26}NO_4$)

Myxofacycline E (**5**)

Colorless solid, IR (film) ν_{max} 2954, 2905, 2889, 724, 1644, 1607, 1464, 1420, 1402, 1385, 1249, 1174, 1027, 966, 926, 870, 852, 729, 657 cm^{-1}, UV (ACN/H_2O) λ_{max} 226, 266 nm, HR-ESI-MS *m/z* 281.18518 $[M+H]^+$ (calc. 281.18597 Δ: 2.80 ppm $C_{15}H_{25}N_2O_3$)

Myxofacycline F (**6**)

Colorless solid, IR (film) ν_{max} 2955, 2930, 2859, 1723, 1660, 1600, 1563, 1459, 1407, 1380, 1251, 1184, 977, 851 cm^{-1}, UV (ACN/H_2O) λ_{max} 226, 264 nm, HR-ESI-MS *m/z* 267.16973 $[M+H]^+$ (calc. 267.17032 Δ: 2.21 ppm $C_{14}H_{23}N_2O_3$)

Myxofacycline G (**7**)

Colorless solid, $[\alpha]_D^{20}$ -2.33 (in MeOH), IR (film) ν_{max} 2954, 2942, 2931, 2868, 1712, 1631, 1544, 1481 cm^{-1}, UV (ACN/H_2O) λ_{max} 220, 328 nm, HR-ESI-MS *m/z* 284.18600 $[M+H]^+$ (calc. 284.18563 Δ:1.27 ppm $C_{15}H_{26}NO_4$)

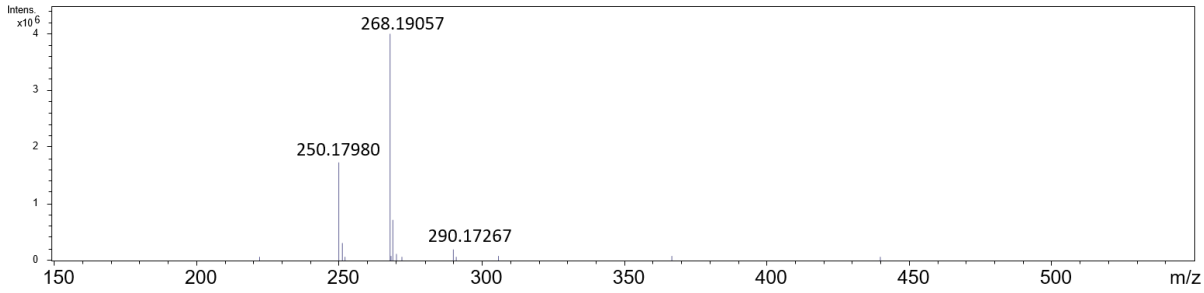

Figure S2. HR-MS spectrum of myxofacycline A (**1**).

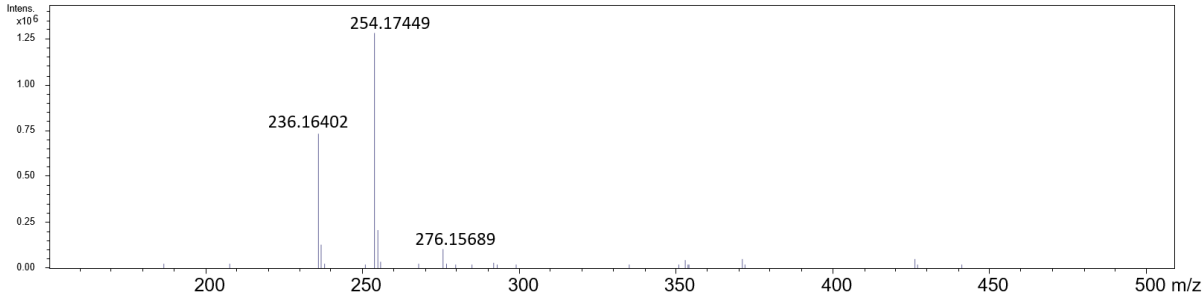

Figure S3. HR-MS spectrum of myxofacycline B (**2**).

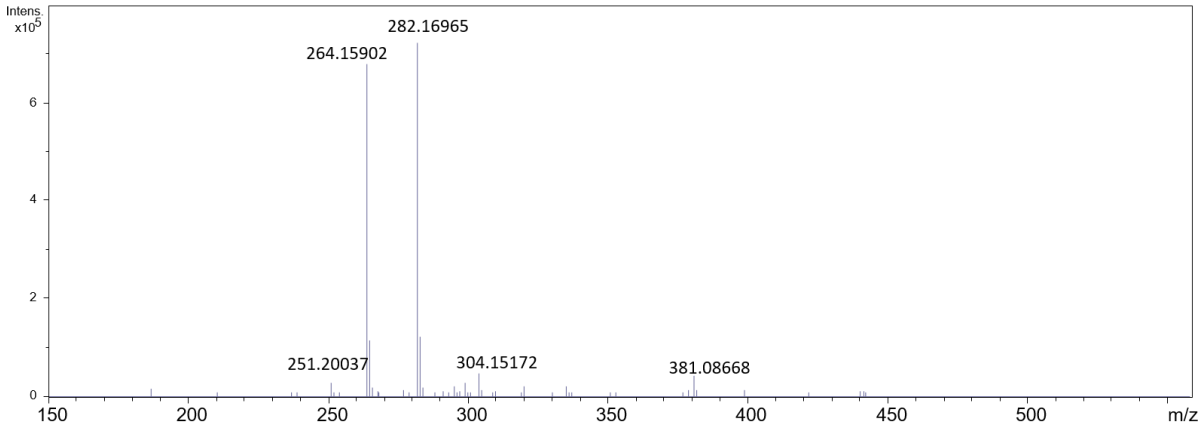

Figure S4. HR-MS spectrum of myxofacycline C (**3**).

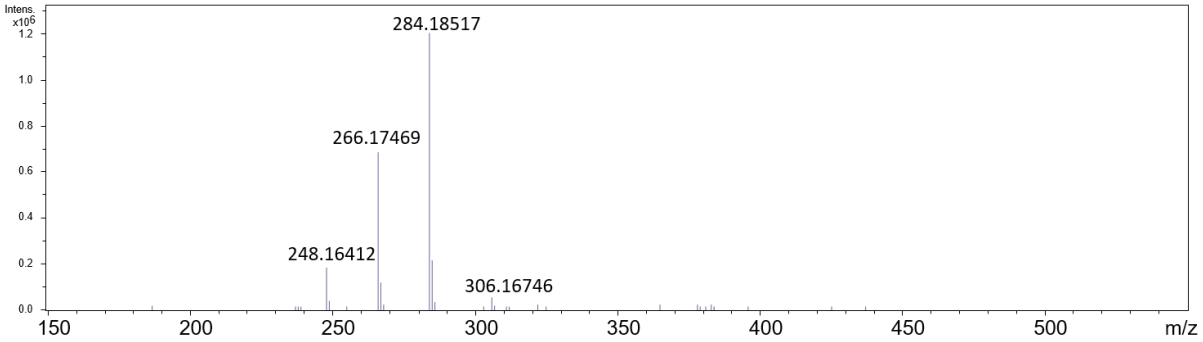

Figure S5. HR-MS spectrum of myxofacycline D (**4**).

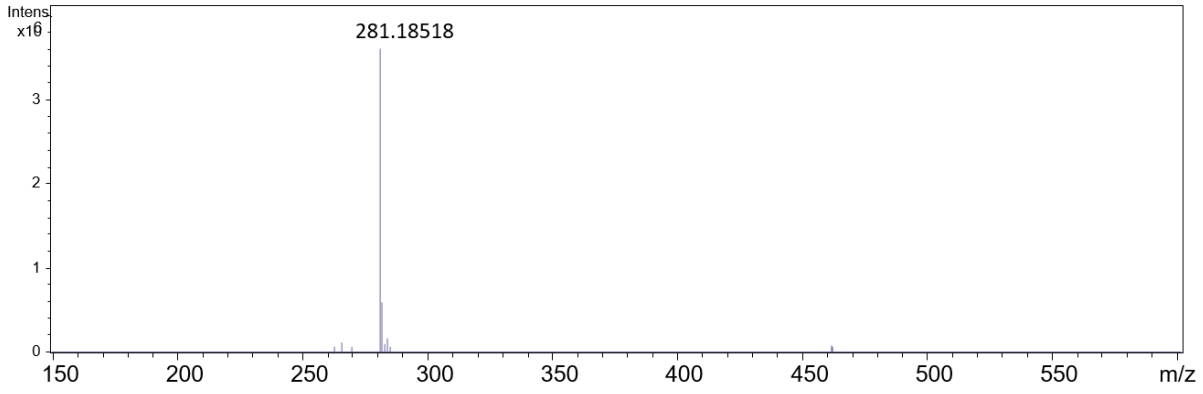

Figure S6. HR-MS spectrum of myxofacycline E (**5**).

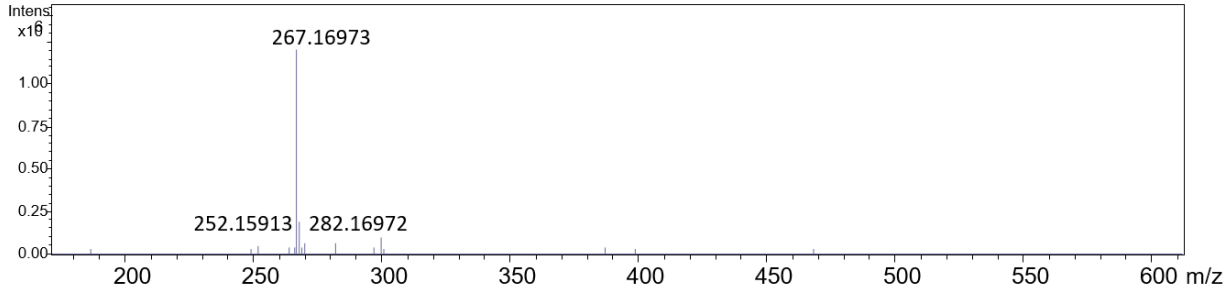

Figure S7. HR-MS spectrum of myxofacycline F (**6**).

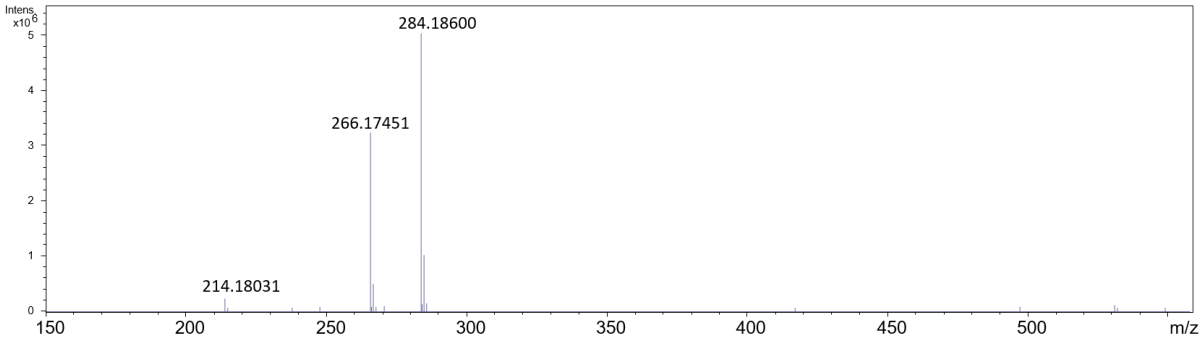

Figure S8. HR-MS spectrum of myxofacycline G (**7**).

2.2 NMR spectroscopic data

Table S8. Spectroscopic values of Myxofacycline A acquired in DMSO-d_6 at 500 MHz.

Position	δ ^{13}C	δ ^{15}N	δ ^{1}H	Multiplicity (J in Hz)	COSY	HMBC
1, 3	22.5	-	0.84	d (6.6)	2	1/3, 2, 4
2	27.4	-	1.49	dquin (13.3, 6.7, 6.7)	1, 3, 4	1, 3,
4	38.3	-	1.13	m	5, 2	1, 2, 3, 6
5	26.4	-	1.27	m	4, 6	4, 6
6	28.7	-	1.28	m	5, 7	5, 4
7	27.0	-	1.60	m	6, 8	5, 6, 9
8	25.9	-	2.68	t (7.6)	7, 10	6, 7, 9, 10
9	173.0	-	-	-	-	-
10	100.7	-	6.15	s	8	8, 9, 11, 14
11	163.0	-	-	-	-	-
12	-	361	-	-	-	-
13	-	-	-	-	-	-
14	24.7	-	2.57	t (7.6)	15	10, 11, 15, 16,
15	23.1	-	1.79	quin (7.5)	16, 14	11, 14, 16, 17
16	33.0	-	2.24	t (7.4)	15	14, 15, 17
17	174.1	-	-	-	-	-
18	-	-	12.05	bs	-	-

Table S9. Spectroscopic values of Myxofacycline B acquired in DMSO-d_6 at 700 MHz.

position	δ ^{13}C	δ ^{1}H	Multiplicity (J in Hz)	COSY	HMBC
1	13.9	0.86	t (7.00)	2	2, 3
2	22.0	1.26	m	1, 3	1, 3
3	31.1	1.24	m	2, 3	1, 2, 4, 5
4	28.4	1.29	m	3, 5	2, 3, 5, 6
5	28.2	1.28	m	6	3, 4, 6, 7
6	27.0	1.60	quin (7.18)	5, 7	4, 5, 7, 8
7	25.8	2.68	t (7.55)	6	5, 6, 8, 9, 10
8	172.9	-	-	-	-
9	100.7	6.14	s	7	7, 8, 10
10	163.0	-	-	-	-
13	24.7	2.57	t (7.63)	14	9, 10, 14, 15
14	23.2	1.79	quin (7.52)	13, 15	10, 13, 15, 16
15	33.1	2.23	t (7.33)	14	13, 14, 16
16	174.1	-	-	-	-
17	-	12.26	bs	-	-

Table S10. Spectroscopic values of Myxofacycline C acquired in DMSO-d_6 at 500 MHz.

position	δ ^{13}C	δ ^{15}N	δ ^{1}H	Multiplicity (J in Hz)	COSY	HMBC
1, 3	22.5	-	0.85	d (6.6)	1/3, 2	1/3, 2, 4
2	27.3	-	1.51	m	1, 3, 4	1, 3, 4
4	38.2	-	1.17	m	2, 5	1, 2, 3, 5, 6
5	26.2	-	1.29	m	4, 6	2, 4, 6, 7
6	23.2	-	1.57	quin (7.16)	5, 7	4, 5, 7, 8
7	39.3	-	2.94	t (7.3)	6	5, 6, 8, 9
8	189.3	-	-	-	-	-
9	165.3	-	-	-	-	-
10	108.6	-	7.29	s	14	8, 9, 11, 14
11	164.4	-	-	-	-	-
12	-	378	-	-	-	-
14	24.7	-	2.71	t (7.6)	15	10, 11, 15, 16
15	23	-	1.85	quin (7.5)	14, 16	11, 14, 16, 17
16	33	-	2.26	t (7.4)	15	14, 15, 17
17	174.1	-	-	-	-	-
18	-	-	12.21	bs	-	-

Table S11. Spectroscopic values of Myxofacycline D acquired in DMSO-d_6 at 500 MHz.

Position	δ ^{13}C	δ ^{15}N	δ ^{1}H	Multiplicity (J in Hz)	COSY	HMBC
1, 3	22.5	-	0.84	d (6.6)	1/3, 2	1/3, 2, 4
2	27.4	-	1.48	dt (13.33, 6.64)	1, 3, 4	1, 3, 4, 5, 6
4	38.4	-	1.13	m	5, 2	1, 2, 3, 5, 6
5	26.6	-	1.26	m	4, 6	4, 6, 7, 8
6	25.0	-	1.29	m	5, 7	4, 5, 7, 8
7	35.7	-	1.68	m	6, 8	5, 6, 8, 9
8	65.2	-	4.61	dd (7.27, 5.77)	7	6, 7, 9, 10, 11
9	175.6	-	-	-	-	-
10	100.3	-	6.23	s	-	7, 8, 9, 11, 14
11	162.8	-	-	-	-	-
12	-	369.2	-	-	-	-
14	24.7	-	2.59	t (7.59)	15	9, 10, 11, 15, 16
15	23.2	-	1.80	quin (7.51)	16, 14	11, 14, 17
16	33.0	-	2.24	t (7.37)	15	14, 15, 17
17	174.1	-	-	-	-	-
18	-	-	12.24	bs	-	-
19	-	-	5.63	bs	-	-

Table S12. Spectroscopic values of Myxofacycline E acquired in DMSO-d_6 at 700 and 500 MHz.

Position	δ ^{13}C	δ ^{1}H	δ ^{15}N	Multiplicity (J in Hz)	COSY	HMBC
1, 3	22.4	0.83	-	d (6.5)	1/3, 2	1/3, 2, 4
2	27.2	1.49	-	dquin (13.3, 6.6)	1, 3, 4	1, 3, 4
4	38.0	1.15	-	m	2, 5	1, 2, 3, 5, 6
5	26.1	1.25	-	m	4, 6	4, 6, 7
6	27.0	1.60	-	quin (7.6)	5, 7	4, 5, 7, 8
7	34.1	2.48	-	m	6	6, 8
8	161.9	-	-	-	-	-
9	-	-	175.0	-	-	-
10	162.6	-	-	-	-	-
11	109.4	5.95	-	s	14	10, 12, 14
12	167.1	-	-	-	-	-
13	-	-	242.0	-	-	-
14	35.8	2.40	-	t (7.5)	11, 15	11, 12, 15, 16
15	22.8	1.78	-	quin (7.5)	14, 1	12, 14, 16, 17
16	32.9	2.21	-	t (7.4)	15	14, 15, 17
17	174.2	-	-	-	-	-
18	-	-	12.19	bs	-	-
19	-	-	12.19	bs	-	-

Table S13. Spectroscopic values of Myxofacycline F acquired in DMSO-d_6 at 500 MHz.

Position	δ ^{13}C	δ ^{1}H	Multiplicity (J in Hz)	COSY	HMBC
1	13.9	0.85	t (7.2)	2,	2, 3
2	22.0	1.25	m	1, 3	1, 3, 4
3	30.9	1.24	m	2, 4	1, 2, 4, 5
4	28.1	1.24	m	3, 5	2, 3, 5, 6
5	26.8	1.62	quin (7.6)	4, 6	3, 4, 6, 7
6	34.1	2.48	m	5	4, 5, 7
7	162.0	-	-	-	-
9	162.7*	-	-	-	-
10	109.3	5.94	s		9, 11, 13
11	167.0*	-	-	-	-
13	35.8	2.39	t (7.5)	14	10, 11, 14, 15
14	23.0	1.77	quin (7.5)	13, 15	15, 13, 11, 16
15	33.2	2.19	br t (7.3)	14	13, 14, 16
16	174.3	-	-	-	-
17	-	12.23	bs	-	-
18	-	12.23	bs	-	-

*chemical shifts obtained from HMBC spectrum

Table S14. Spectroscopic values of Myxofacycline G acquired in DMSO-d_6 at 500 MHz.

Position	$\delta^{13}C$	$\delta^{1}H$	Multiplicity (J in Hz)	COSY	HMBC
1, 3	22.5	0.82	d (6.6)	2	1/3, 2, 4
2	27.3	1.46	m	1, 3, 4	1/3, 4, 5
4	38.4	1.09	m	2, 5	1/3, 2, 5, 6
5	27.0	1.18	m	4, 6	2, 4, 6, 7
6	22.6	1.18	m	5, 7	2, 4, 5, 7
7	36.5	1.49	m	6	5, 6, 8, 9
8	87.5	-	-	-	-
9	201.0	-	-	-	-
10	93.0	4.62	d (0.38)	12, 13	8, 9, 11, 13
11	179.8	-	-	-	
12	-	8.06	-	10	8, 9, 10, 11, 13
13	29.0	2.36	t (7.6)	10, 14	10, 11, 14, 15
14	21.9	1.77	td (7.4, 2.6)	13, 15	11, 13, 15, 16
15	32.9	2.26	t (7.5)	14	13, 14, 16
16	174.1	-	-	-	-
17	-	5.87	bs	-	-
18	-	n.d.	-	-	-

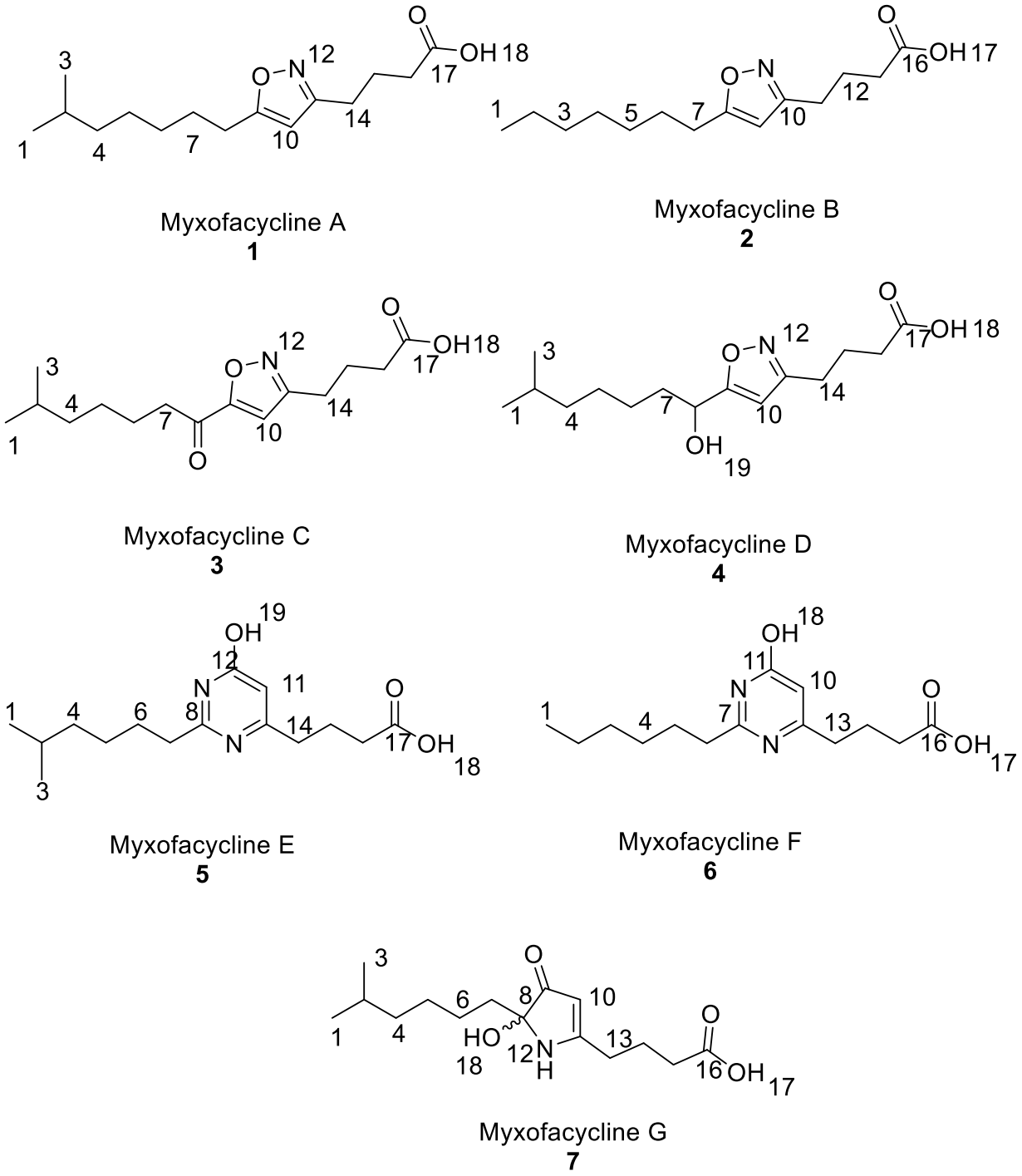

Figure S9. Structure and numbering of myxofacyclines A–G (**1–7**).

2.4 Feeding experiments

L-Leucine d_3 and $^{13}C_2$ acetate

The isotopic patterns of myxofacycline congeners **1**, **3**, **4**, **5** and **7** showed intensified peaks at m/z 271 and 272 corresponding to a mass shift of +3 Da, caused by the incorporation of L-leucine d_3, as exemplarily shown for **1** in **Figure S10** and **5** in **Figure S11**. The incorporation of the branched-chain amino acid L-leucine d_3 can be explained through its conversion to isovaleryl-CoA, which serves as a starter unit during the biosynthesis of myxofacycline A. Similarly, acetate $^{13}C_2$ supplementation shows intensified peaks at m/z 270, 271 and 272 in the isotopic patterns of all myxofacyclines corresponding to a mass shift of +2 Da.

L-glutamine $^{15}N_2$ $^{13}C_6$, L-asparagine $^{15}N_2$ $^{13}C_6$, L-valine d_8, L-glutamic acid N_{15}, glycine N_{15} C_{13}

The isotopic patterns of myxofacycline congeners **1–7** showed no respective specific intensified peaks after the supplementation of L-glutamine $^{15}N_2$ $^{13}C_6$, L-asparagine $^{15}N_2$ $^{13}C_6$, L-valine d_8, L-glutamic acid N_{15} or glycine N_{15} C_{13} except for marginally intensified peaks corresponding to a mass shift of +1 Da (in particular the changed ratio between $[M+H]^+$ and $[M+H]^+$ + 1Da). (Data not shown). Potential incorporation of L-glutamine $^{15}N_2{}^{13}C_6$ and L-asparagine $^{15}N_2$ $^{13}C_6$ can be explained through an aminotransferase-initiated catalysis in the heterocyclization of the myxofayclines.

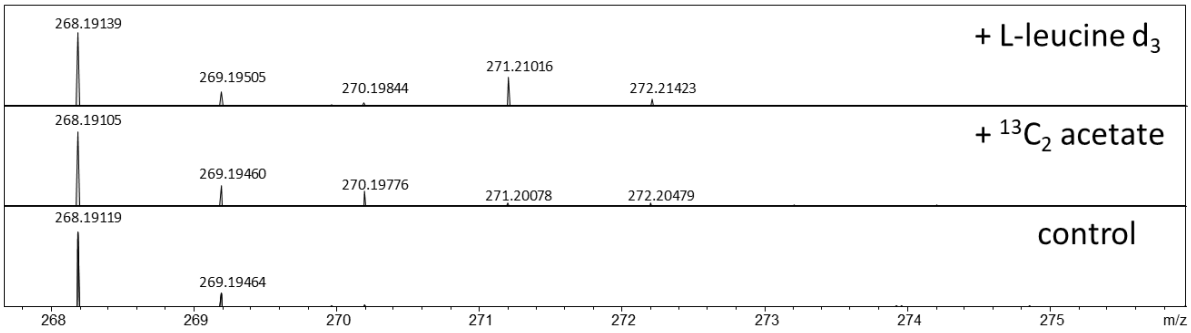

Figure S10. Partial ESI+MS spectra for myxofacycline A with L-leucine d_3 and acetate $^{13}C_2$ supplementation and culture broth without precursor supplementation as control.

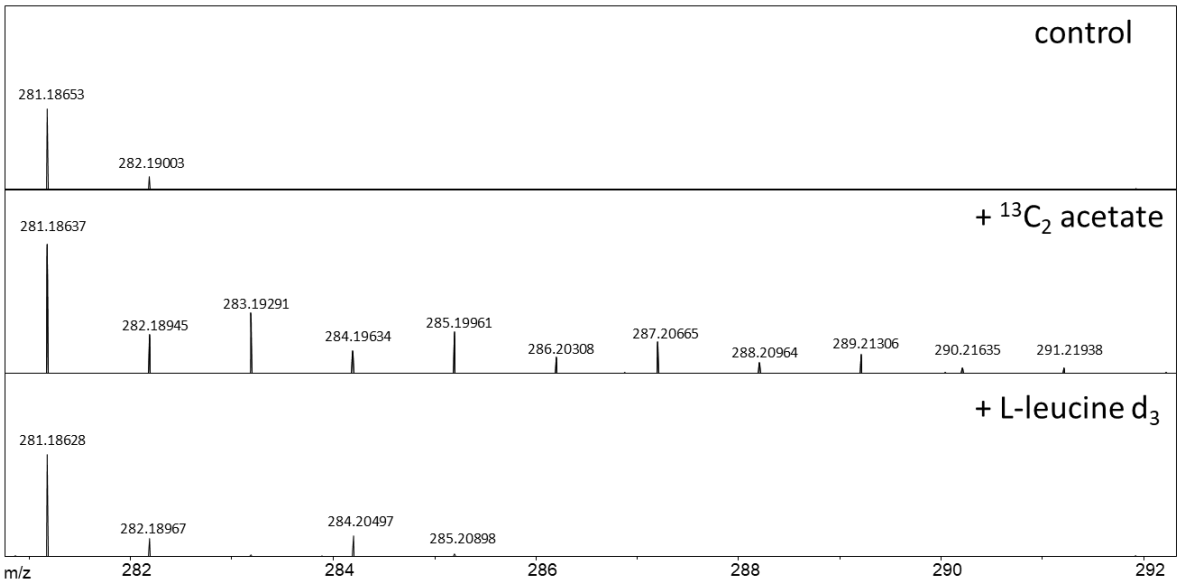

Figure S11. Partial ESI+MS spectra for myxofacycline E with L-leucine d_3 and acetate $^{13}C_2$ supplementation and culture broth without precursor supplementation as control.

2.5 *In silico* investigation of the myxofacycline biosynthesis

Genes encoded in the myxofacycline gene cluster (*iso1–9*)

Table S15. Table of all open reading frames assigned to the myxofacycline biosynthetic gene cluster (*iso1–9*) in *M. xanthus* Mx x48 with proposed function and closest homologue according to blastp search in the nr (non-redundant protein sequences) protein database at NCBI.

Gene name	Length (bp)	Proposed function	Closest homologue	Coverage/ identity (%)
iso1	414	thioesterase	WP_108068573.1	99/96
iso2	3699	starter unit tethering FAAL-ACP	WP_158619977.1	99/76
iso3	843	fatty acid desaturase	WP_120624300.1	96/86
iso4	843	oxidation	WP_143901697.1	99/85
iso5	2766	PKS biosynthesis KS-AT	WP_108069076.1	88/77
iso6	3288	PKS/NRPS biosynthesis ACP-Amt-C-domain	WP_143901701.1	99/75
iso7	375	Standalone ACP	WP_161665324.1	99/69
iso8	1581	Adenylation domain	WP_161665323.1	99/85
iso9	7383	PKS biosynthesis KS-AT-DH-ER-KR-ACP-TE	WP_143901706.1	98/79

The identified biosynthetic gene cluster was also found in the genome sequence of the myxobacterial strains *Corallococcus* sp. Z5C101001, *Corallococcus sicarius* sp. nov. (CA040B^T = DSM 108850^T = NBRC 113890^T)[17], *Vitiosangium* sp. GDMCC 1.1324[18] and *Corallococcus* sp. c25j21. The comparison of these strains assisted to determine precisely the exact biosynthetic gene cluster borders, since upstream of *iso1* and downstream of *iso9* the genetic region is significantly different between the different producers.

iso1

The gene *iso1* encodes a thioesterase (TE) which is a member of the thioesterase family 13 (TE13)[19] such as the phenylacetic acid degradation protein PaaI[20]. Typical TEs in PKS and NRPS pathways are classified as type I thioesterase (TE I; thioesterase family 16) integrated in the multimodular architecture of FASs, PKSs, or NRPs such as the TE in Iso9 or type II thioesterase (TE I; thioesterase family 18) which are independently working TEs[21]. These TEs feature a α/β-hydrolase fold[22], whereas the structure of Iso1 putatively exhibits a Hotdog fold[23] such as other members of TE13. The function of *iso1* remains elusive, since all myxofacyclines can be produced without Iso1, as shown for the genetically engineered *M. xanthus* Mx x48 mutants, which harbors the vanillate-inducible promoter system in front of *iso2*, which most probably nullifies the expression of *iso1*; additional confirmation is provided by the heterologous production of all myxofacyclines in DK1622, which only harbors the genetic operon *iso2–9* in the respective mutants.

iso2

The gene *iso2* encodes a fatty acyl AMP ligase (FAAL), an acyl CoA dehydrogenase (DH) domain and an ACP domain. The FAAL shows the highest structural similarity according Phyre2 analysis to the FAAL from *L. pneumophila (Lp*FAAL, PDB: 3KXW)[24]. The FAAL in Iso2 features the insertion motif (distinguishing it from FACLs), the hinge region, the gate motif and the highly conserved loop region within the C domain, which are interacting with each other for substrate binding and product release[25]. The product is then transferred to the ACP on Iso2. The ACP is not featuring the motif with the catalytic serine of (D/E)xGxDSL or any related DSL/R motif[26]. A similar ACP is described for AmbG, responsible for the biosynthesis of ambruticin[27][28]. The optional *β*-oxidation, of the fatty acid substrate, is catalyzed by the Acyl-CoA DH in Iso2. The Acyl-CoA DH has the highest sequence similarity with the Acyl-CoA DH NocC in *Nostoc* sp. CCAP 1453/38[29].

iso3

In silico prediction based on the amino acid sequence proposes a structure for Iso3, with the closest similarity to stearoyl-CoA desaturases (c4zyoA, c4ymkA) (**Figure S12**).

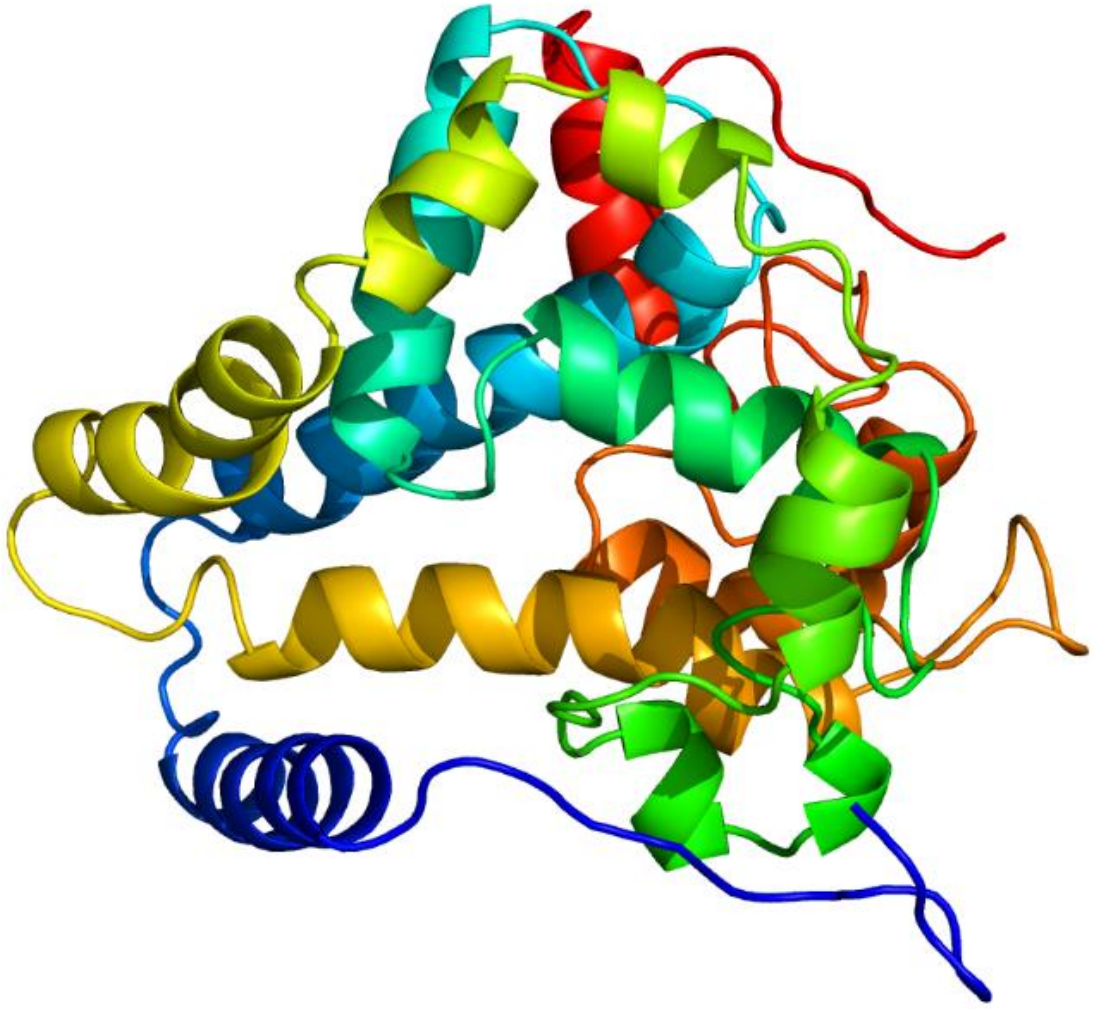

Figure S12. Phyre-2 structure homology model of the putative stearoyl-CoA desaturase encoded by *iso3* (model based on template c4zyoA; figure colored by rainbow *N* → *C* terminus.

iso4

The gene *iso4* putatively encodes a cryptic protein, which might be responsible for the hydroxylation of the generated free secondary amine. Iso4 shows low sequence similarity with the imidazolonepropionase (BBA66509.1) from the biosynthesis of actinoallolides[30] and low structural similarity to crystal structure of a tena/thi-4 domain-containing protein from *Sulfolobus solfataricus* (PDB: 4LQX) and the oxygenase PqqC. The proposed mechanism could work by using molecular oxygen to generate the oxime[31].

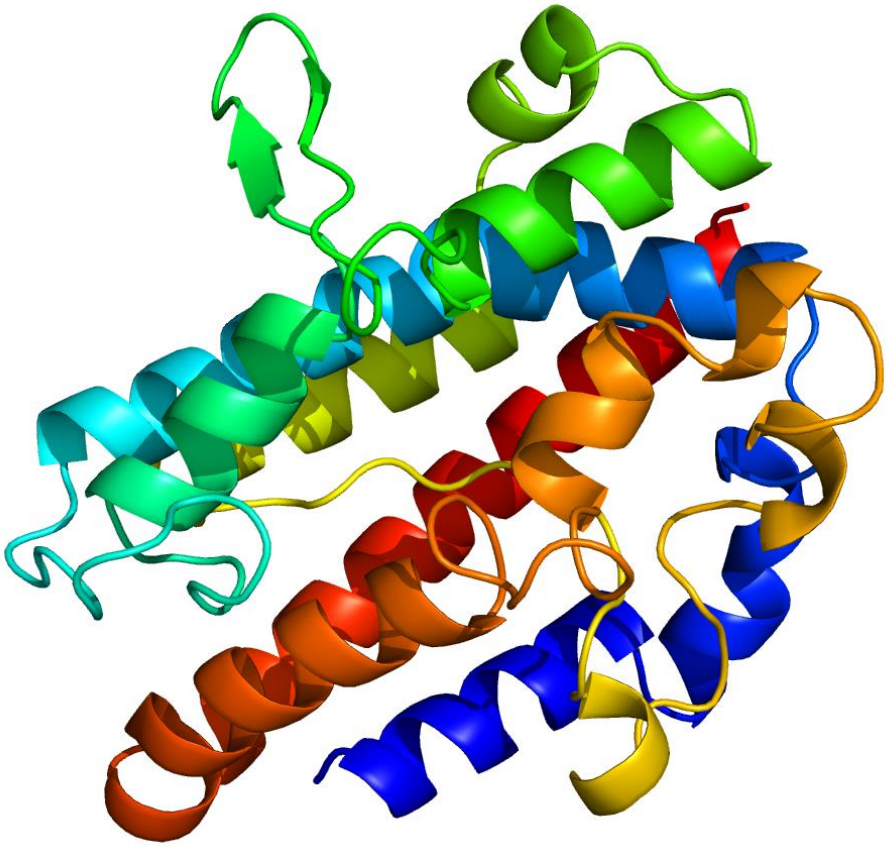

Figure S13. Phyre-2 structure homology model of a putative tena/thi-4 domain-containing protein (oxidoreductase, PDB: 4LQX) encoded by *iso4* (model based on template d1otva; figure colored by rainbow *N* → *C* terminus.

iso5

The gene *iso5* encodes a KS and AT domain responsible for conventional polyketide chain extension incorporating malonyl-CoA building blocks. The active site residue of the AT domain of Iso5 and Iso9 (**Tab. S16 and Tab. S17**) and clearly indicates that the extension building block has to be malonyl-CoA rather than being methylmalonate CoA or any other unusual substrate. Iso5 might act iteratively on the octanoic acid-based precursors as hypothesized.

Table S16. Acyl transferase (AT) active residues that correlate with domain specificity.

Domain /residue	**11**	**63**	**90**	**91**	**92**	**93**	**94**	**117**	**200**	**201**	**231**	**250**	**255**
Methylmalonate cons.	Q	Q	G	H	S	QMI	G	R	S	H	T	NS	V
malonate cons.	Q	Q	G	H	S	LVIFAM	G	R	FP	H	ANTGEDS*	NHQ	V
epoC_AT_1	Q	Q	G	H	S	I	G	R	F	H	N	H	V
epoA_AT_1	Q	Q	G	H	S	I	G	R	F	H	N	H	V
epoB_AT_1	Q	Q	G	H	S	M	G	R	S	H	N	H	V
Iso5 AT	Q	Q	G	H	S	L	G	R	F	H	T	N	V
Iso9 AT	Q	Q	G	H	S	V	G	R	F	H	N	H	V

Table S17. Acyl transferase (AT) additional conserved residues that correlate with domain specificity.

Domain/residue	**15**	**58**	**59**	**60**	**61**	**62**	**70**	**72**	**197**	**198**	**199**
Methylmalonate cons.	W	REDQ	VIDA	D	V	VLI	MAEQ	SAG	D	YV	A
Malonate cons.	R	RQED	T	GRLE	YWFW	TAS	EQ	AG	SN	H	A
epoC_AT_1	T	E	T	A	F	T	E	A	S	H	A
epoA_AT_1	T	Q	T	A	F	T	E	A	S	H	A
epoB_AT_1	W	R	I	D	V	V	A	A	D	V	A
Iso5 AT	F	D	T	H	A	A	E	A	R	H	A
Iso9 AT	Y	Q	T	K	Y	T	E	A	S	H	A

iso6

iso6 encodes module 3, harboring an ACP, an Amt domain and a C domain. The ACP features the typical D/ExGxDSL motif with the catalytically active serine. The ACP-Amt didomain architecture shows striking similarity to the ACP-Amt fusion domain found in the mycosubtilin pathway (PDB: c6kfuA) (**Figure S14**). The C domain found in Iso6 is hypothesized to perform the cyclization of the generated oximes to yield the heterocyclic scaffold presented in the different myxofacyclines. Phylogenetic analysis of this C domain reveals that it might represent a distinct novel clade besides the six C domain subtypes distinguished by Rausch *et al.*[32] and the new C domain subtype described by Pogorevc *et al.*[33]. However, the C domain in Iso6 features the common catalytic motif HHxxxDG and is not replaced through the motif DxxxxDxxS which is described for several heterocyclization domains[34].

Figure S14. Phyre2 structure homology model of the ACP-Amt di-domain encoded by *iso6* (model based on template c6kfuA4; figure colored by rainbow *N* → *C* terminus).

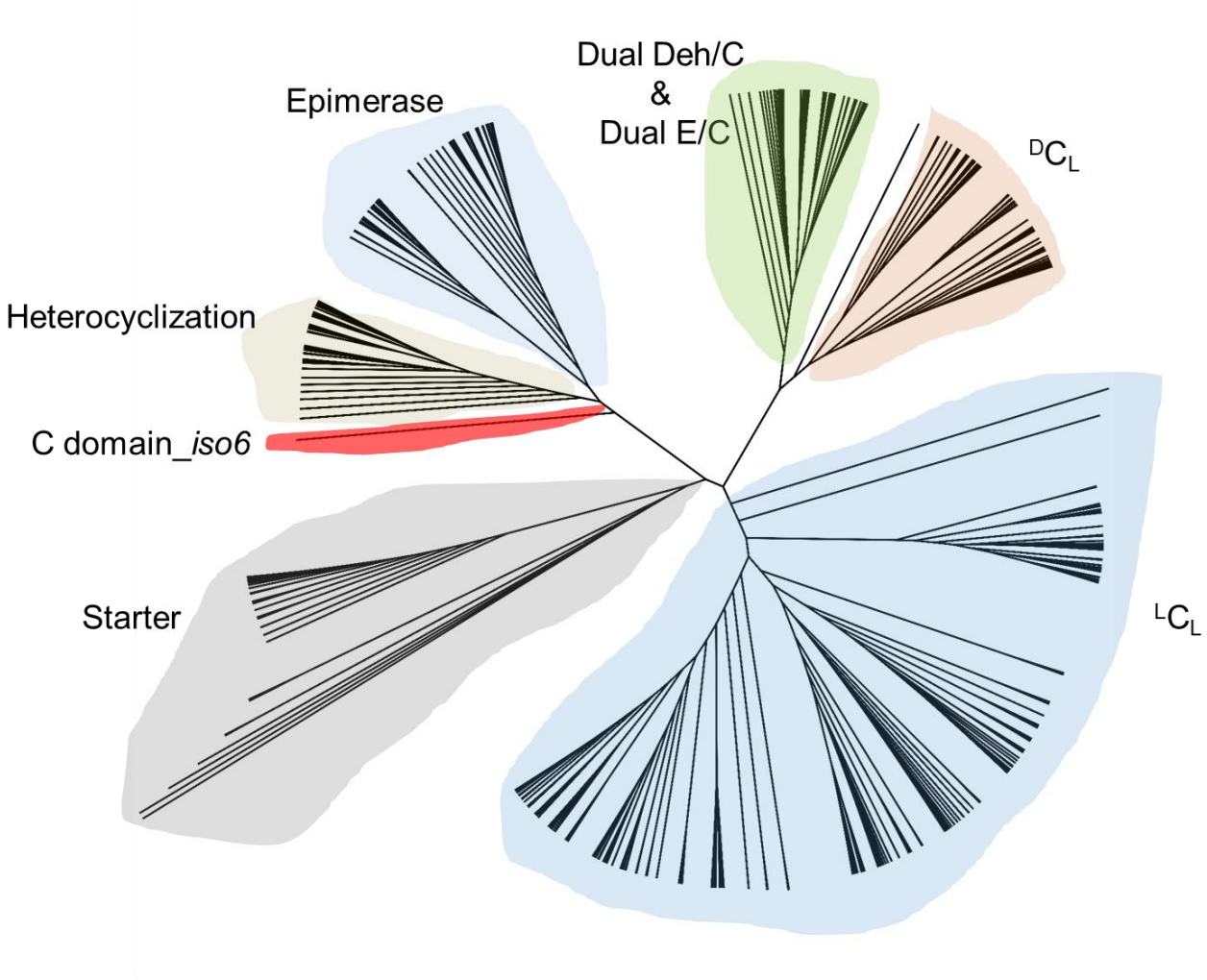

Figure S15. Phylogenetic tree of different C domain subtypes. Phylogenetic tree of all known C domain subtypes ($^{L}C_{L}$, $^{D}C_{L}$, starter, dual E/C, dual Deh/C, epimerization and heterocyclization domains). The phylogeny was reconstructed by using phyml, a gamma-distributed rate variation with four categories and employing the JTT model of amino acid substitution. Support values are based on 100-fold bootstrapping. The C domain list includes in total 538 domains from phylogenetic studies by Rausch *et al.*[32] and Pogorevc *et al.*[33]. The C-domain from the NRPS module Iso6 seems to be phylogenetically closely related to heterocyclization domains such as described for epothilone or myxothiazol biosynthesis[35].

iso7

iso7 encodes a standalone ACP domain. The ACP domain shows similarity with the structure of the acyl carrier 2 protein domain from module 2 of the 6-deoxyerythronolide b_3 synthase[36] (**Figure S16**).

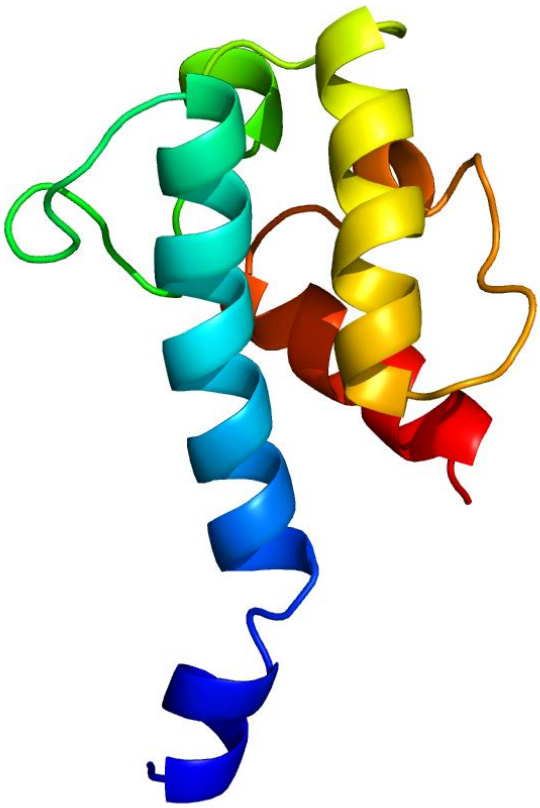

Figure S16. Phyre2 structure homology model of the standalone ACP-Amt encoded by *iso7* (model based on template c2ju2A; figure colored by rainbow *N*→*C* terminus).

iso8

iso8 encodes a standalone A domain. The specificity-conferring code of adenylation domains in NRPSs (Stachelhaus code[37]) implies that the substrate of Iso8 cannot be an α-amino acid, since residue 235 features a histidine rather an aspartic acid (**Table S18**). The exact role of Iso8 remains elusive.

Table S18. Stachelhaus code sequence of different A domains including the standalone A domain Iso8.

Name /Position	**235**	**236**	**239**	**278**	**299**	**301**	**322**	**330**	**331**	**517**	**building block**
Iso8	H	V	W	A	V	G	N	N	M	K	---
AIL50189.1 (BGC0000213)	F	G	C	G	F	G	A	I	C	K	aminolevulinic acid
AMU1	D	A	W	T	I	A	A	I	C	K	Phe
cdaps003_A_002_1amu	D	G	W	A	V	A	S	V	C	K	Trp
ATY72527.1 (BGC0001574)	V	G	W	C	V	G	I	A	C	K	fatty acyl
natF (BGC0001695)	H	G	V	W	L	Y	V	G	P	K	2-amino benzoic acid
AZF85933.1 (BGC0001963)	I	G	W	C	A	G	L	N	T	K	fatty acyl

Accession number according the MIBiG database are shown in brackets.

iso9

iso9 encodes a PKS module consisting of an AT, ACP and KS domain equipped with the full set of accessory domains (KR, DH and ER) to catalyze a full reductive loop onto the β-keto thioester during condensation. *In silico* analysis and the conducted genetic disruption experiment of *iso9* confirmed the functionality of the last module, which provides optional backbone extension of the myxofacyclines.

2.6 Biosynthetic investigation and genetic manipulation of the myxofacycline biosynthesis in the producer *M. xanthus* Mx x48

Generation of gene-disruption and induced-gene mutants of *M. xanthus* Mx x48 to connect the identified genes to the production of myxofacycline

A 317–1373 bp homology sequence of the genes *iso1*, *iso2*, *iso3*, *iso4*, *iso5*, *iso6*, *iso8* and *iso9* have been PCR amplified by the primers as shown in **Table S2**. The specific homology sequence was subcloned via conventional restriction ligation (HindIII, SpeI) into the pCR2.1 vector from the TOPO-TA cloning kit (Thermo scientific TOPO-TA cloning Kit). Similarly to the construction of the disruption constructs, a 1117 bp homology sequence starting from the translational start (not the RBS, but the coding sequence) of the gene *iso2* encoding the starter module has been PCR amplified by the primers as shown in **Table S2.** The homology sequence was subcloned via conventional restriction ligation into the pFP_{Van} vector (NdeI, EcoRI), which has been constructed and utilized previously to express several genes in myxobacteria[8,38]. The pFP_{Van} vector is a derivative of the pCR2.1 vector featuring a vanillate-inducible promoter which is fused to the vanillate-responsive repressor as described in literature[39]. Additional mutants of *M. xanthus* Mx x48 were generated with the plasmid pMycoMar (**Table S4**, plasmid No. 6), confers kanamycin resistance to the respective transformants. This plasmid allows very efficient random integration into myxobacterial genomes through the usage of a Himar1-dervied transposable element[10]. The procedure to generate these mutants were not only useful to develop a transformation protocol for *M. xanthus* Mx x48 (see below) but also to use these mutants as controls to scrutinize pleiotropic effects regarding the production of myxofacyclines after mutagenesis in *M. xanthus* Mx x48. As outcome, these transposon mutants did not show differences in the myxofacycline production, when compared with the wild type strain *M. xanthus* Mx x48.

Transfer and chromosomal integration of the constructs into the host *M. xanthus* Mx x48

The procedure to test *M. xanthus* Mx x48 for electrocompetence with 4–6 µL of pMycoMar vector solution (100–200 ng/µL) and CTT media has been described elsewhere[11]. This testing and the evaluation via the amount of resulting transformants led to the conclusion, that the same parameters as applied for *M. xanthus* DK1622 are optimal for the succesful transformation of *M. xanthus* Mx x48.

According to a previously established electroporation procedure for *M. xanthus* DK1622[40] the strain *M. xanthus* Mx x48 was transformed with the generated disruption and induced-gene constructs (**Table S6**, genetic constructs 1–6). *M. xanthus* Mx x48 transformants were routinely cultivated at 30 °C in CTT medium or CTT agar. Liquid cultures were grown in Erlenmeyer flasks on an orbital shaker at 180 rpm for 3–6 days. *M. xanthus* Mx x48 transformants were selected by adding 50 µg/mL kanamycin to the fermentation culture. Correct chromosomal integration of the expression constructs via homologous recombination into the site-specific locus was confirmed by PCR (**Figure S17**). PCRs were performed according to the settings described above. Genomic DNA of the transformants were isolated using the Gentra® Puregene® Yeast/Bact. Genomic DNA Purification Kit (Qiagen) according to manufacturer's instructions. For each expression construct, correct chromosomal integration was confirmed using two different primer combinations revealing PCR products of the expected sizes:

- Construct No. 1, Seq. primer No.1/3 (1495 bp), and primer No.4/2 (1609 bp)
- Construct No. 2, Seq. primer No.5/7 (1844 bp), and primer No.8/6 (1836 bp)
- Construct No. 3, Seq. primer No.9/11 (1659 bp), and primer No.12/10 (1449 bp)
- Construct No. 4, Seq. primer No.13/15 (1561 bp), and primer No.16/14 (1548 bp)
- Construct No. 5, Seq. primer No.17/19 (1789 bp), and primer No.20/18 (2037 bp)
- Construct No. 6, Seq. primer No.21/23 (1928 bp), and primer No.24/22 (2079 bp)
- Construct No. 7, Seq. primer No.25/27 (2032 bp), and primer No.28/26 (1533 bp)
- Construct No. 8, Seq. primer No.29/31 (1970 bp), and primer No.32/30 (1859 bp)
- Construct No. 9, Seq. primer No.33/35 (1620 bp), and primer No.36/34 (1745 bp)

Genomic DNA of *M. xanthus* Mx x48 was used as negative control. A complementary experiment using the following primer combinations revealed a specific PCR product for *M. xanthus* Mx x48, but not for any of the transformants of *M. xanthus* Mx x48 harboring one of the generated constructs.

- Construct No.1, Seq. primer No.1/2 (1716 bp PCR product for *M. xanthus* Mx x48 wild type)
- Construct No.2, Seq. primer No. 5/6 (1442 bp PCR product for *M. xanthus* Mx x48 wild type)
- Construct No.3, Seq. primer No. 9/10 (1634 bp PCR product for *M. xanthus* Mx x48 wild type)
- Construct No.4, Seq. primer No. 13/14 (1455 bp PCR product for *M. xanthus* Mx x48 wild type)
- Construct No.5, Seq. primer No.17/18 (1627 bp PCR product for *M. xanthus* Mx x48 wild type)

- Construct No.6, Seq. primer No. 21/22 (1681 bp PCR product for *M. xanthus* Mx x48 wild type)
- Construct No.7, Seq. primer No.25/26 (1549 bp PCR product for *M. xanthus* Mx x48 wild type)
- Construct No.8, Seq. primer No. 29/30 (1487 bp PCR product for *M. xanthus* Mx x48 wild type)
- Construct No.9, Seq. primer No. 33/34 (1754 bp PCR product for *M. xanthus* Mx x48 wild type)

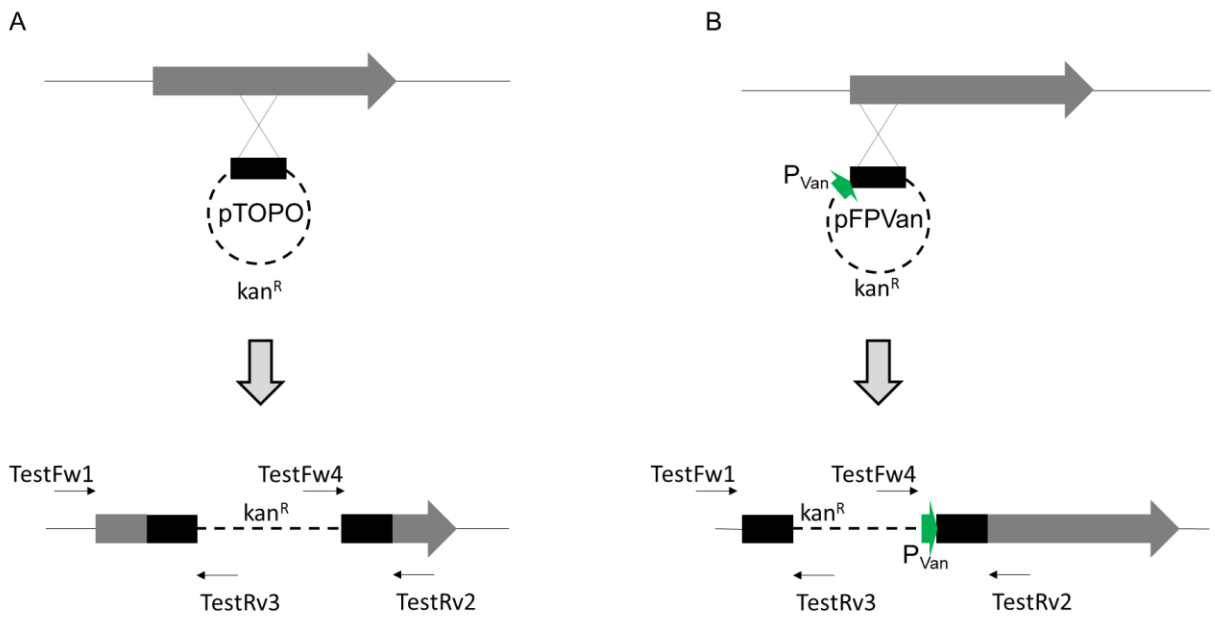

Figure S17. Genotypic verification procedure using PCR. Correct chromosomal integration of the genetic disruption (**A**) and induced-gene expression constructs were verified by multiplex PCR using four primers: two integrations site-specific primers (TestFw1 and TestRv2) and two vector specific primers (Test Rv3 and Test Fw4).

Analysis of secondary metabolism of genetic mutants

Table S19. Secondary metabolites associated with BGC *iso1–9* in *M. xanthus* Mx x48 and in the heterologous host *M. xanthus* DK1622. *Production after *iso9* gene disruption

No.	RT [min]	Mass $[M+H]^+$	Sum formula	Identification	Metabolite	*After iso9*-KO*
1	5.37	266.17480	$C_{15}H_{24}NO_3$	*iso1/2* activation	---	No
2	5.44	239.13980	$C_{12}H_{19}N_2O_3$	*iso9* disruption	Myxofacycline F1 **6a**	Yes
3	5.83	270.17022 (252.15864)	$C_{14}H_{24}NO_4$ ($C_{14}H_{22}NO_3$)	*iso1/2* activation	---	No

4	6.03	267.17060	$C_{14}H_{23}N_2O_3$	*iso1/2* activation	Myxofacycline F **6**	No
5	6.15	256.15481	$C_{13}H_{22}NO_4$	*iso9* disruption	Myxofacycline G1 **7a**	Yes
6	6.43	253.1553	$C_{13}H_{20}N_2O_3$	*iso9* disruption	Myxofacycline E1 **5a**	Yes
7	6.70	284.18599 (266.17454)	$C_{15}H_{26}NO_4$ ($C_{15}H_{24}NO_3$)	*iso1/2* activation	Myxofacycline G **7**	No
8	6.93	281.18557	$C_{21}H_{25}N_2O_3$	*iso1/2* activation	Myxofacycline E **5**	No
9	7.29	266.17542	$C_{15}H_{24}NO_3$	*iso1/2* activation	--	No
10	7.31	228.19573	$C_{13}H_{26}NO_2$	*iso1/2* activation	---	No
11	7.61	325.21214	$C_{17}H_{29}N2O_4$	*iso1/2* activation	---	No
12	7.63	518.2861	$C_{27}H_{40}N_3O_7$	*iso9* disruption	C_2H_4- precursor of No.14	Yes
13	8.04	546.3182	$C_{29}H_{44}N_3O_7$	*iso1/2* activation	---	No
14	8.52	270.17027 (252.15920)	$C_{14}H_{24}NO_4$ ($C_{14}H_{22}NO_3$)	*iso1/2* activation	---	No
15	8.80	256.15382	$C_{13}H_{22}NO_4$	*iso9* disruption	Myxofacycline D1 **4a**	Yes
16	9.37	284.18612 (266.17462) (248.16495)	$C_{15}H_{26}NO_4$ $C_{15}H_{24}NO_3$ $C_{15}H_{22}NO_2$	*iso1/2* activation	Myxofacycline D **4**	No
17	9.57	282.1706	$C_{15}H_{24}NO_4$	*iso1/2* activation	---	No
18	9.91	268.19042	$C_{15}H_{26}NO_3$	*iso1/2* activation	---	No
19	10.24	254.13901	$C_{13}H_{20}NO_4$	*iso9* disruption	Myxofacycline C1 **3a**	Yes
20	10.35	226.14361	$C_{12}H_{20}NO_3$	*iso9* disruption	Myxofacycline B1 **2a**	Yes
21	10.88	282.17043 (264.15929)	$C_{15}H_{24}NO_4$ ($C_{15}H_{22}NO_3$)	*iso1/2* activation	Myxofacycline C **3**	No
22	11.01	254.17528	$C_{14}H_{24}NO_3$	*iso1/2* activation	---	No
23	11.11	254.17555	$C_{14}H_{24}NO_3$	*iso1/2* activation	Myxofacycline B **2**	No
24	11.18	240.15910	$C_{13}H_{22}NO_3$	*iso9* disruption	Myxofacycline A1 **1a**	No
25	11.33	266.12050	$C_{17}H_{16}NO_2$	*iso1/2* activation	---	Yes
26	11.80	268.19192	$C_{15}H_{26}NO_3$	*iso1/2* activation	---	
27	11.91	268.19192	$C_{15}H_{26}NO_3$	Initial target compound	Myxofacycline A **1**	No
28	12.03	266.1757	$C_{15}H_{24}NO_3$	*iso1/2* activation	Myxofacycline A double bond derivative?	No

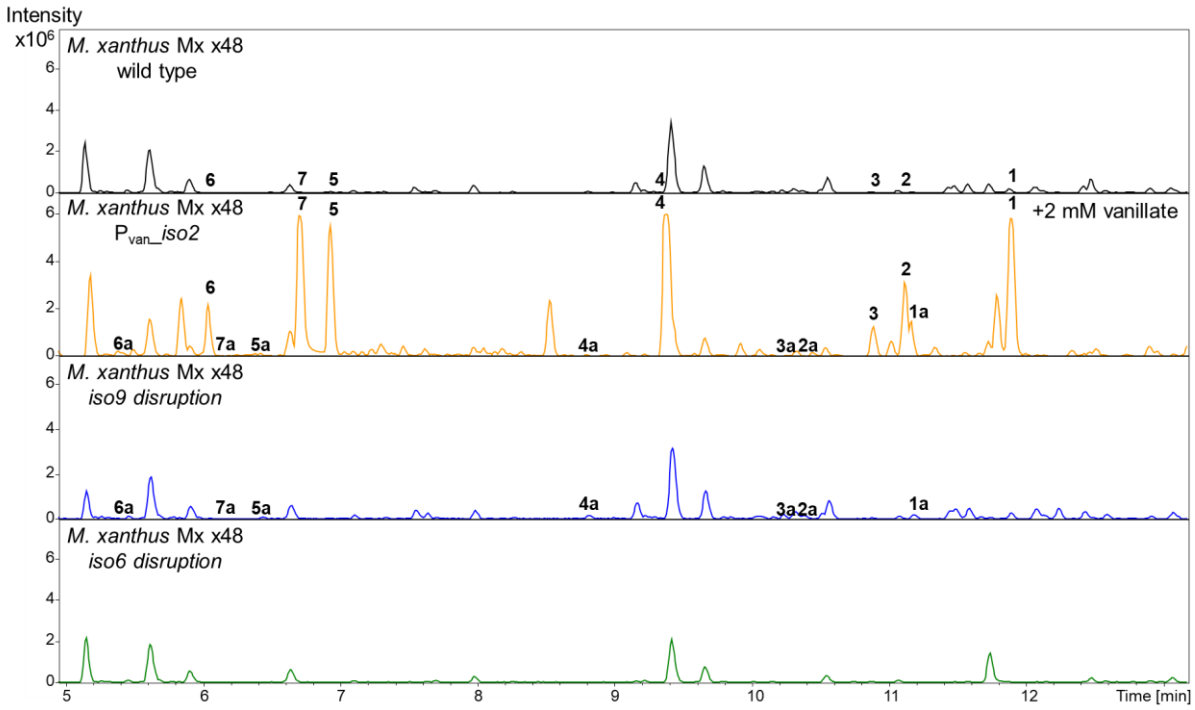

Figure S18. High-performance liquid chromatography-mass spectrometry base peak chromatogram (HPLC-MS BPC) of crude extracts of *M. xanthus* Mx x48 wild type (**A**), *M. xanthus* Mx x48 P_{van}*_iso2* supplemented with 2mM vanillate (**B**), *M. xanthus* Mx x48 *iso9* disruption mutant (**C**) and *M. xanthus* Mx x48 *iso6* disruption mutant representative for the gene disruption mutants *iso1–6*. Although *iso1* seems not to be essential for the production of the myxofacyclines (**see Figure S19**), the production of all myxofacyclines were abolished probably due to the disruption of the genetic operon and its expression.

2.7 Heterologous expression of the myxofacycline biosynthetic gene cluster in the heterologous host *M. xanthus* DK1622

Mobilization genetic modification of the myxofacycline BGC originating from *Stigmatella aurantiaca* Sg a32

Cosmid library construction of the myxobacterial strain *S. aurantiaca* Sg a32 was conducted by Explogen LLC (EXG) (https://explogen.com.ua/about/) according a previously established procedure[41]. The plasmid backbone pCos15AtetMx8-For-31/37 was used to generate this cosmid library. End-sequencing of the generated cosmid library (with the Sequencing primer pair No.37/38) revealed that the *E. coli* transformant on position E06 of the 96-well plate No. 13 harbors the whole myxofacycline BGC. Since the respective cosmid contains not only the biosynthetic operon *iso1–9* but also five full additional genes upstream and two additional genes downstream two sequential genetic modifications were conducted, in order to narrow down the necessary genes for the formation of the myxofacyclines. Both steps are based on Red αβ recombineering[9,13], which enables via homologous recombination not only efficient introduction of genetic constructs but also deletions on the vector backbone. The first modification was designed to replace the five additional genes upstream of *iso1 or iso2* and

replace this region at the same time with the vanillate-inducible promoter system including the kanamycin resistance gene *kanR*. (**Table S6**, genetic constructs 10 and 11). The second modification removes in a similar manner the two superfluous genes downstream of *iso9* and also the vector backbone genes *leu2 (*yeast selection marker), the p15A origin of replication, and the two antibiotic selection markers *cat* (confers chloramphenicol resistance) and *tetR* (confers tetracycline resistance). Simultaneously the selection marker *ampR* (confers resistance towards ampicillin) and the origin from pBR322 has been introduced to the vector backbone (**Table S6**, genetic constructs 12 and 13).

Transfer and chromosomal integration of the constructs into the host *M. xanthus* Mx x48

The heterologous host *M. xanthus* DK1622 was transformed with the generated constructs harboring the full myxofacycline BGC (Genetic constructs 10–13 (**Table S6**) and plasmid No.4 (**Table S4**) according the same procedure as described above. *M. xanthus* DK1622 transformants were selected by adding the respective required antibiotic (kanamycin (working concentration: 50 µg/mL), ampicillin (working concentration: 100 µg/mL tetracycline (working concentration: 10 µg/mL to the fermentation culture. Correct chromosomal integration of the expression constructs (via homologous recombination into the mx8 attachment site was confirmed by PCR as described elsewhere[7] (**Table S6,** primer No.39–42). PCRs and Genomic DNA purification of the respective mutants were performed according to the settings described above.

The four generated genetic constructs facilitates the associated mutant strains to produce all previously identified myxofacyclines. Interestingly, there was no significant difference in the production profile between the generated heterologous expression platforms. The generated mutant *M. xanthus* DK1622 harboring the non-engineered cosmid containing the myxofacycline BGC from *Stigmatella aurantiaca* Sg a32 did not lead to any observable production of associated natural products. (**Figure S19**)

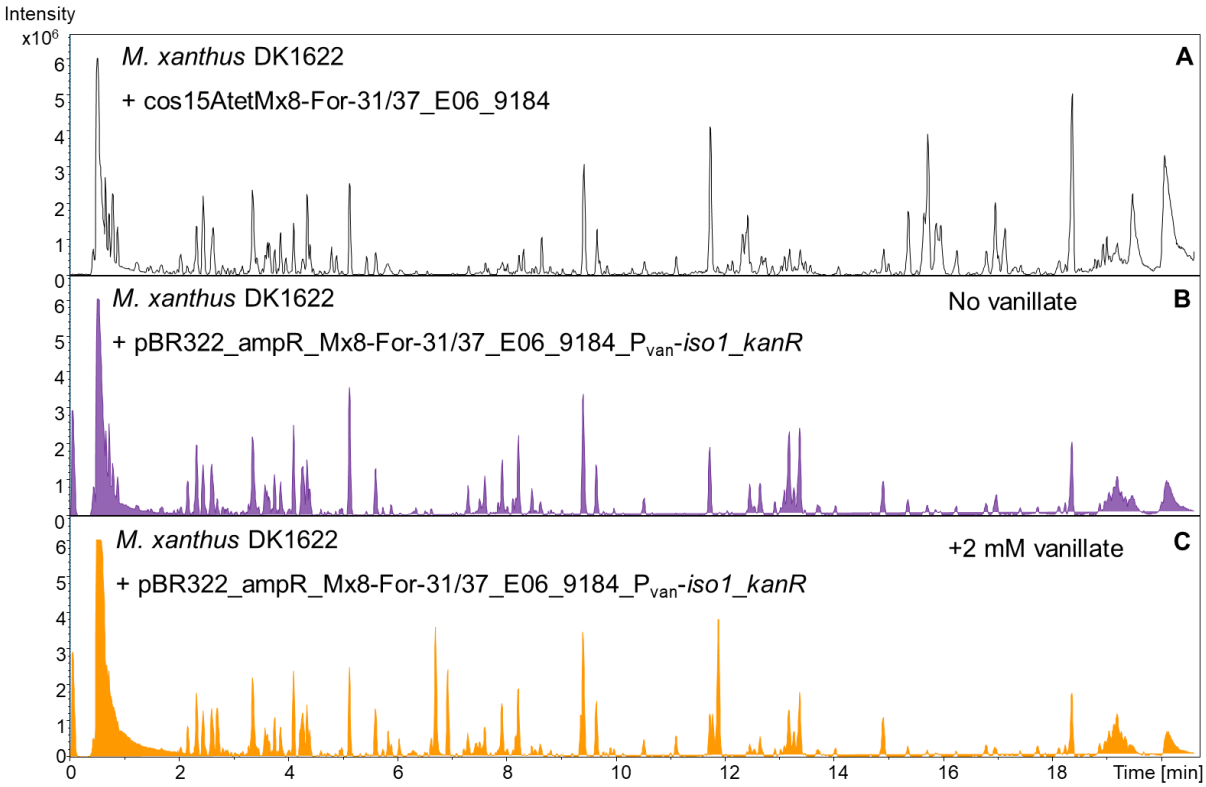

Figure S19. Heterologous production of myxofayclines. Heterologous expression of the genetic operon *iso1–9* based on the non-engineered cosmid expression vector resulted in no production of myxofacyclines (**A**), whereas the engineered cosmid including an inserted vanillate-inducible promoter in front of iso1 or iso2 (iso2 not shown) revealed the production of all previously identified myxofacyclines with and without supplementation of 2 mM vanillate (B and C).

2.7 Biological function of myxofacyclines

Cell based bioactivity profiling

Antimicrobial assay

Standard sterile microbiological techniques were maintained throughout. All microorganisms were handled according to standard procedures and were obtained from the German Collection of Microorganisms and Cell Cultures (Deutsche Sammlung für Mikroorganismen und Zellkulturen, DSMZ) or were part of our internal strain collection. Myxofacyclines were tested in microbroth dilution assays on the following panel of microorganisms: *Escherichia coli* DSM-1116, *E. coli* JW0451-2 (*acrB*-efflux pump deletion mutant of *E. coli* BW25113), *Pseudomonas aeruginosa* PA14, *Bacillus subtilis* DSM-10, *Mycobacterium smegmatis* mc2-155, *Staphylococcus aureus* Newman, *Candida albicans* DSM-1665, *Citrobacter freundii* DSM 30039, *Pichia anomala* DSM-6766 and *Acinetobacter baumannii* DSM30007. For microdilution assays, overnight cultures were prepared from cryo-preserved cultures and were diluted to achieve a final inoculum of 10^4–10^5 cfu/mL. Serial dilutions of compounds were prepared in

sterile 96-well plates in the respective test medium. The cell suspension was added and microorganism were grown for 18–48 h at either 30 °C or 37 °C. Growth inhibition was evaluated by visual inspection and given minimum inhibitory concentration (MIC) values are the lowest concentration of antibiotic at which no visible growth was observed. The MIC of myxofacycline A against *Mucor hiemalis* DSM2656 was observed at 32 µg/mL. No inhibition of one of the above-mentioned tested microorganisms was observed at concentration up to 64 µg/mL for myxofacyclines B–G.

Cytotoxic activity

Cell lines were obtained from the German Collection of Microorganisms and Cell Cultures (Deutsche Sammlung für Mikroorganismen und Zellkulturen, DSMZ) or were part of our internal collection and were cultured under conditions recommended by the depositor. HCT-116 (human colon carcinoma cell line, DSMZ No. ACC 581) and KB-3-1 (cervix carcinoma cell line, DSMZ No. ACC 158) cells were seeded at 6 x 10^3 cells per well of 96-well plates in 180 µL complete medium and treated with myxofacycline in serial dilution after 2 h equilibration. After 5 days incubation, 20 µL of 5 mg/mL MTT (thiazolyl blue tetrazolium bromide) in phosphate buffered saline (PBS) was added per well and it was further incubated for 2 h at 37°C. The medium was discarded and cells were washed with 100 µL PBS before adding 100 µL isopropanol/10 N HCl (250:1) in order to dissolve formazan granules. The absorbance at 570 nm was measured using a microplate reader (Tecan Infinite M200Pro), and cell viability was expressed as percentage relative to the respective MeOH control. IC_{50} values were determined by sigmoidal curve fitting. The IC_{50} of myxofacycline A against KB-3-1 cells was determined to 24.06 µg/mL. None of the tested myxofacyclines B–G showed cytotoxic bioactivity up to a concentration of 37 µg/mL.

2.8 ^{1}H and ^{13}C NMR spectra of myxofacyclines

NMR data myxofacycline A

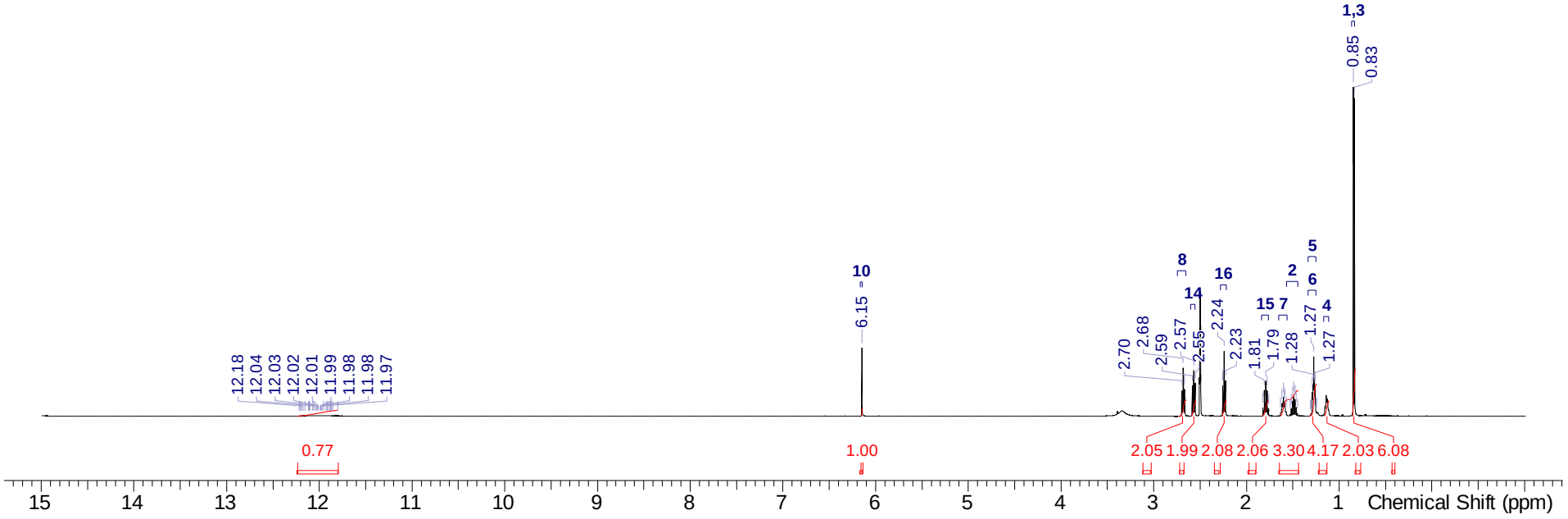

Figure S20. ^{1}H NMR spectrum myxofacycline A acquired in DMSO-*d6* at 500 MHz.

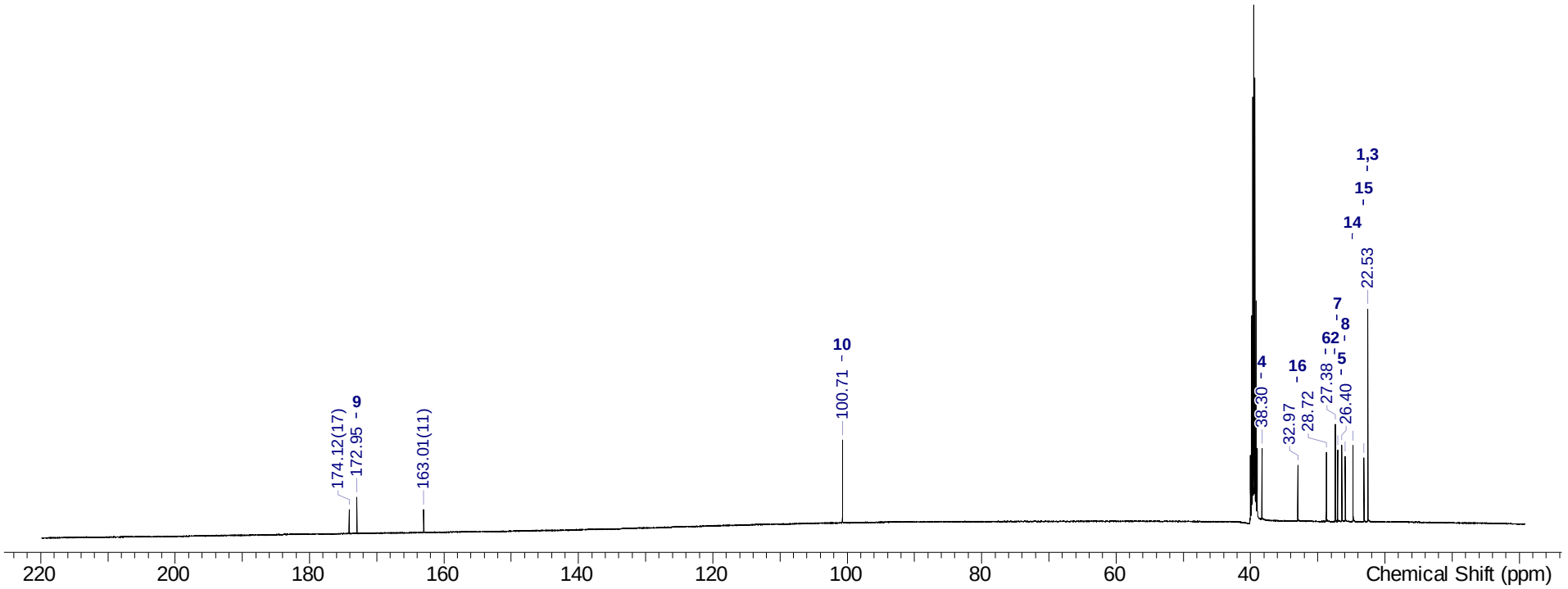

Figure S21. ^{13}C NMR spectrum myxofacycline A acquired in DMSO *d6* at 125 MHz.

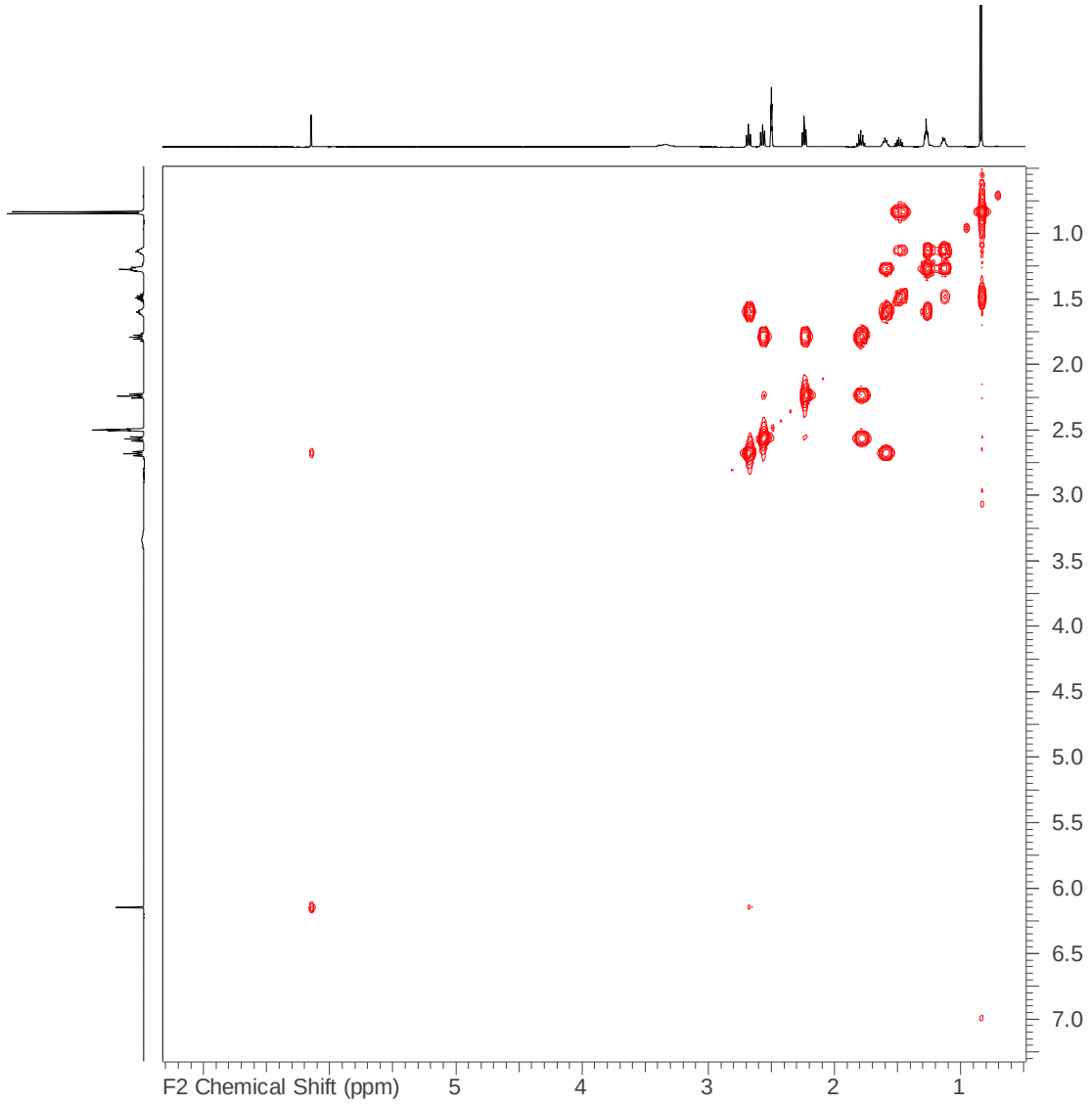

Figure S22. H-H COSY spectrum myxofacycline A acquired in DMSO d6 at 500 MHz.

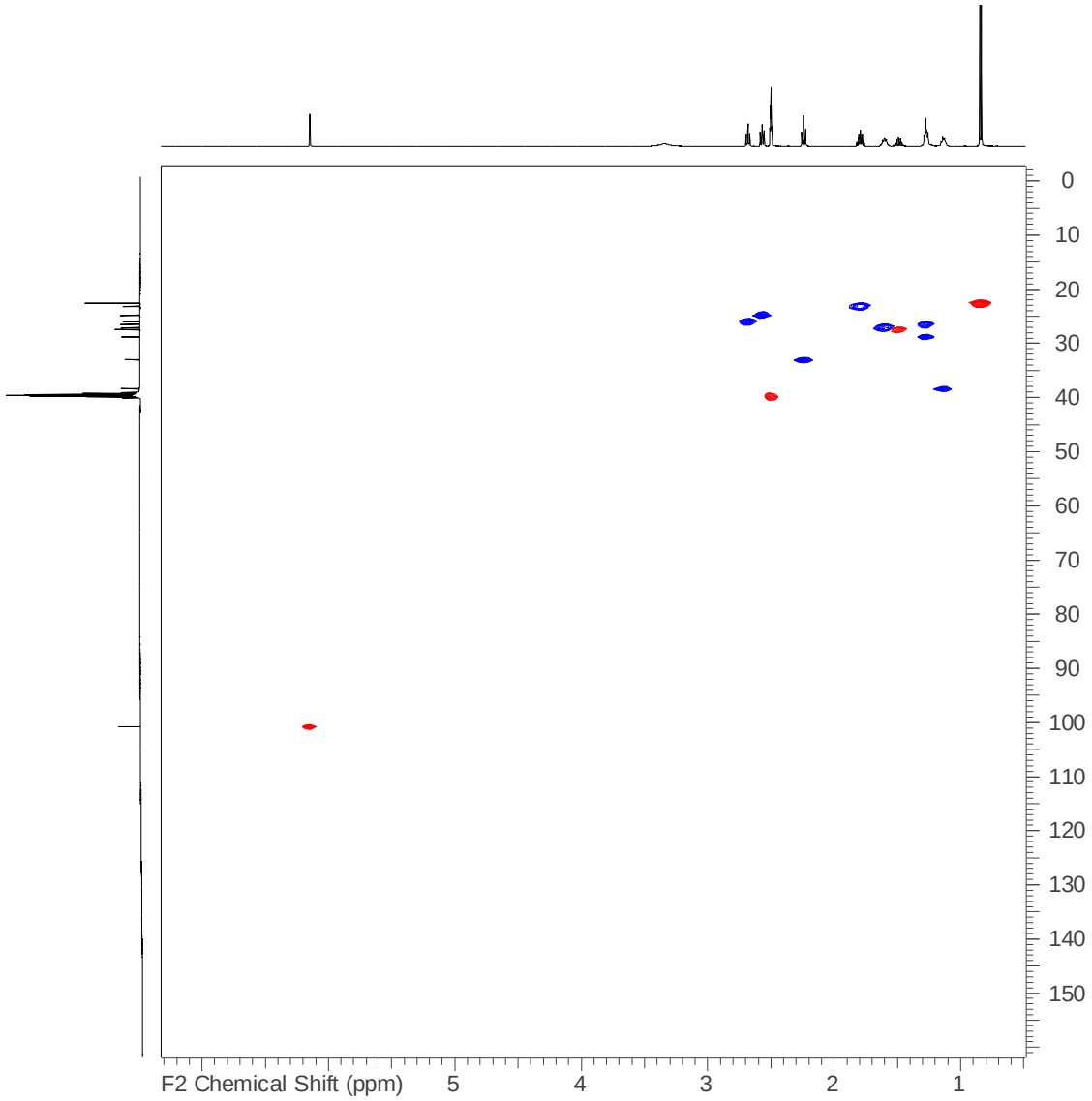

Figure S23. HSQC spectrum of myxofacycline A acquired in DMSO d6 at 500/125 MHz.

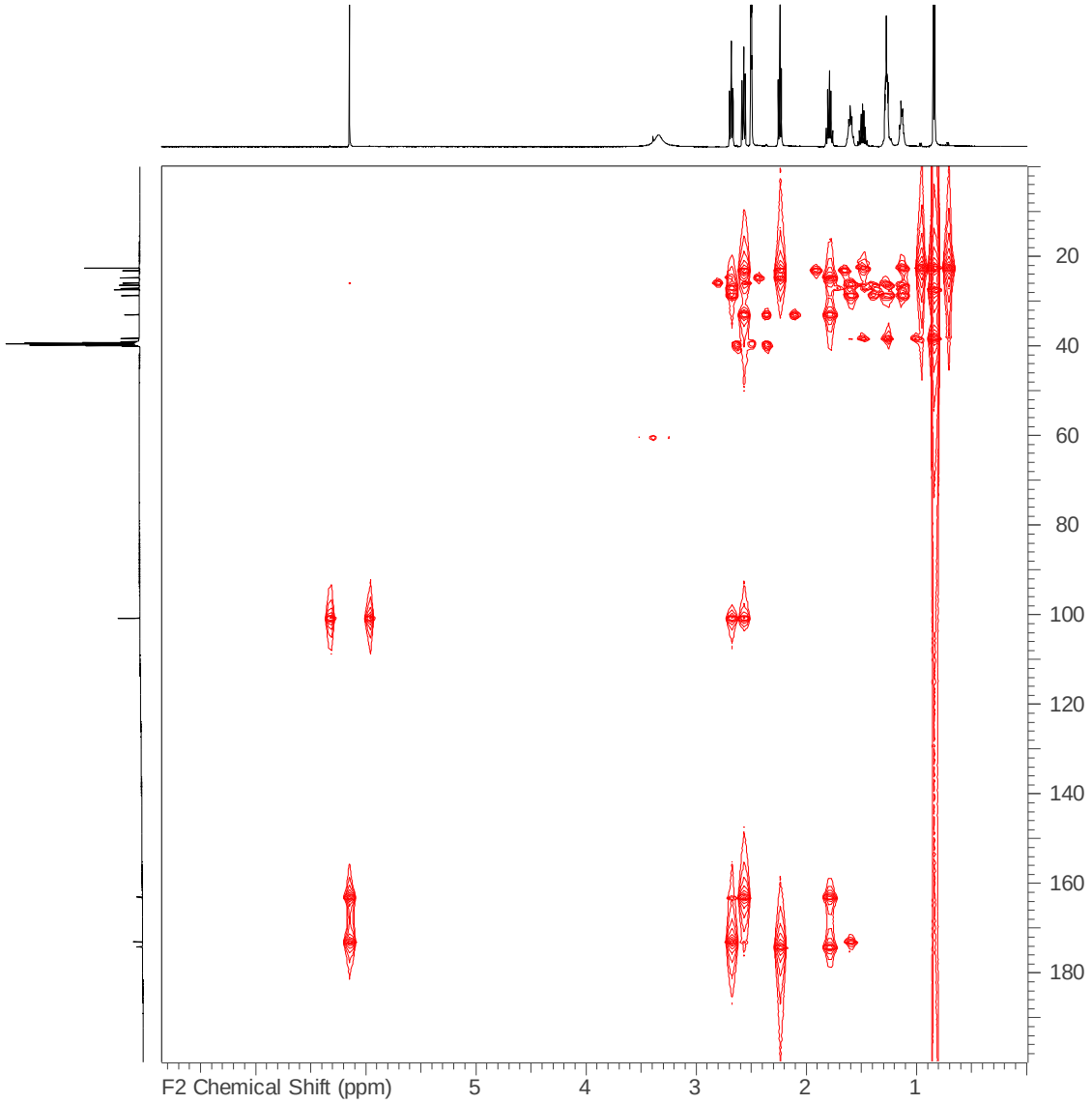

Figure S24. HMBC spectrum of myxofacycline A acquired in DMSO d6 at 500/125 MHz.

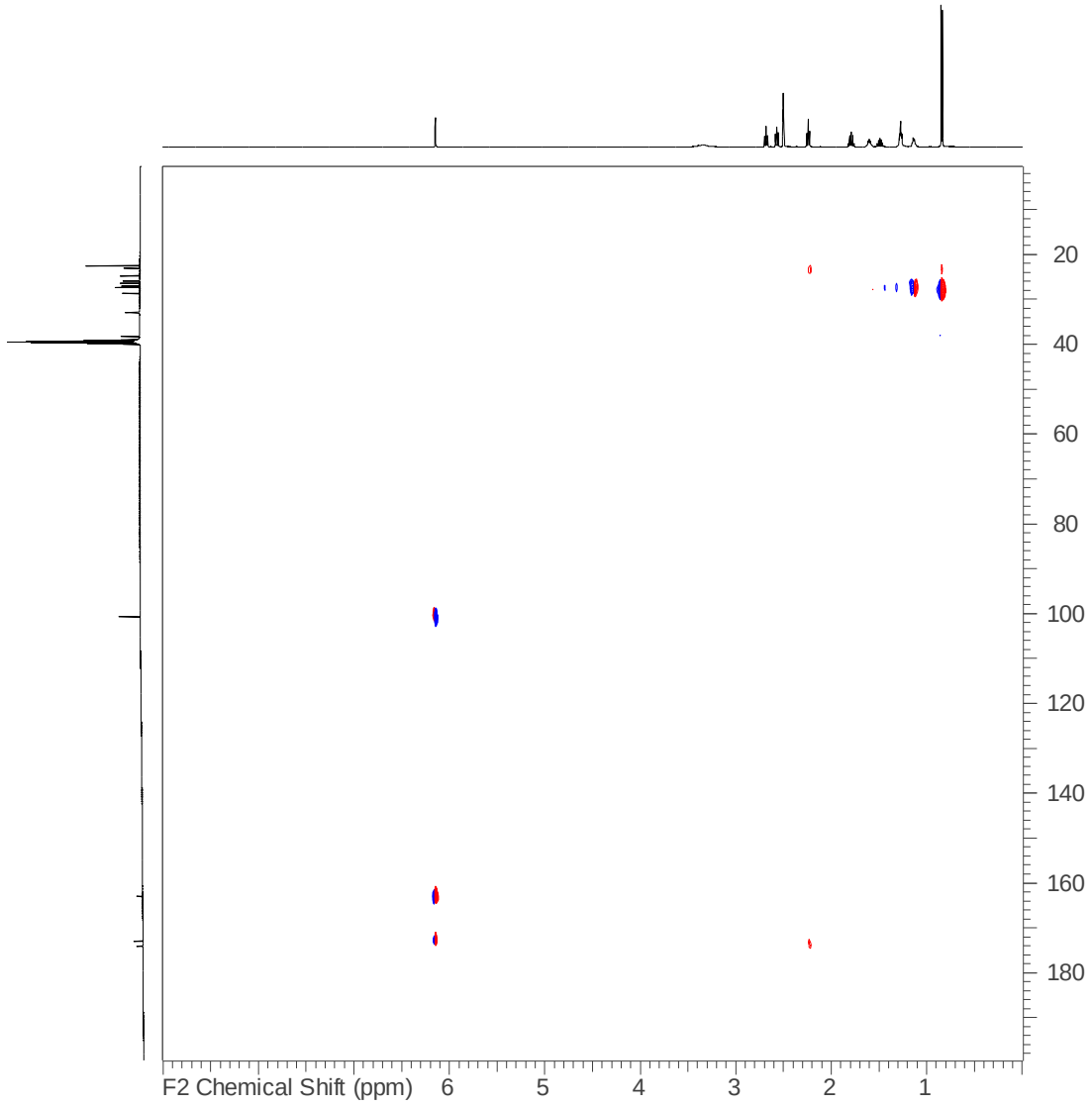

Figure S25. 1,1 ADEQUATE spectrum of myxofacycline A acquired in DMSO d6 at 700/175 MHz.

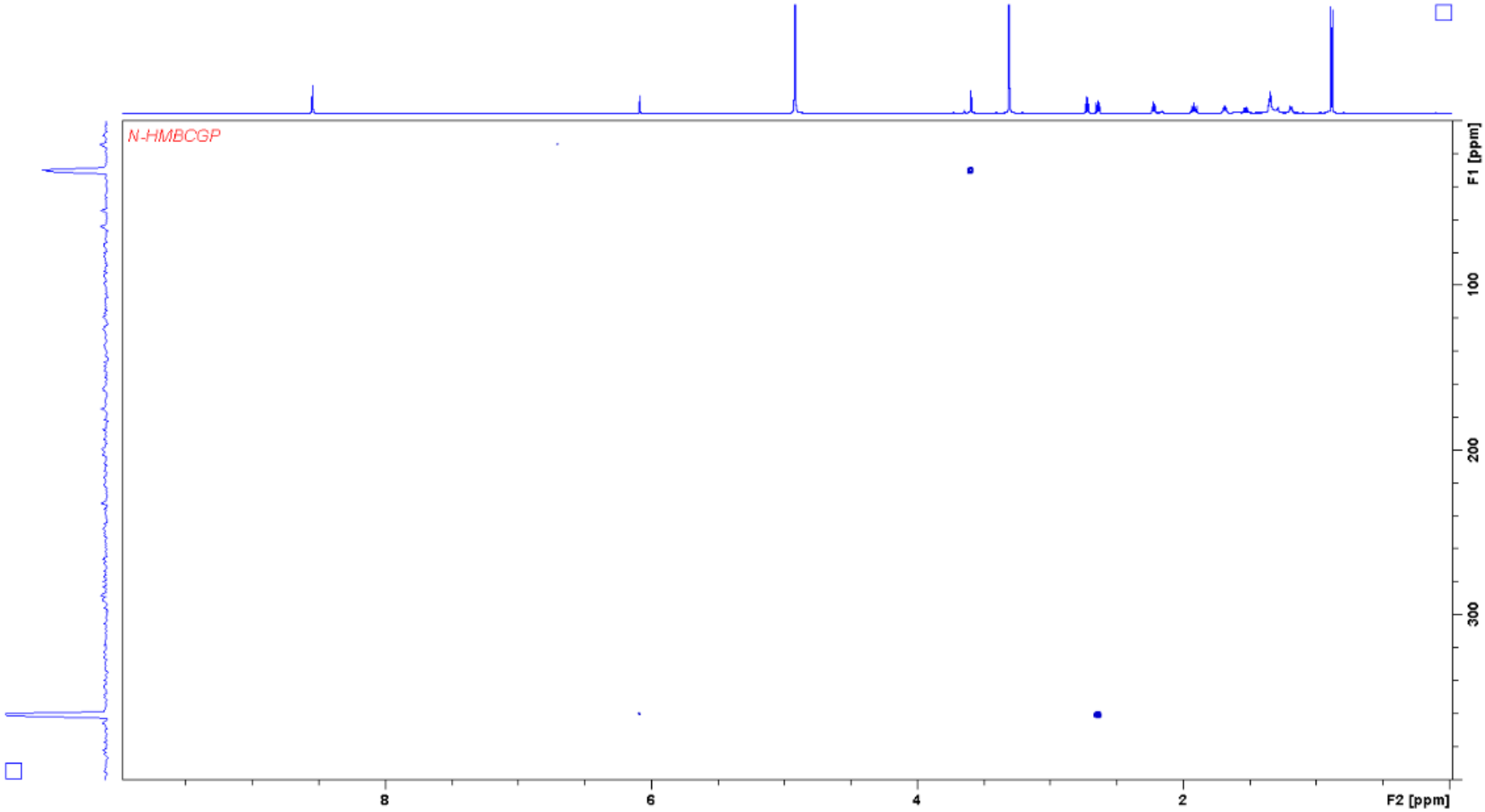

Figure S26. ^{15}N-HMBC spectrum of myxofacycline A acquired in MeOD d6 at 700/70 MHz.(Spectrum was acquired in MeOD; signal at δ_H3.8 δ_N 35 is an impurity).

NMR data myxofacycline B

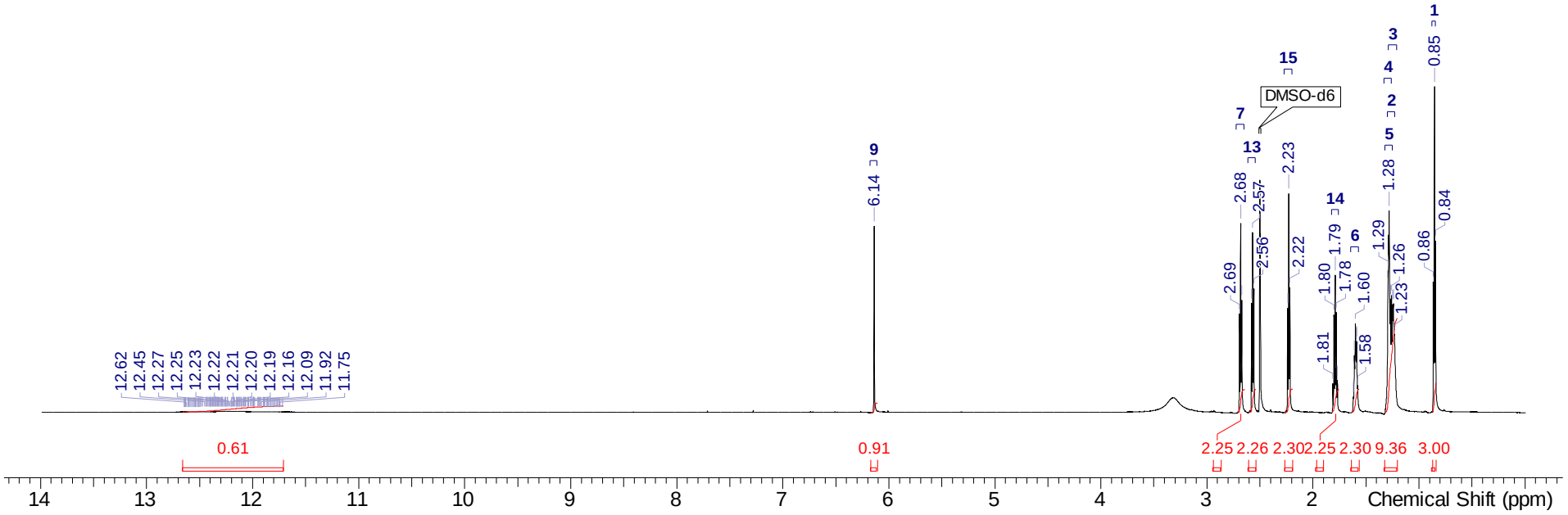

Figure S27. ^{1}H NMR spectrum myxofacycline B acquired in DMSO d6 at 700 MHz.

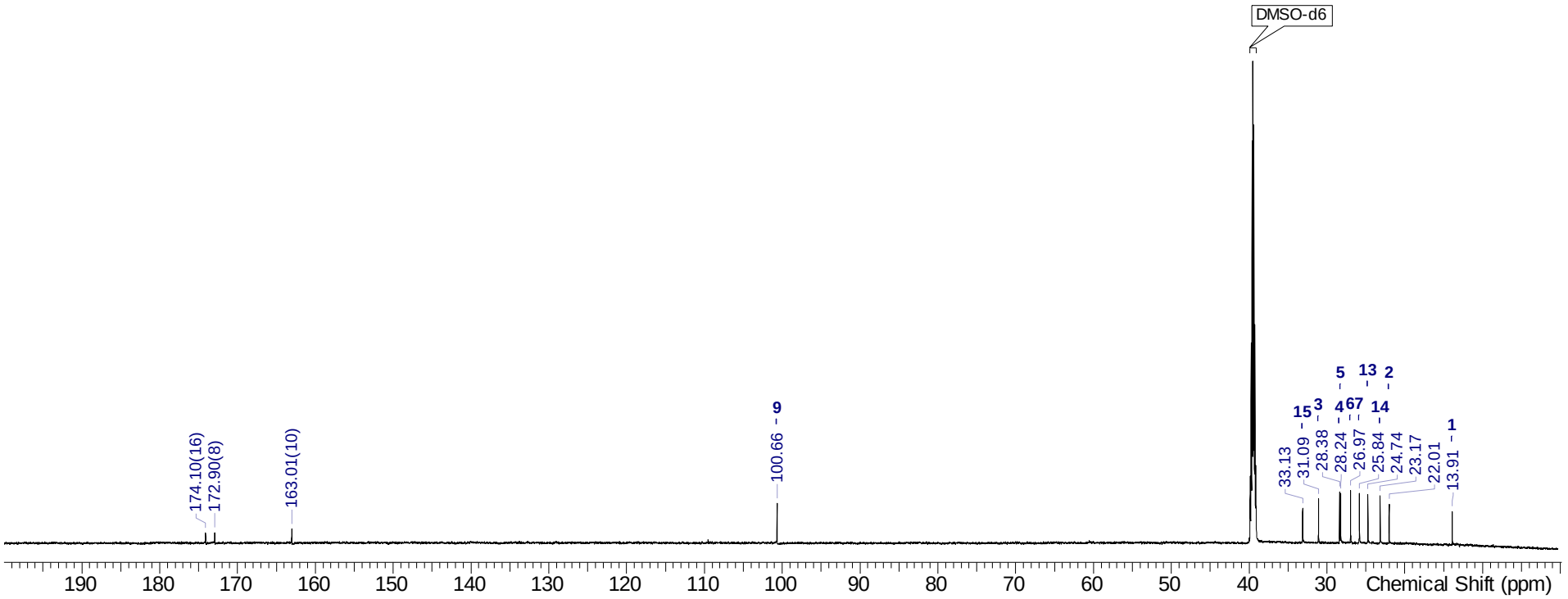

Figure S28. ^{13}C NMR spectrum myxofacycline B acquired in DMSO d6 at 175 MHz.

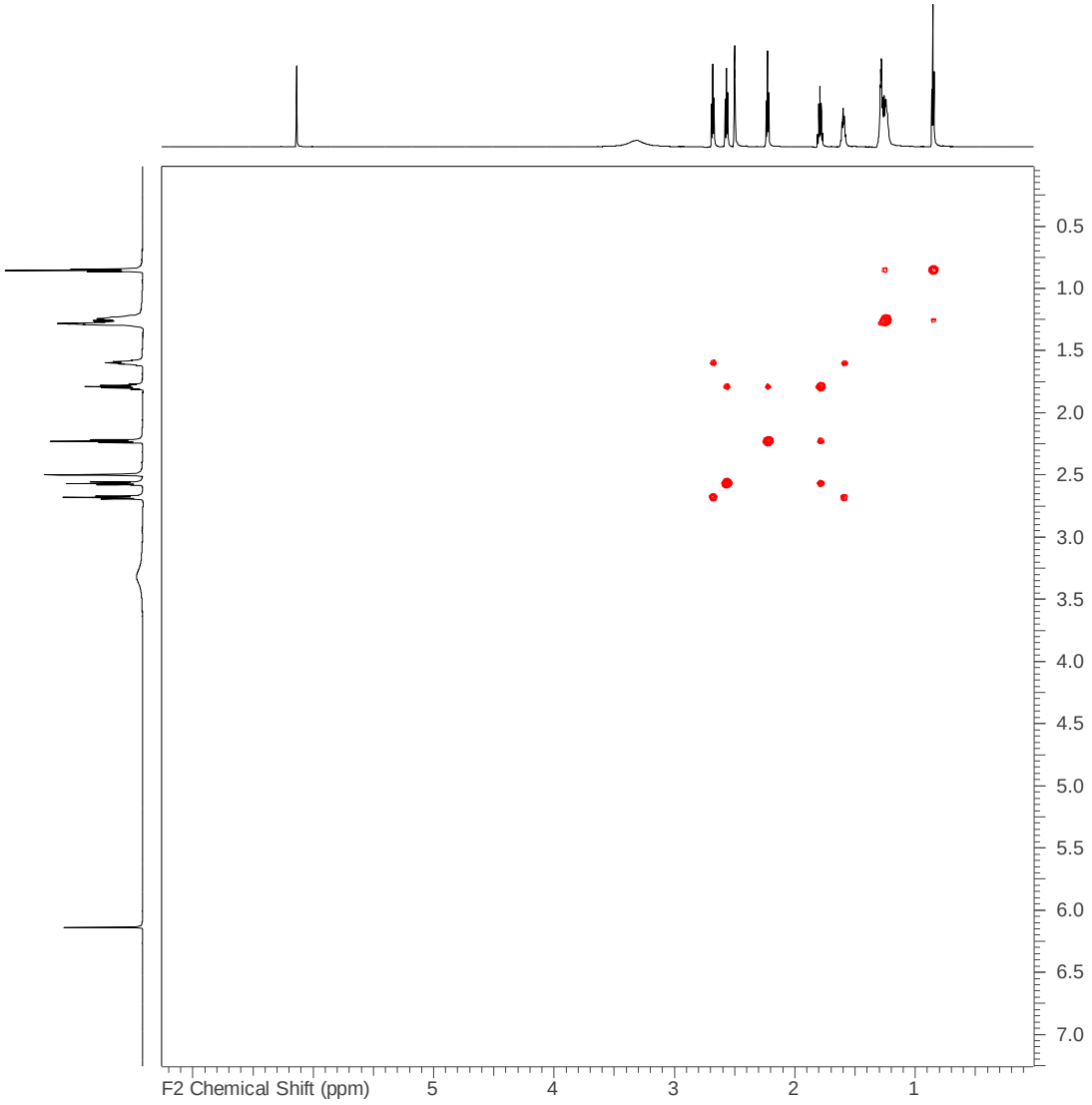

Figure S29. H-H COSY spectrum myxofacycline B acquired in DMSO d6 at 700 MHz.

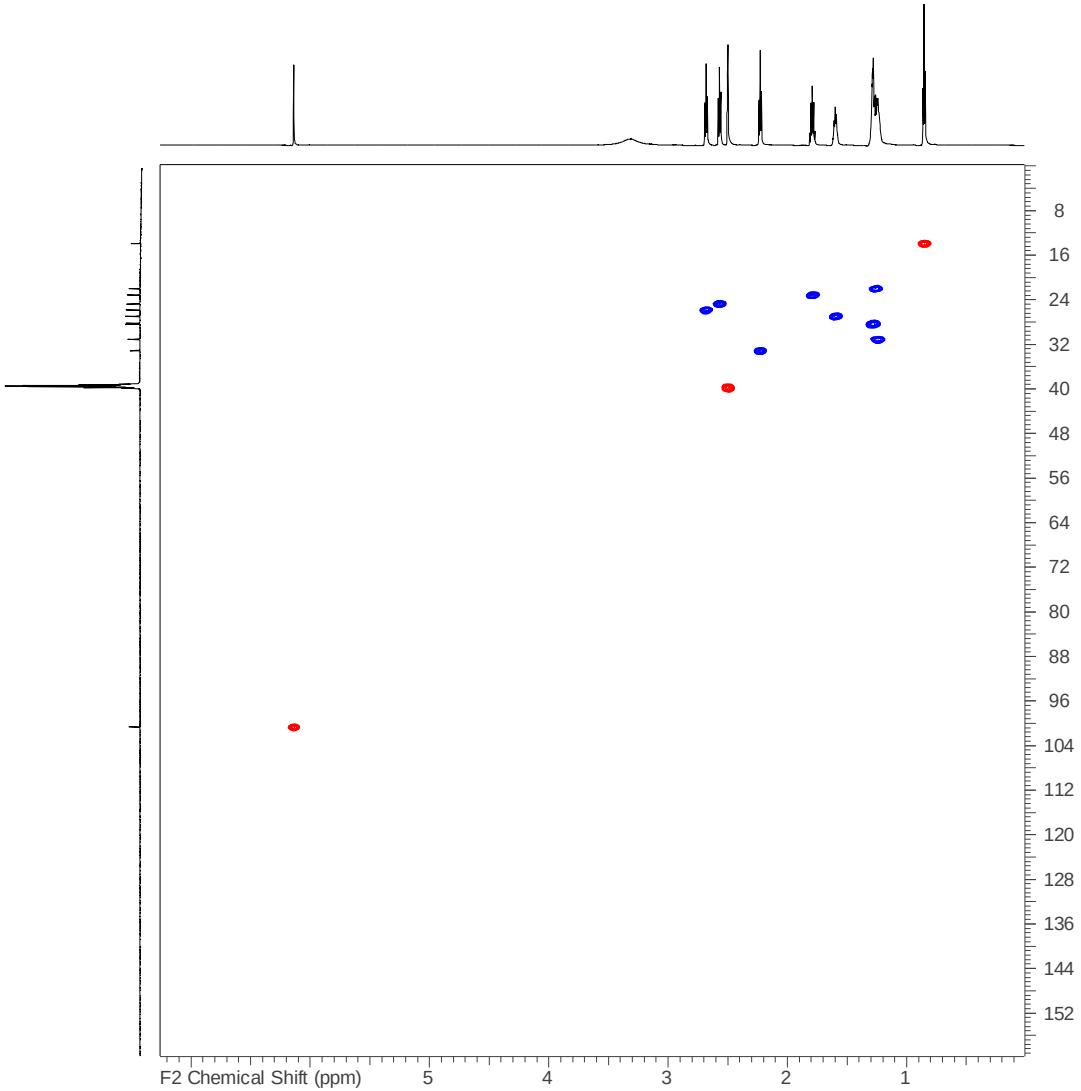

Figure S30. HSQC spectrum of myxofacycline B acquired in DMSO d6 at 700/175 MHz.

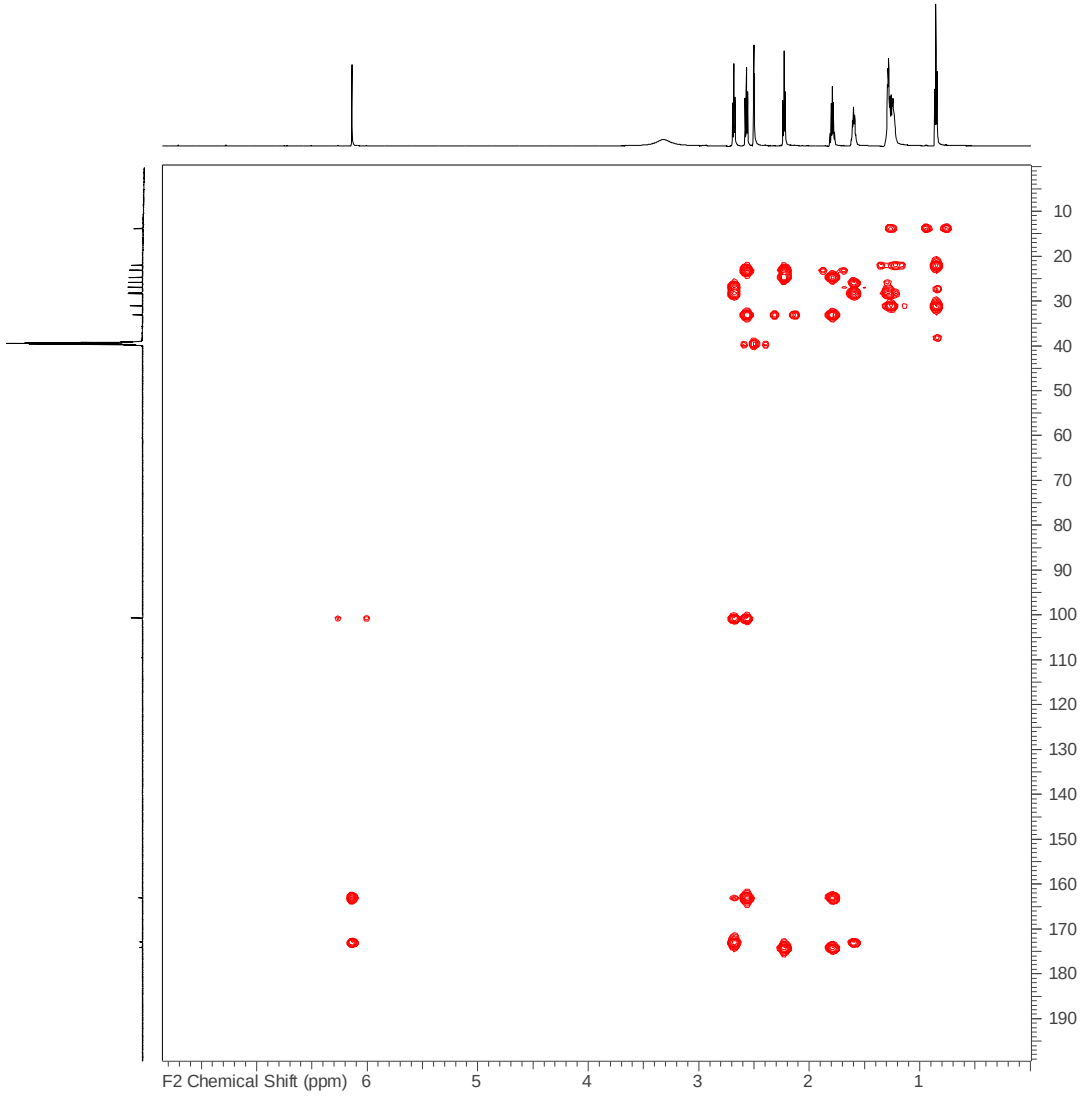

Figure S31. HMBC spectrum of myxofacycline B acquired in DMSO d6 at 700/175 MHz.

NMR data myxofacycline C

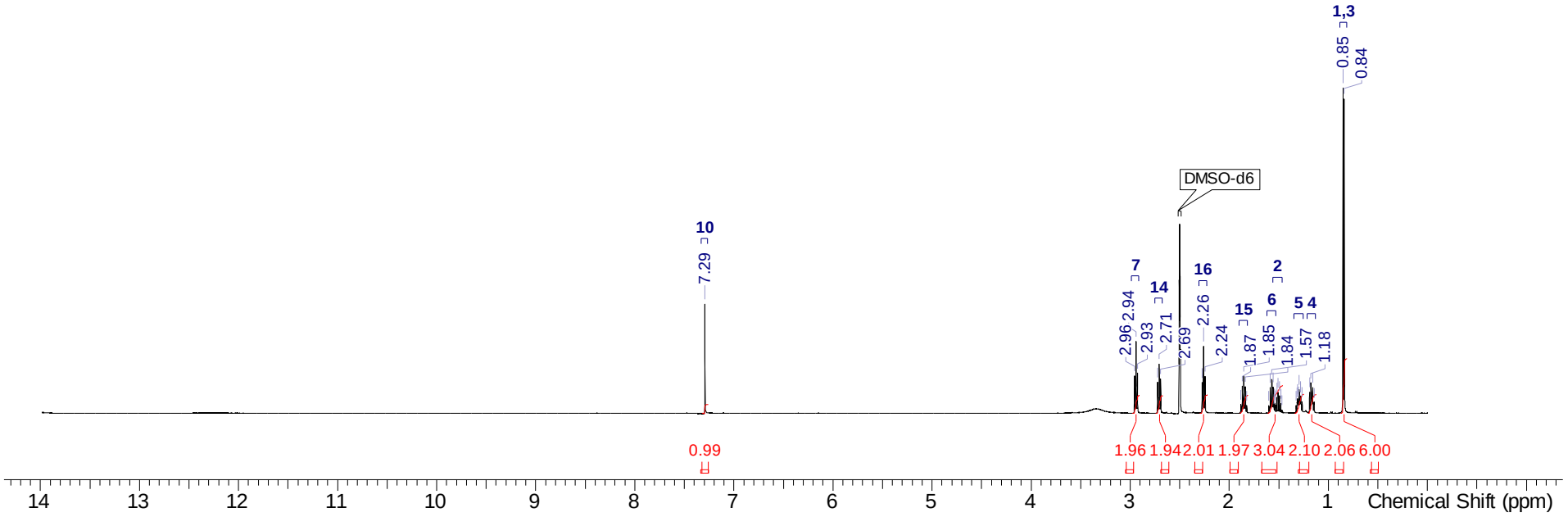

Figure S32. ^{1}H NMR spectrum myxofacycline C acquired in DMSO d6 at 500 MHz.

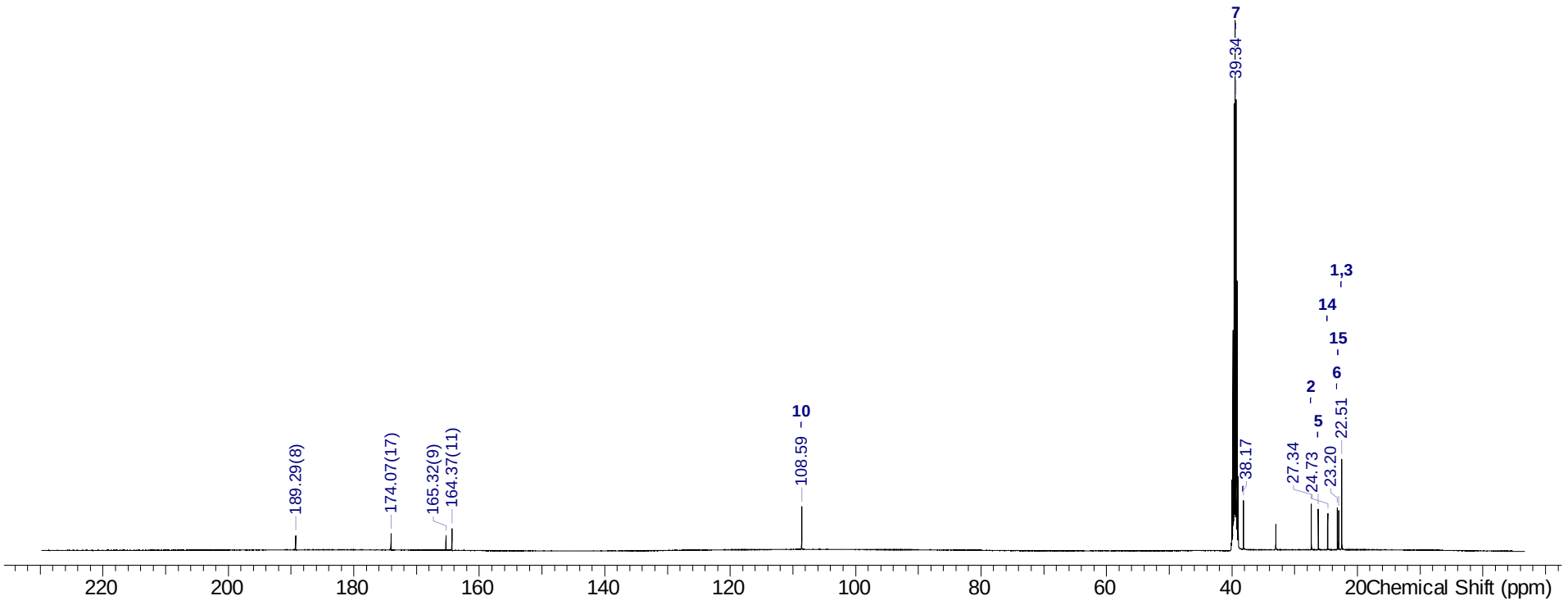

Figure S33. ^{13}C NMR spectrum myxofacycline C acquired in DMSO d6 at 125 MHz.

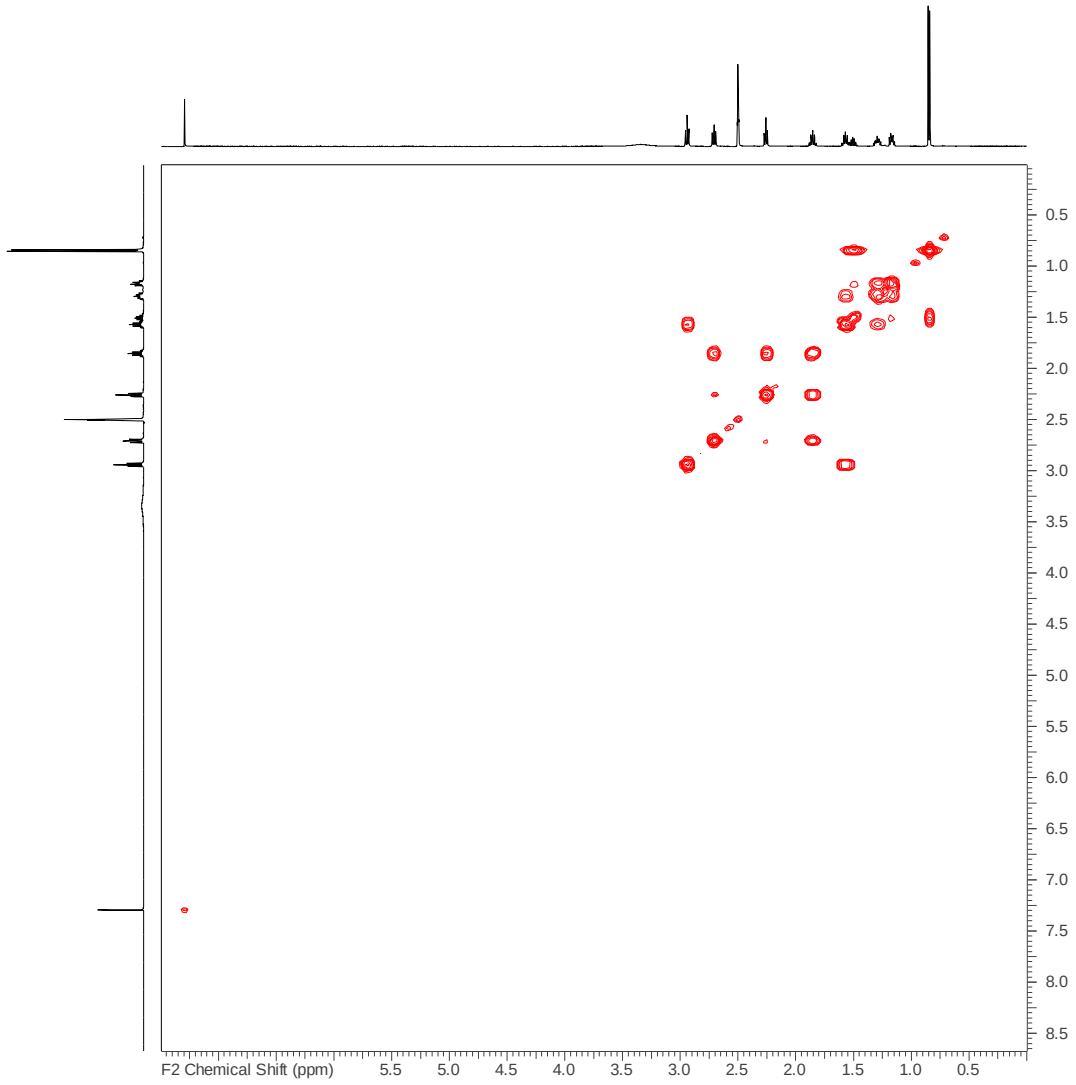

Figure S34. H-H COSY spectrum myxofacycline C acquired in DMSO d6 at 500 MHz.

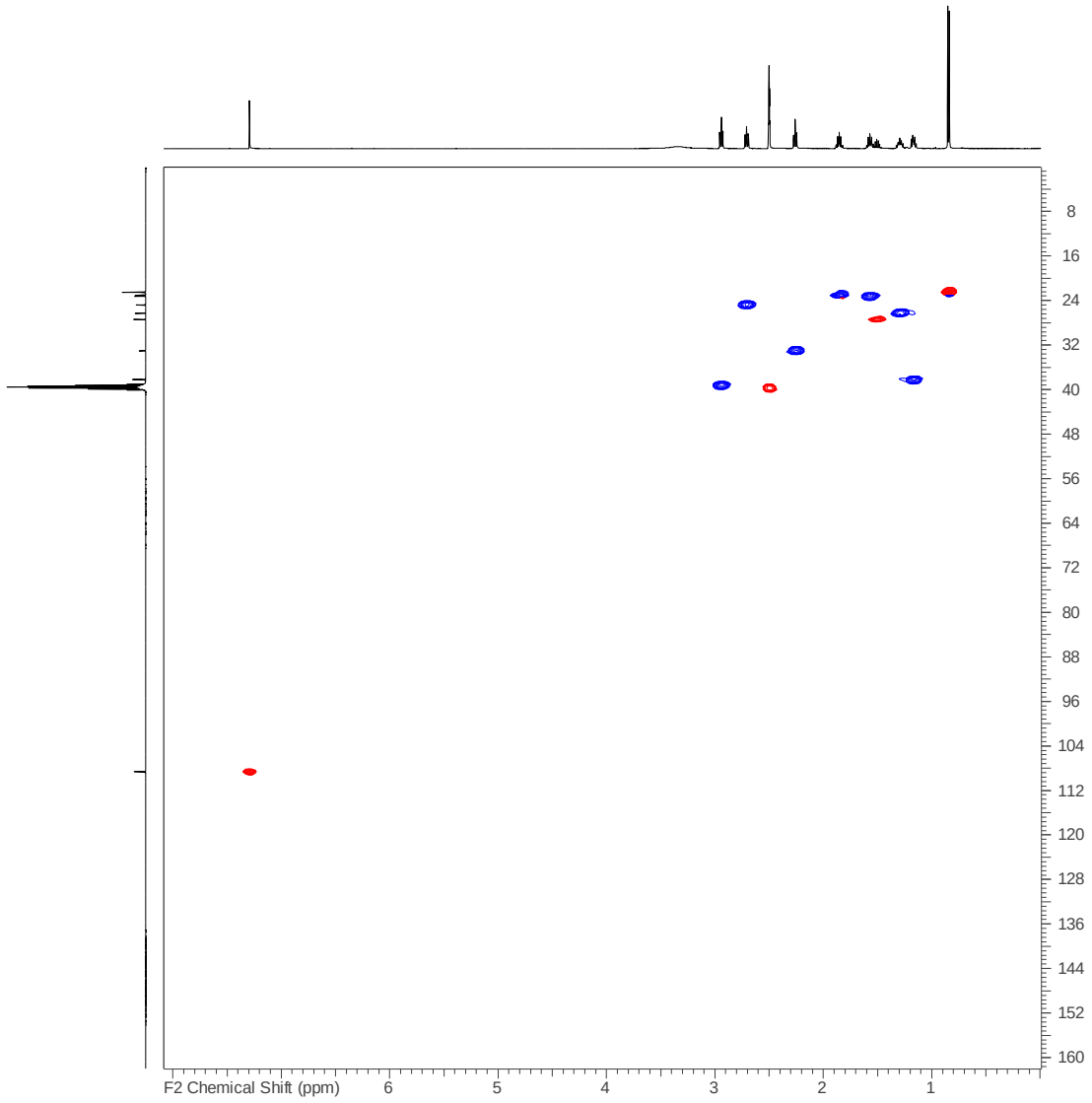

Figure S35. HSQC spectrum of myxofacycline C acquired in DMSO d6 at 500/125 MHz.

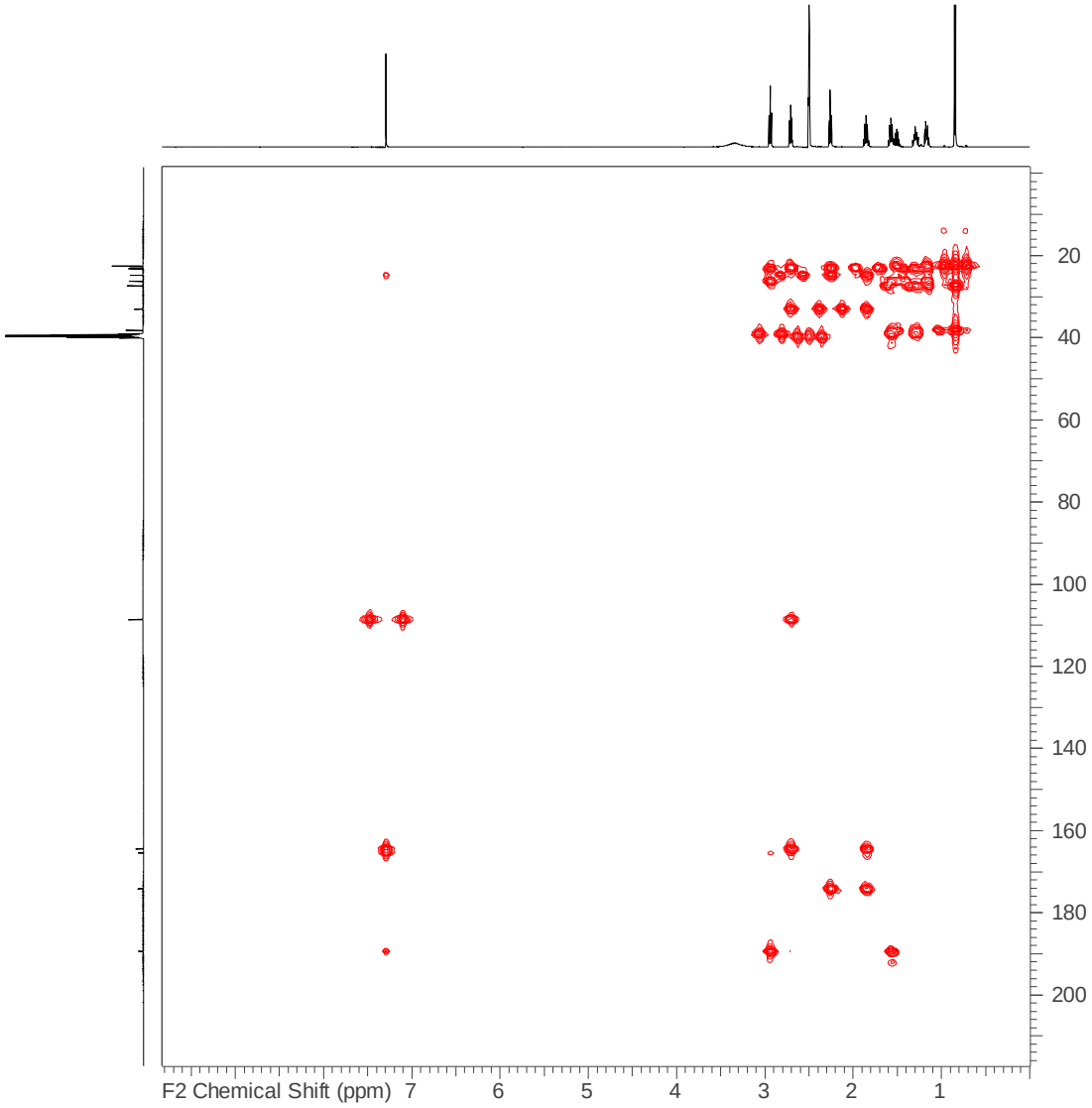

Figure S36. HMBC spectrum of myxofacycline C acquired in DMSO d6 at 500/125 MHz.

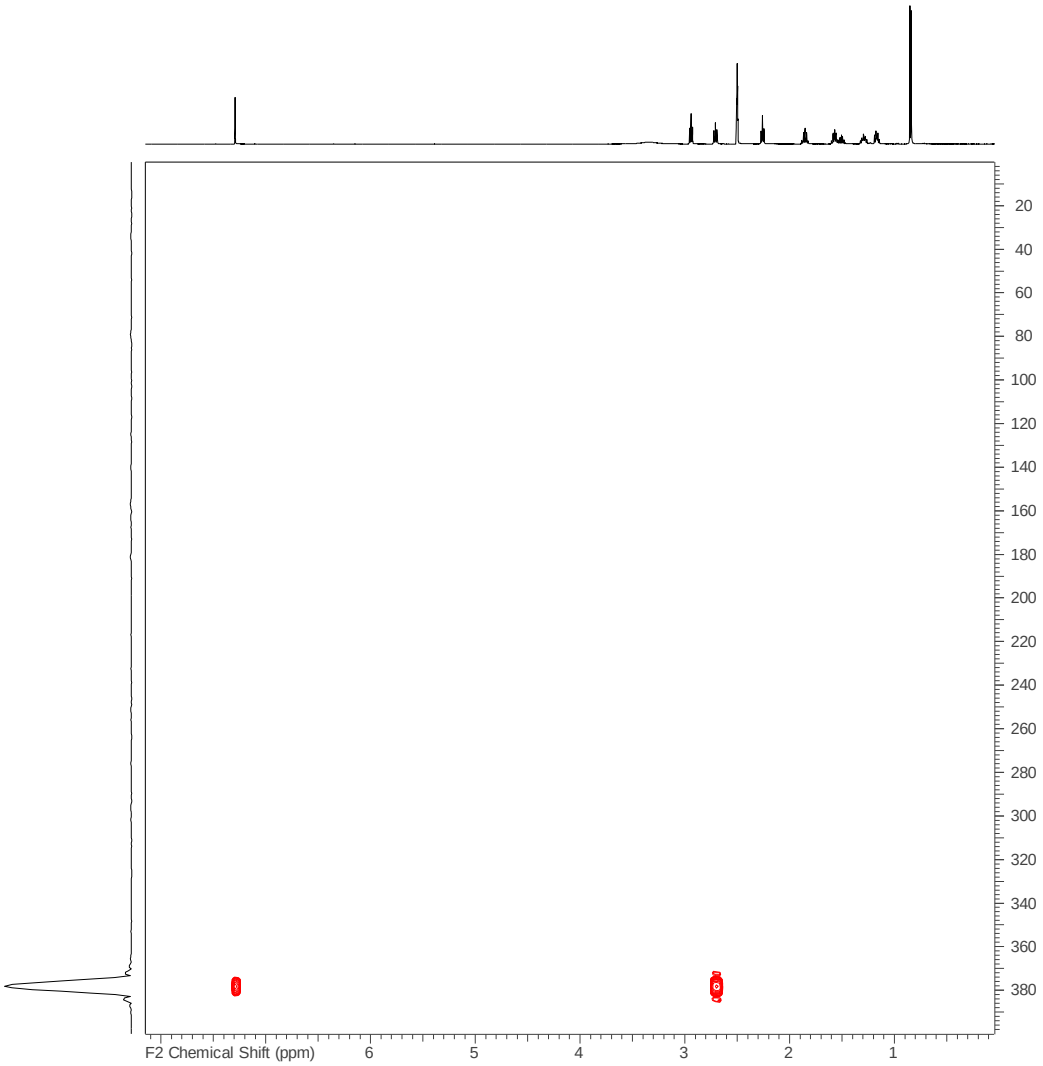

Figure S37. ^{15}N-HMBC spectrum of myxofacycline C acquired in DMSO d6 at 500/50 MHz.

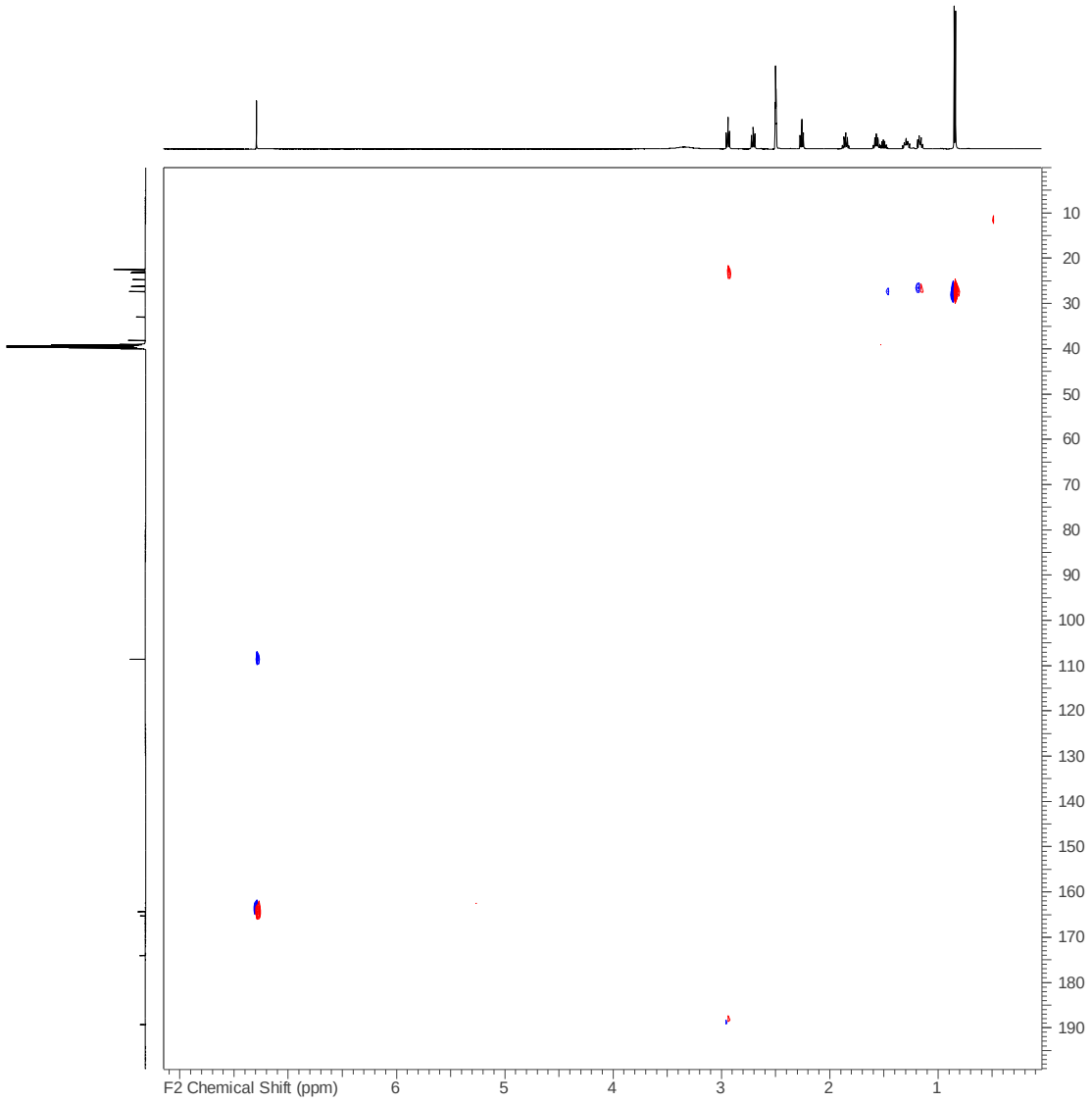

Figure S38. 1,1 ADEQUATE spectrum of myxofacycline C acquired in DMSO d6 at 700/175 MHz.

NMR data myxofacycline D

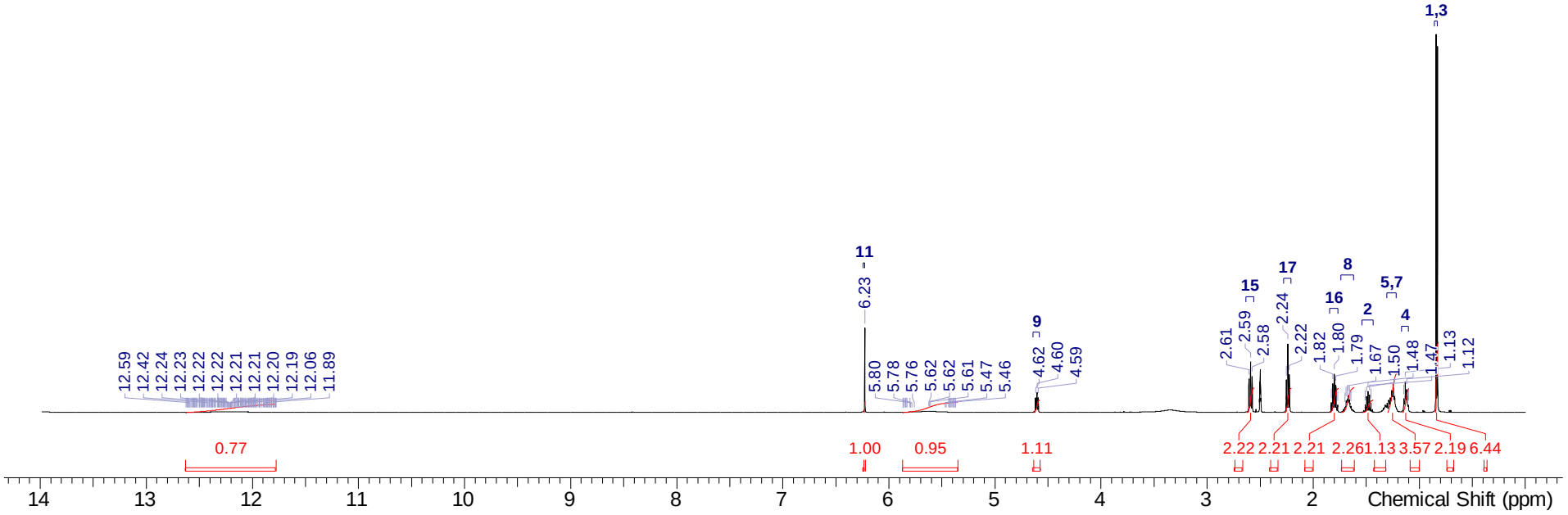

Figure S39. *^{1}H NMR* spectrum myxofacycline D acquired in DMSO d6 at 500 MHz.

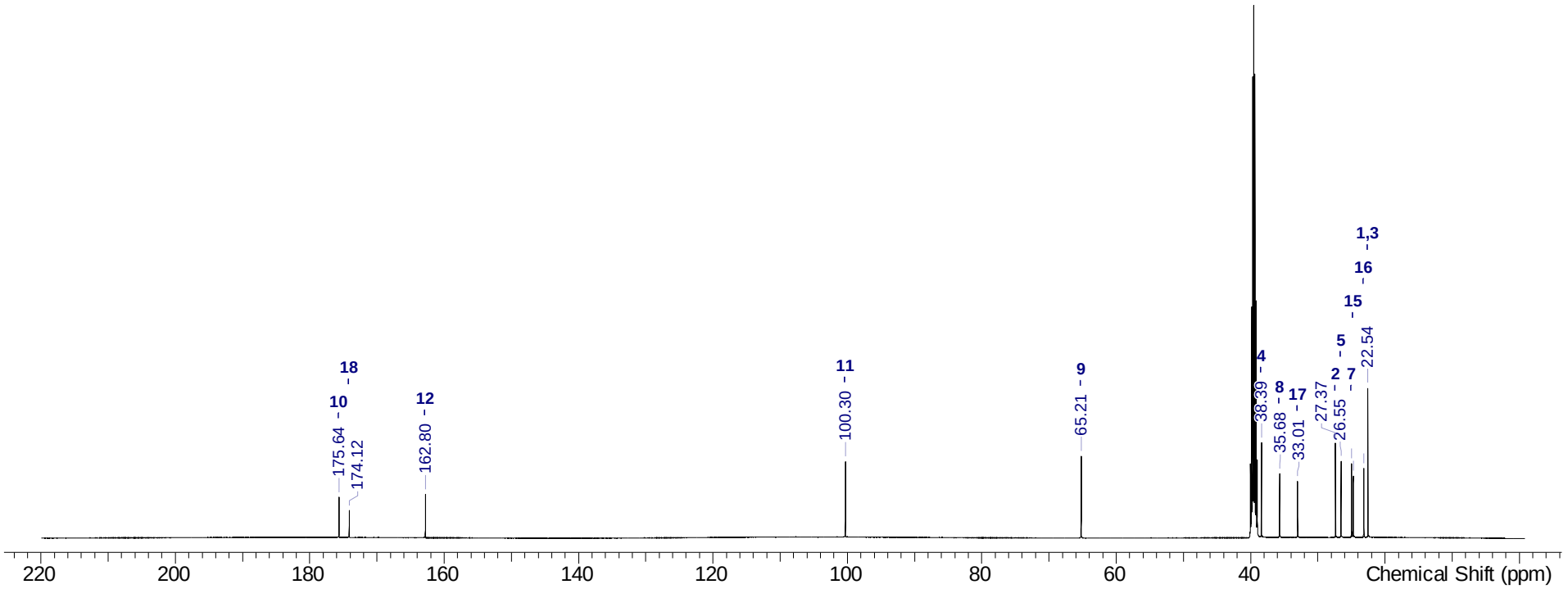

Figure S40. *^{13}C NMR* spectrum myxofacycline D acquired in DMSO d6 at 125 MHz.

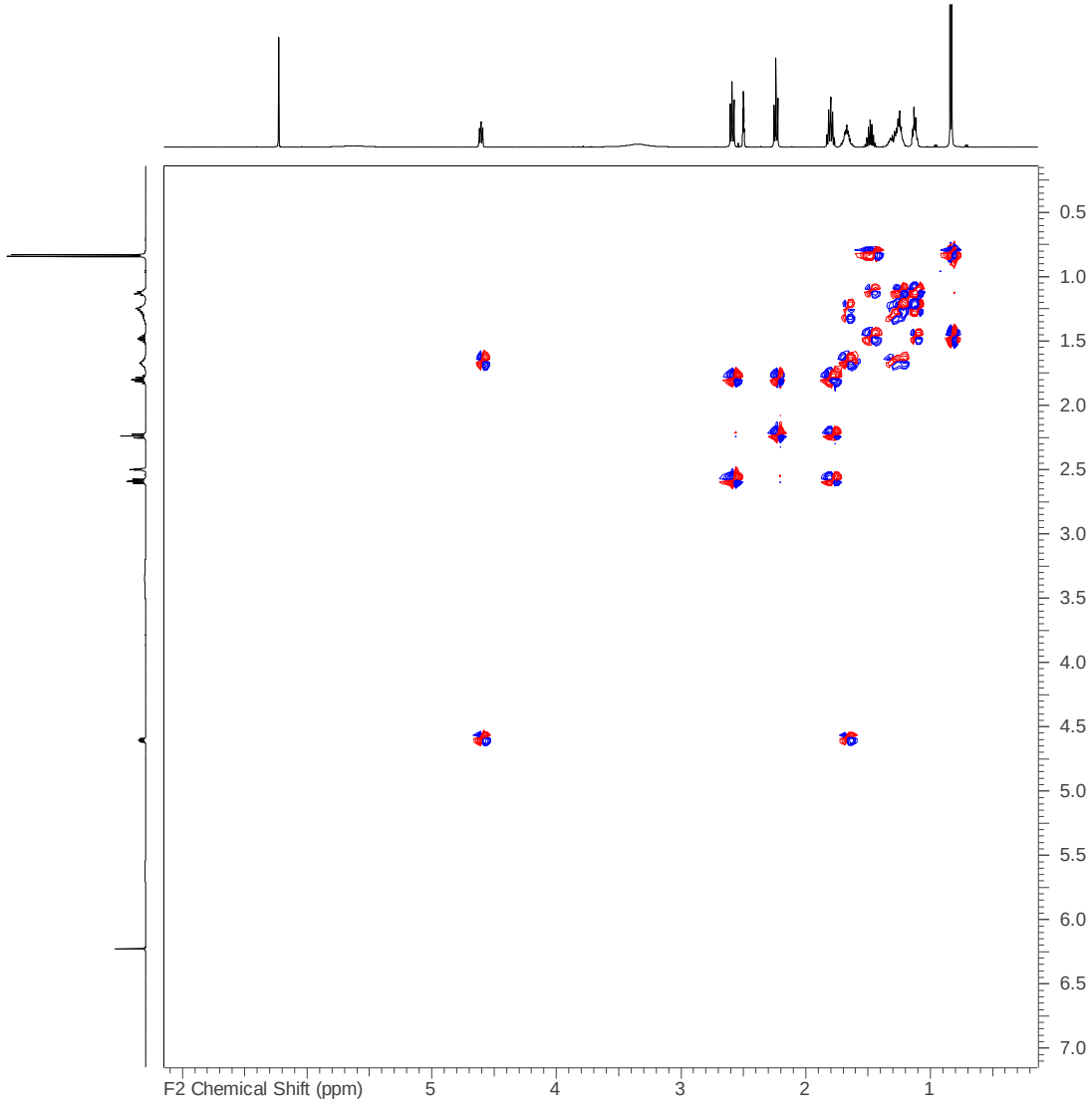

Figure S41. *H-H DQF-COSY* spectrum myxofacycline D acquired in DMSO d6 at 500 MHz.

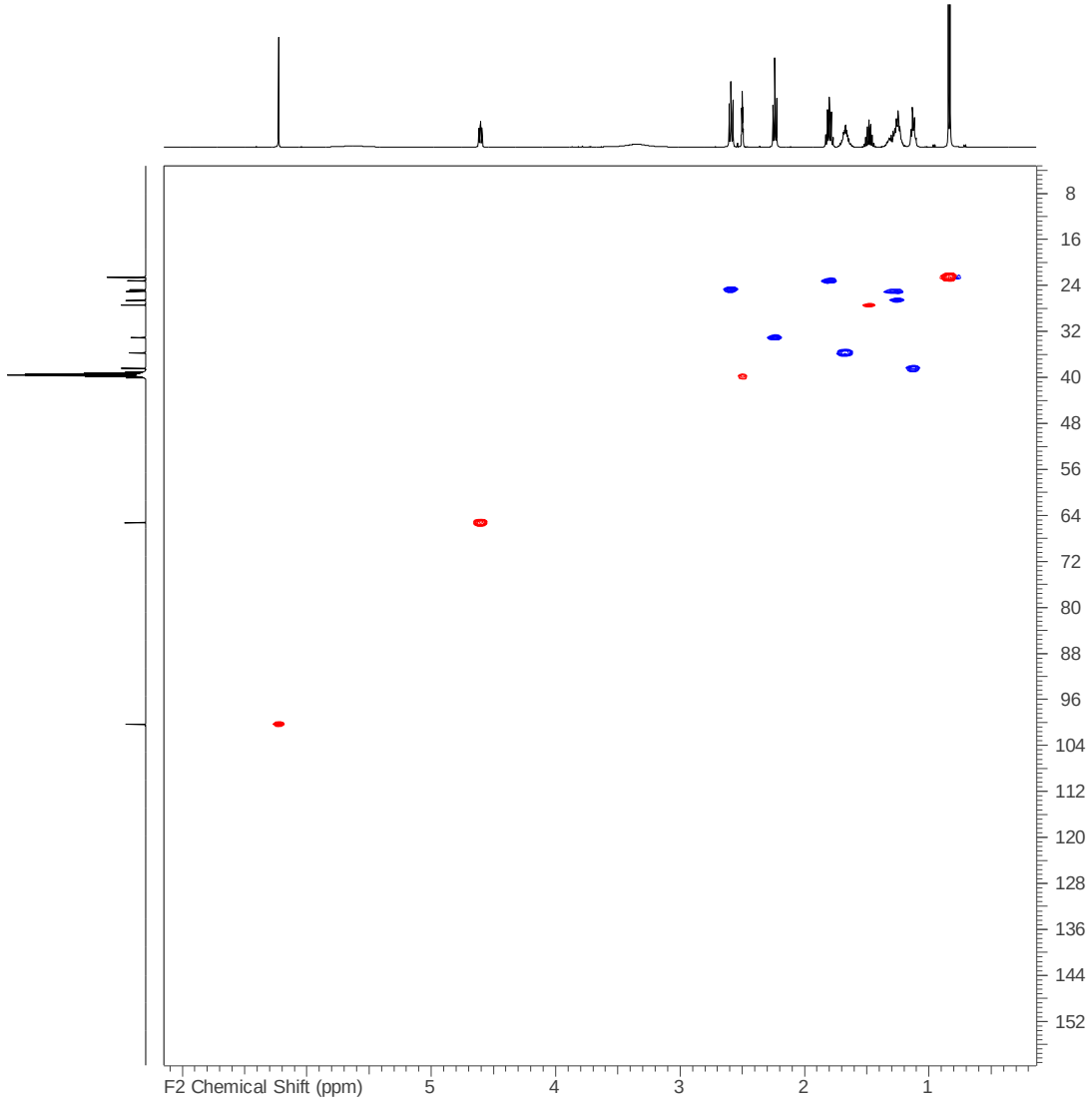

Figure S42. HSQC spectrum of myxofacycline D acquired in DMSO d6 at 500/125 MHz.

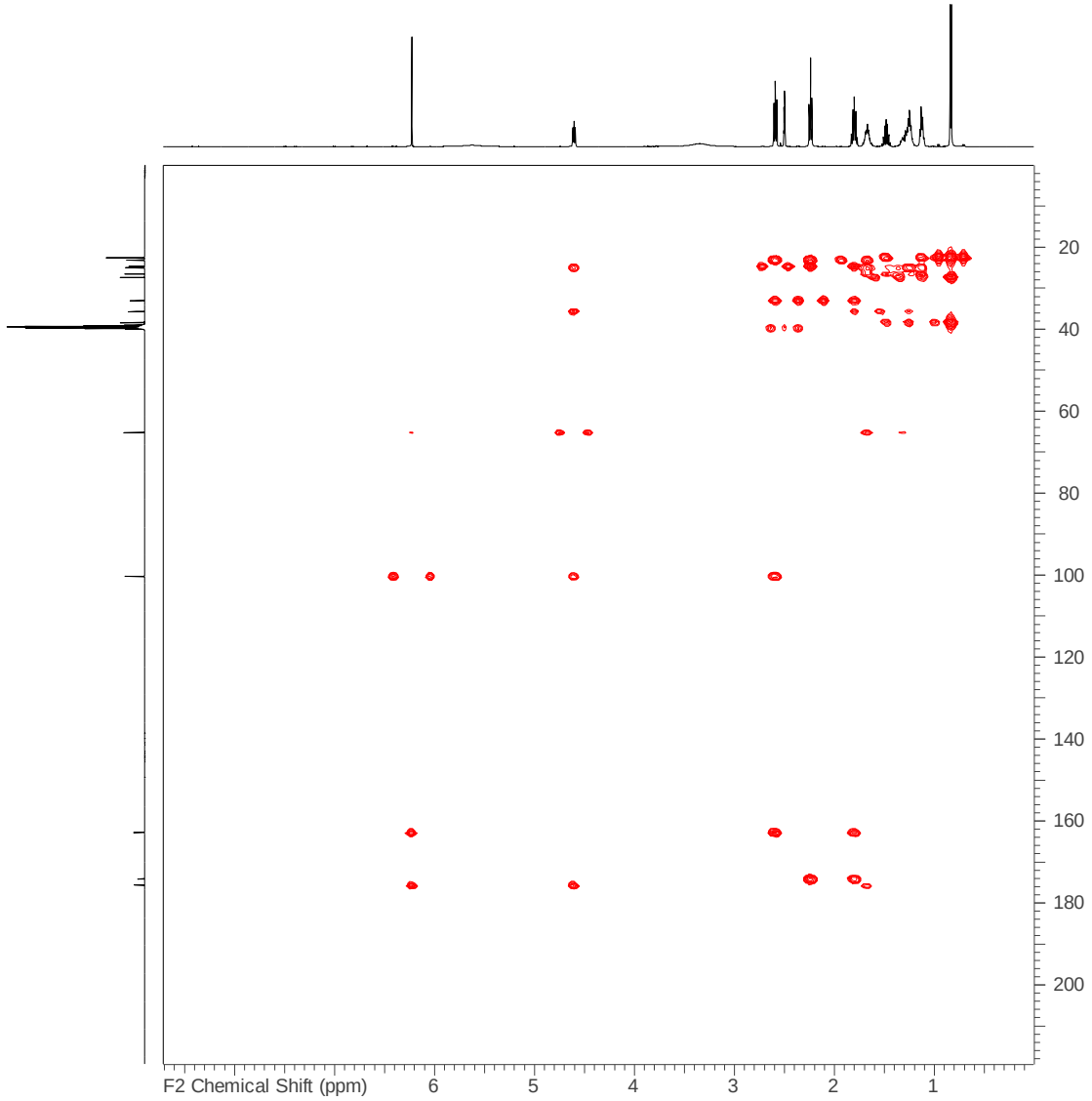

Figure S43. HMBC spectrum of myxofacycline D acquired in DMSO d6 at 500/125 MHz.

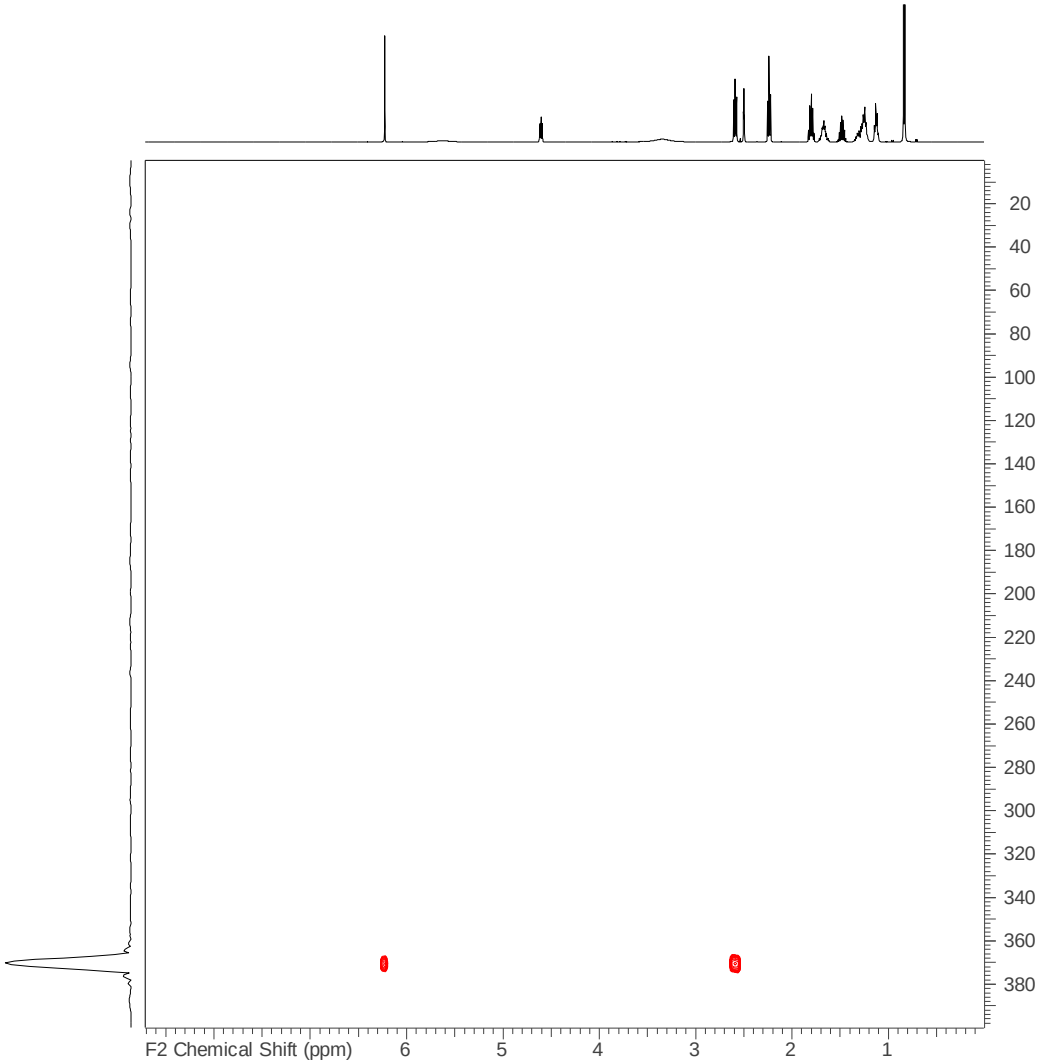

Figure S44: ^{15}N-HMBC spectrum of myxofacycline D acquired in DMSO d6 at 500/125 MHz.

NMR data myxofacycline E

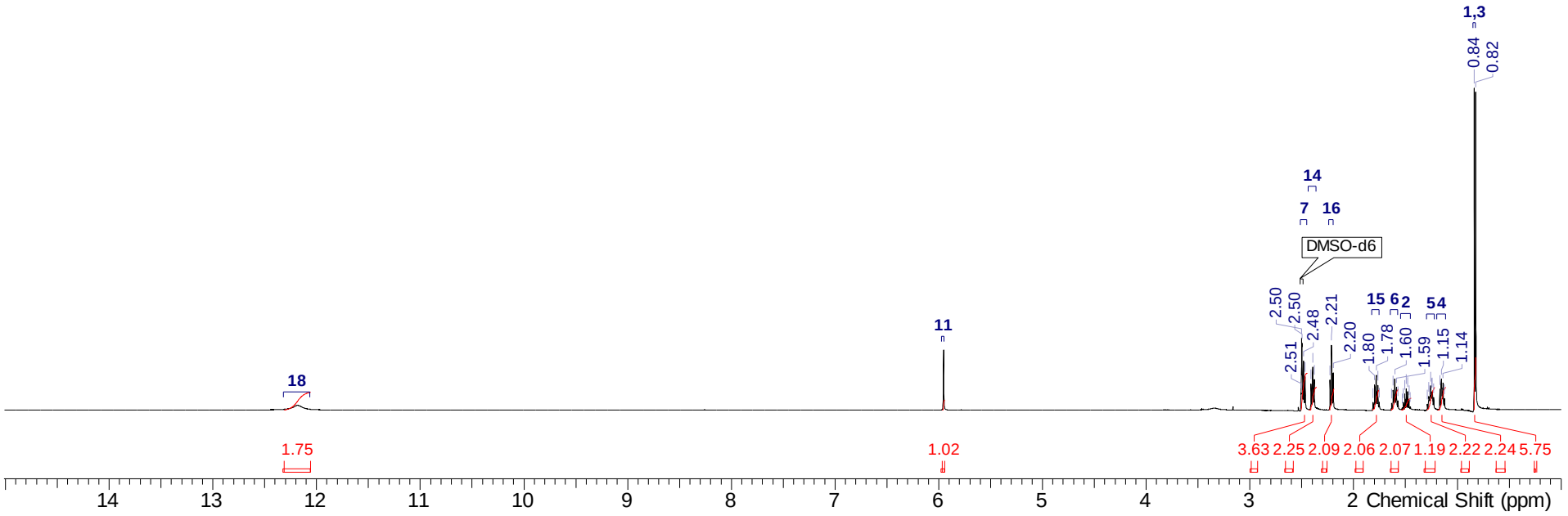

Figure S45. ^{1}H NMR spectrum myxofacycline E acquired in DMSO d6 at 500 MHz.

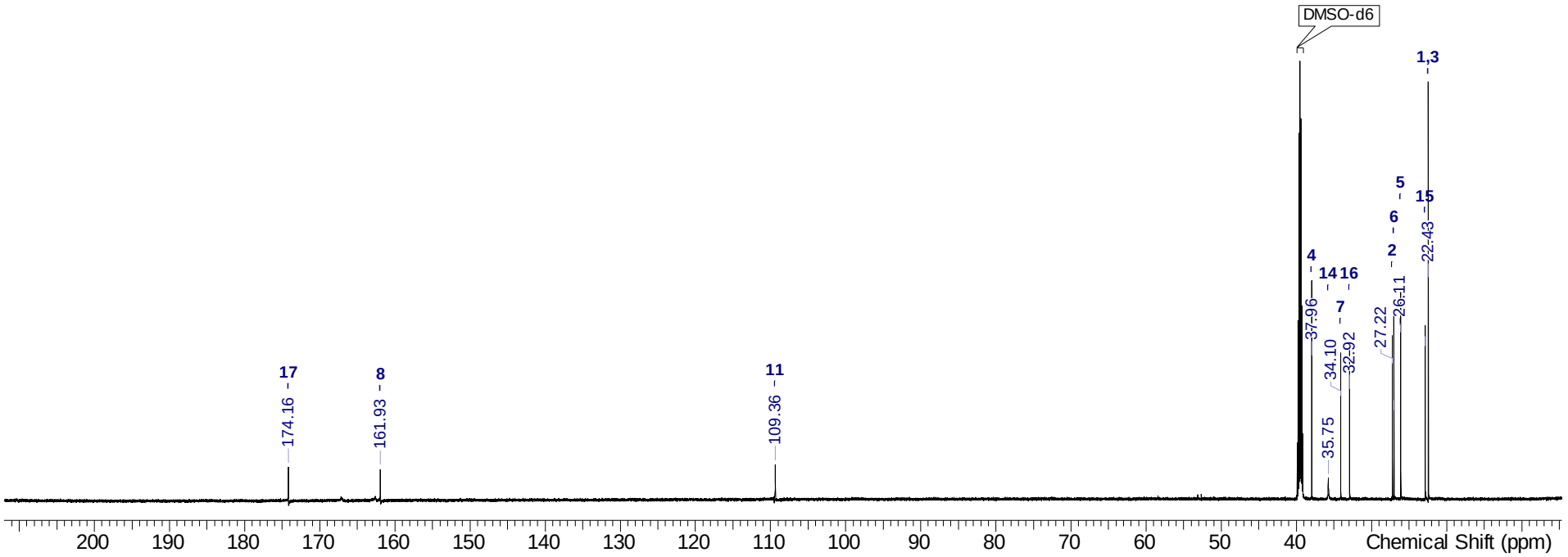

Figure S46. ^{13}C NMR spectrum myxofacycline E acquired in DMSO d6 at 125 MHz.

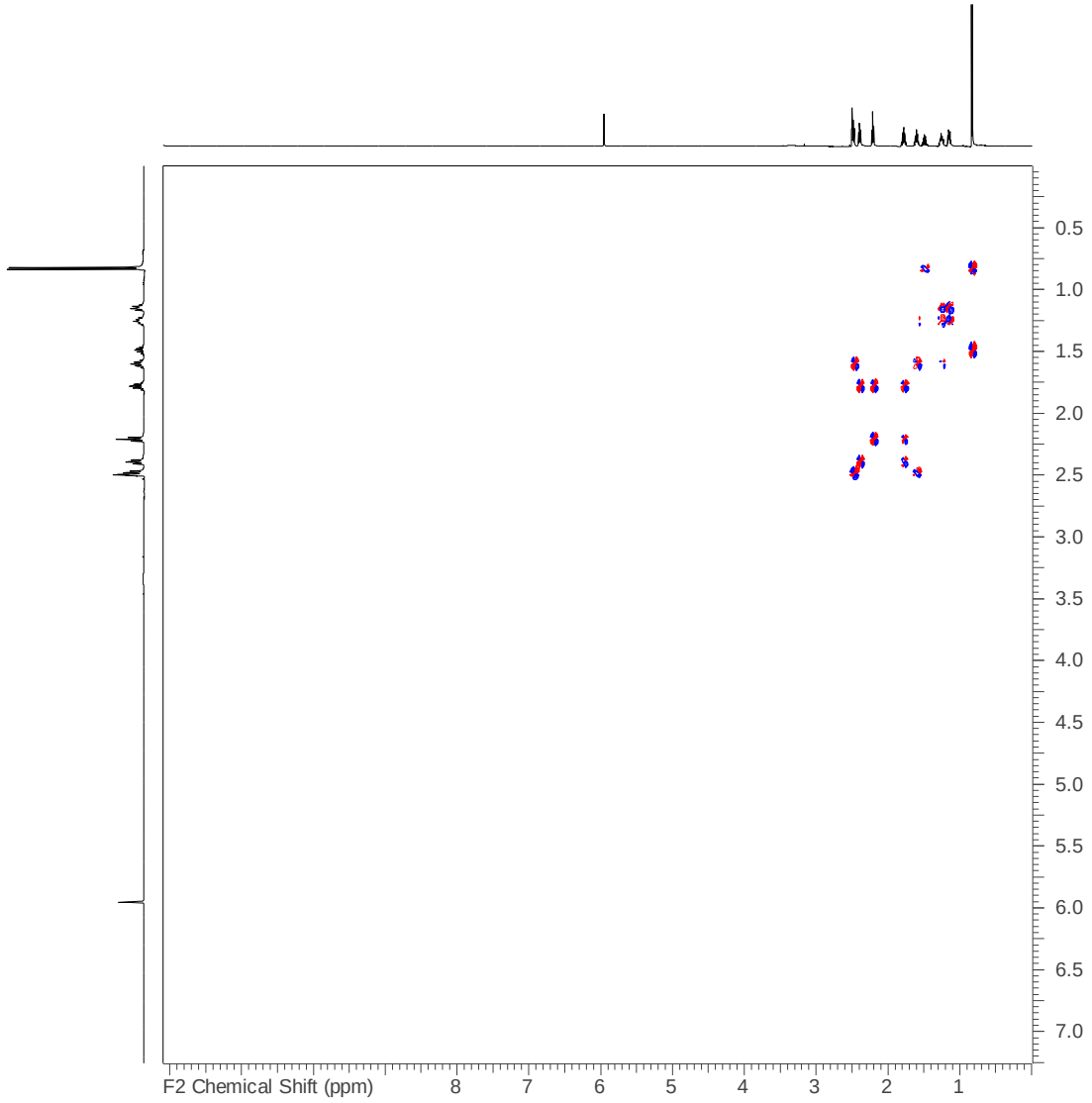

Figure S47. DQF-COSY spectrum myxofacycline E acquired in DMSO d6 at 500 MHz.

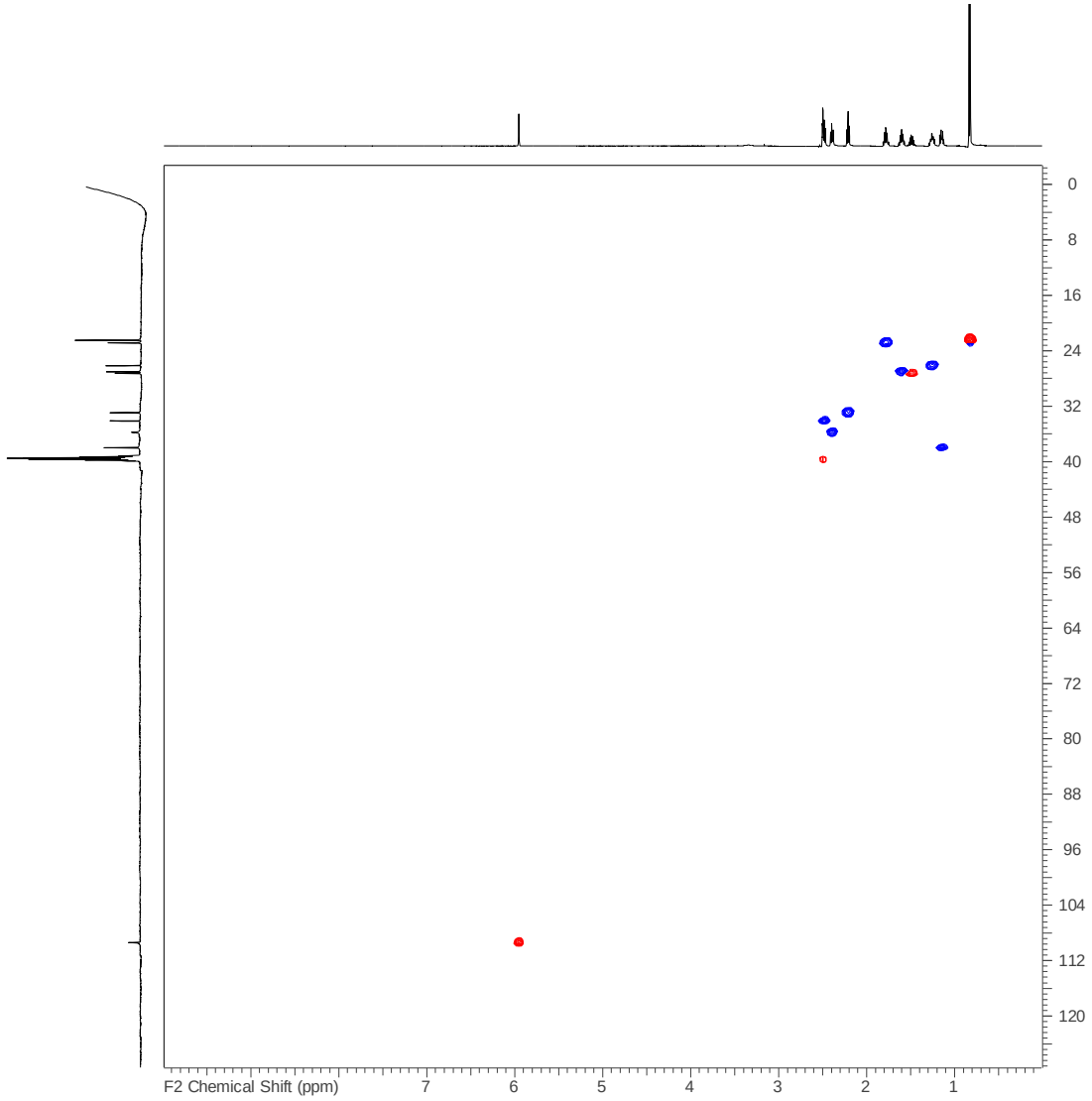

Figure S48. HSQC spectrum of myxofacycline E acquired in DMSO d6 at 500/125 MHz.

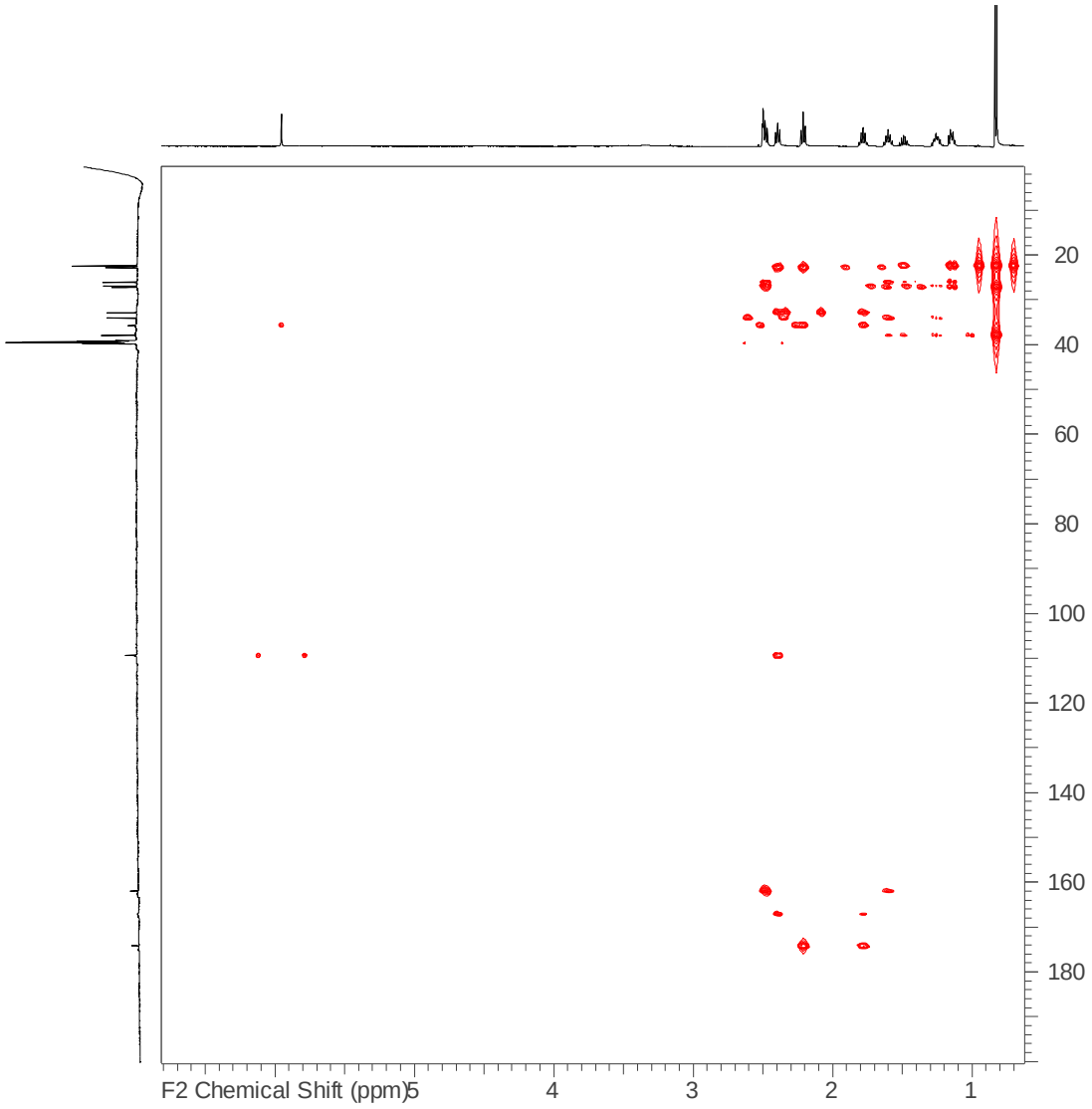

Figure S49. HMBC spectrum of myxofacycline E acquired in DMSO d6 at 500/125 MHz.

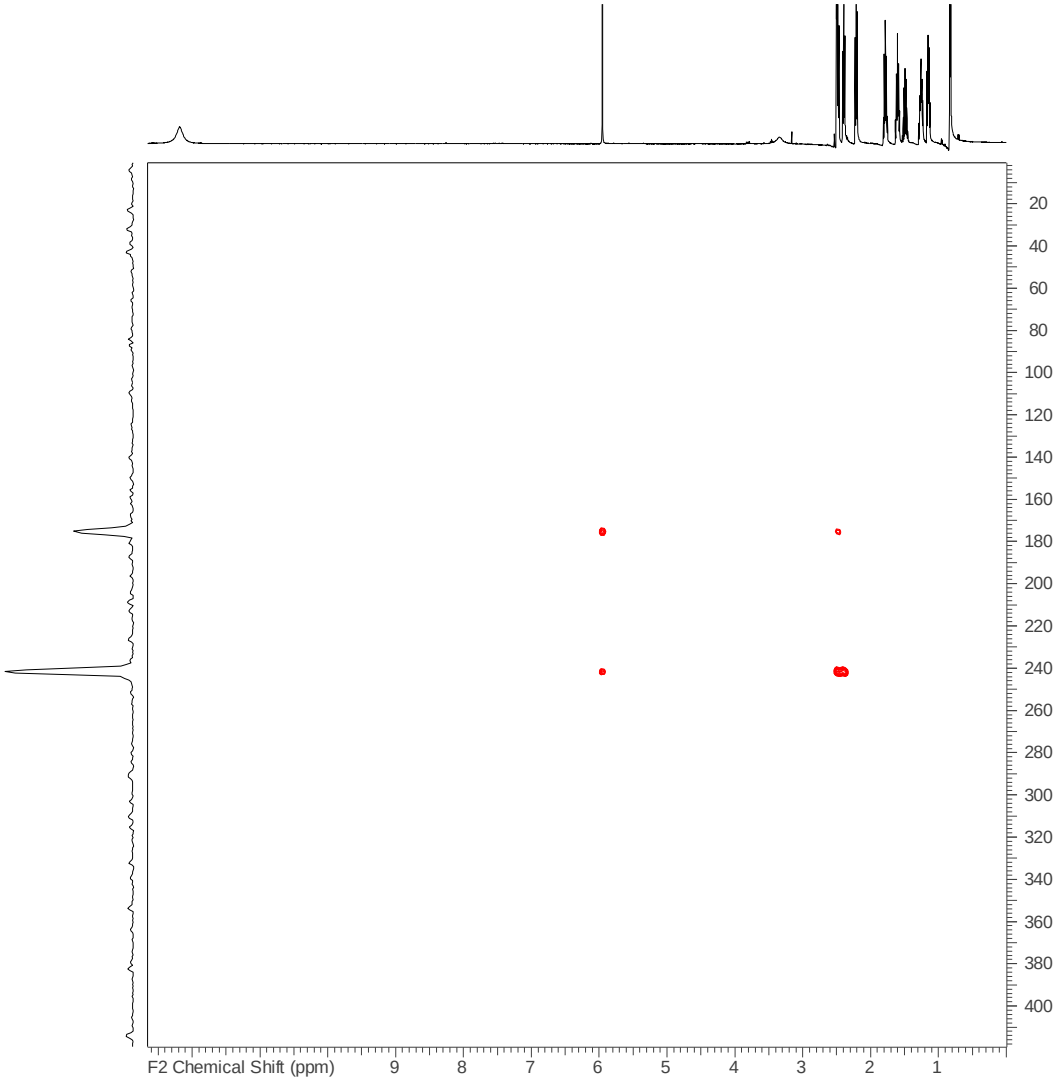

Figure S50. ^{15}N-HMBC spectrum of myxofacycline E acquired in DMSO d6 at 500/50 MHz.

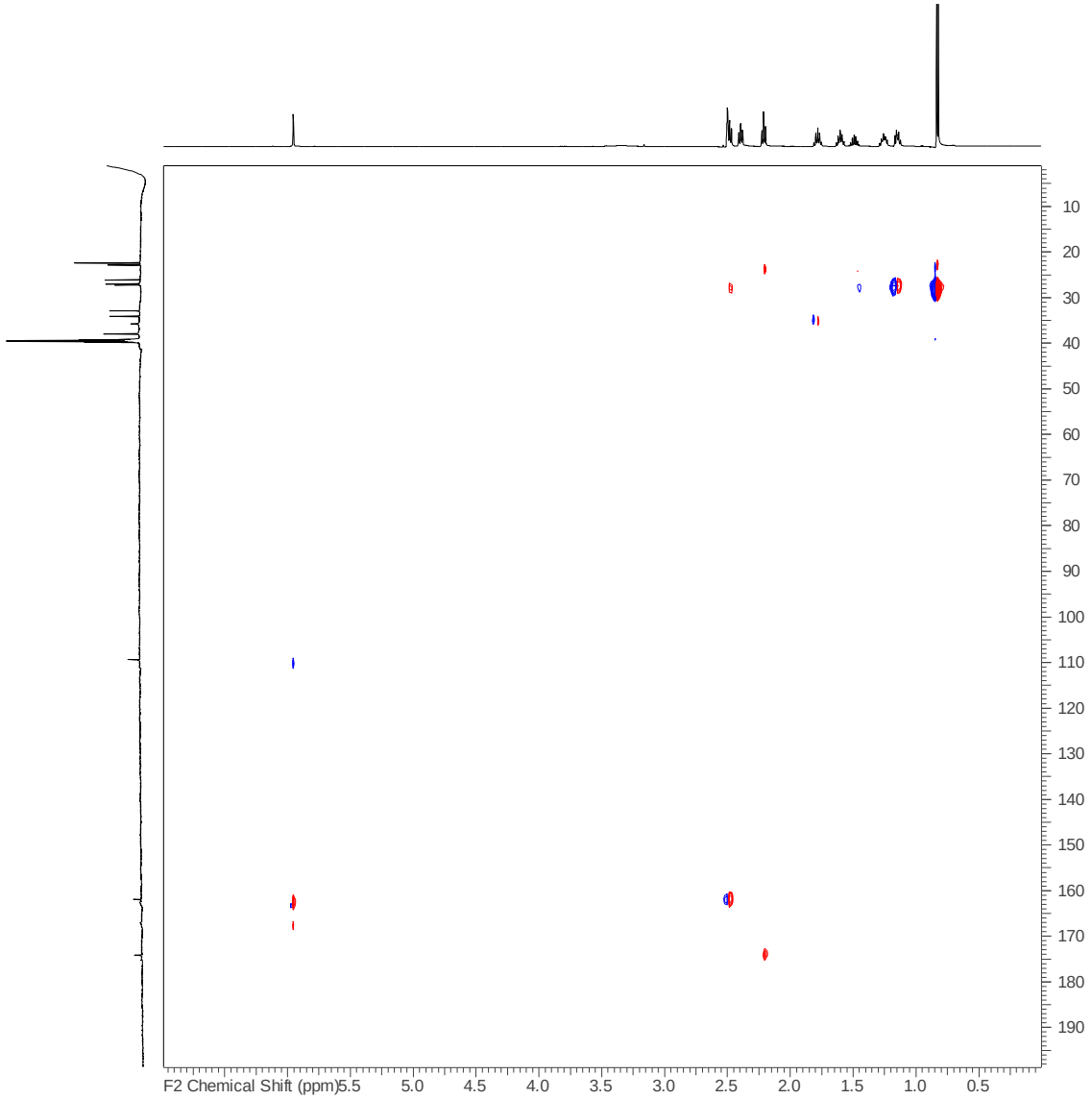
10
20
30
40
50
60
70
80
90
100
110
120
130
140
150
160
170
180
190
F2 Chemical Shift (ppm)5.5
5.0
4.5
4.0
3.5
3.0
2.5
2.0
1.5
1.0
0.5

Figure S51. 1,1 ADEQUATE spectrum of myxofacycline E acquired in DMSO d6 at 700/175 MHz.

NMR data myxofacycline F

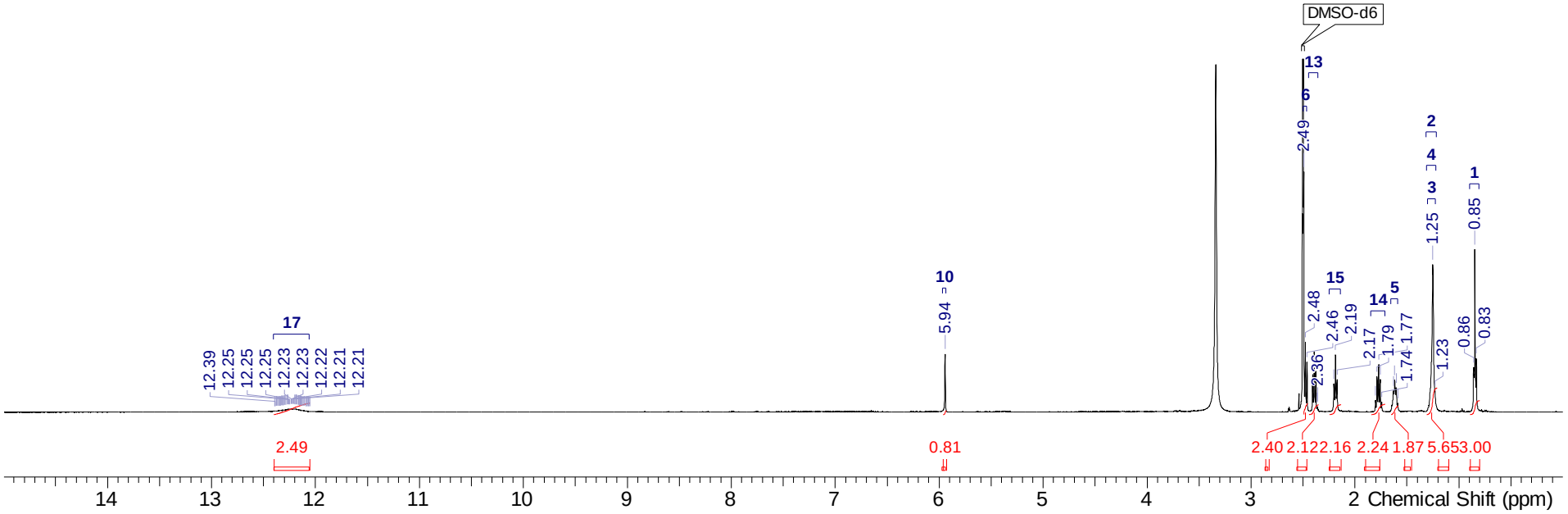

Figure S52. ^{1}H NMR spectrum myxofacycline F acquired in DMSO d6 at 500 MHz.

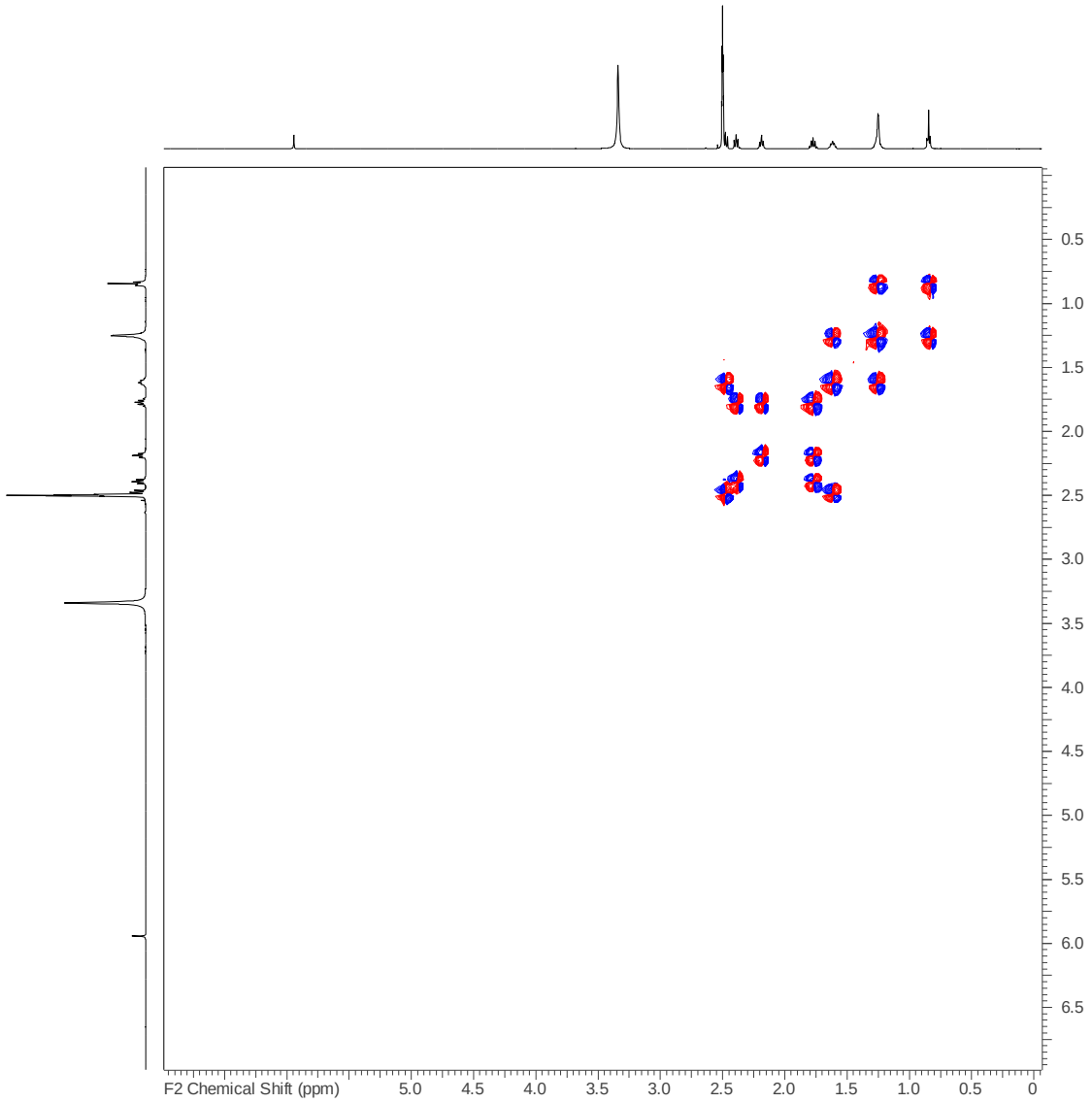

Figure S53. DQF-COSY spectrum myxofacycline E acquired in DMSO d6 at 500 MHz.

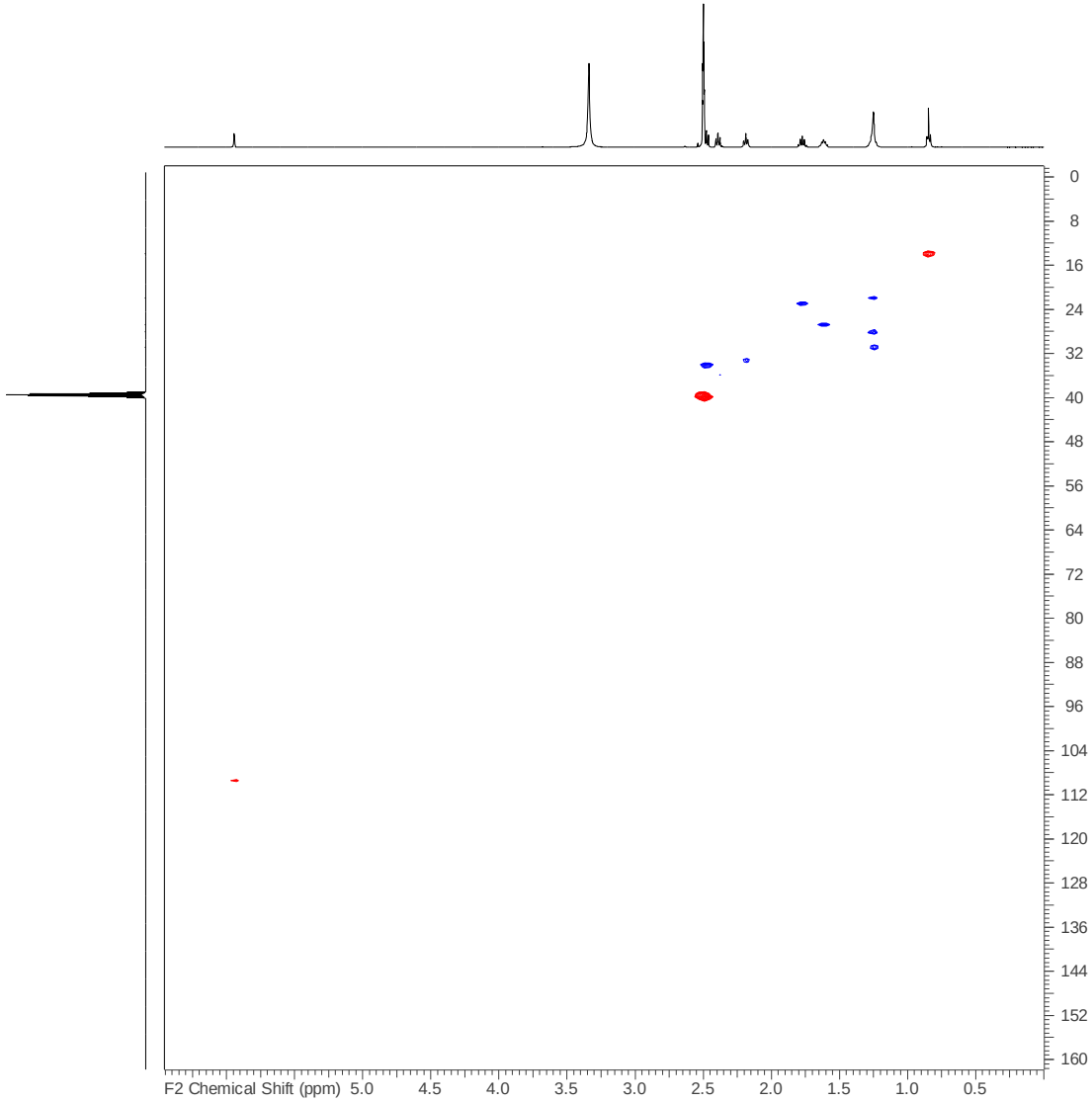

Figure S54. HSQC spectrum of myxofacycline F acquired in DMSO d6 at 500/125 MHz.

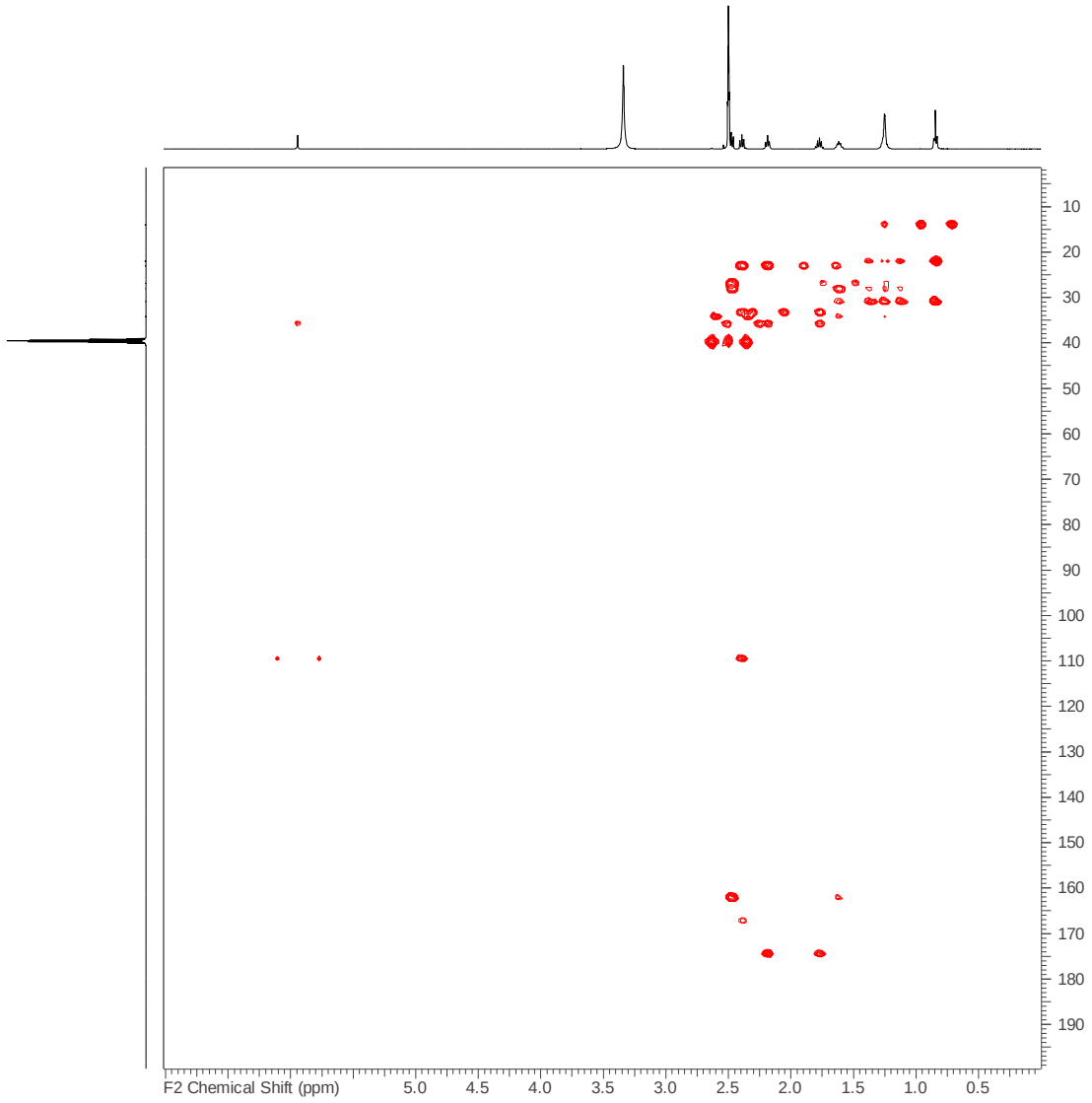

Figure S55. HMBC spectrum of myxofacycline F acquired in DMSO d6 at 500/125 MHz.

NMR data myxofacycline G

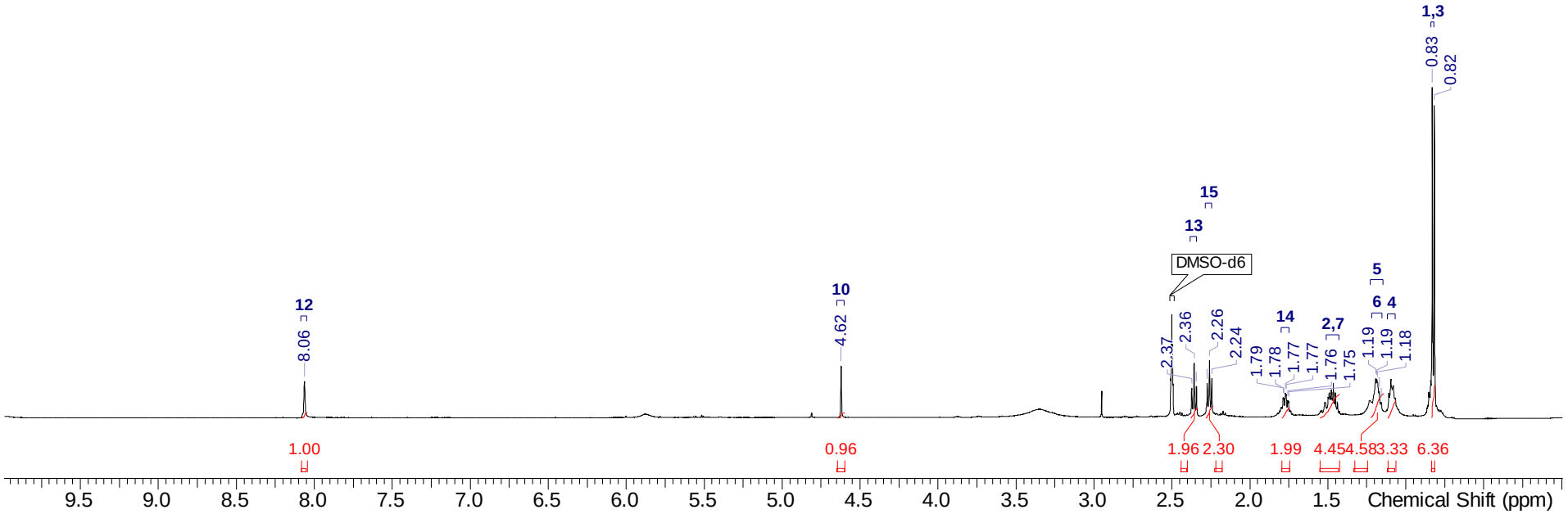

Figure S56. ^{1}H NMR spectrum myxofacycline G acquired in DMSO d6 at 500 MHz.

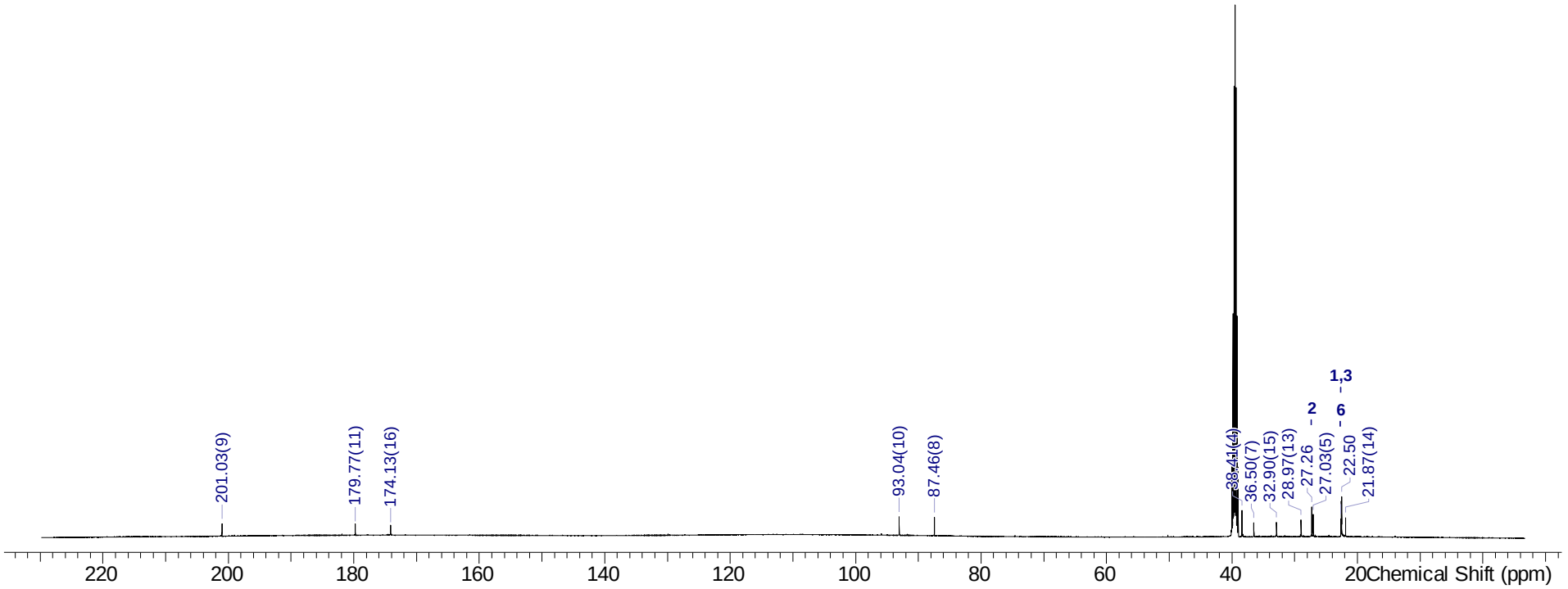

Figure S57. ^{13}C NMR spectrum myxofacycline G acquired in DMSO d6 at 125 MHz.

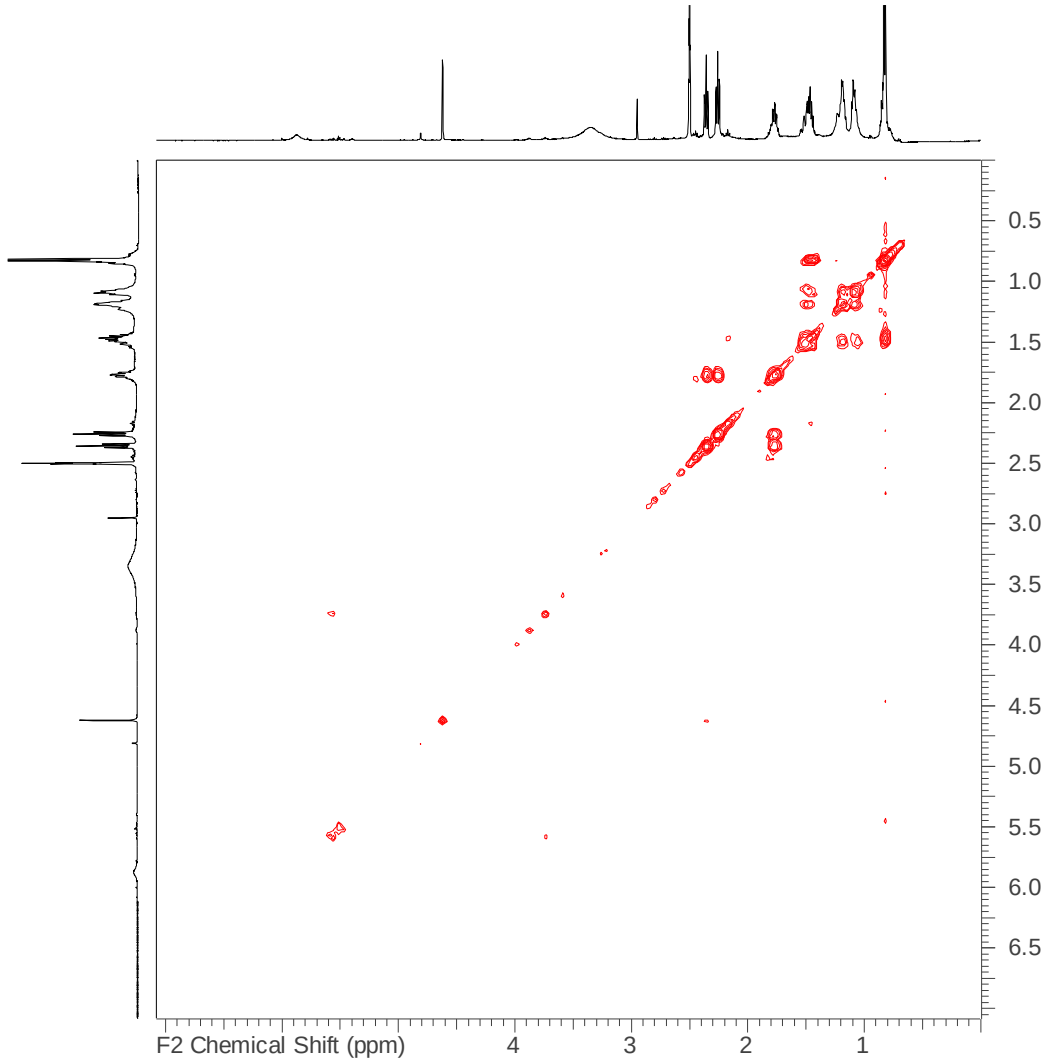

Figure S58. H-H COSY spectrum myxofacycline G acquired in DMSO d6 at 500 MHz.

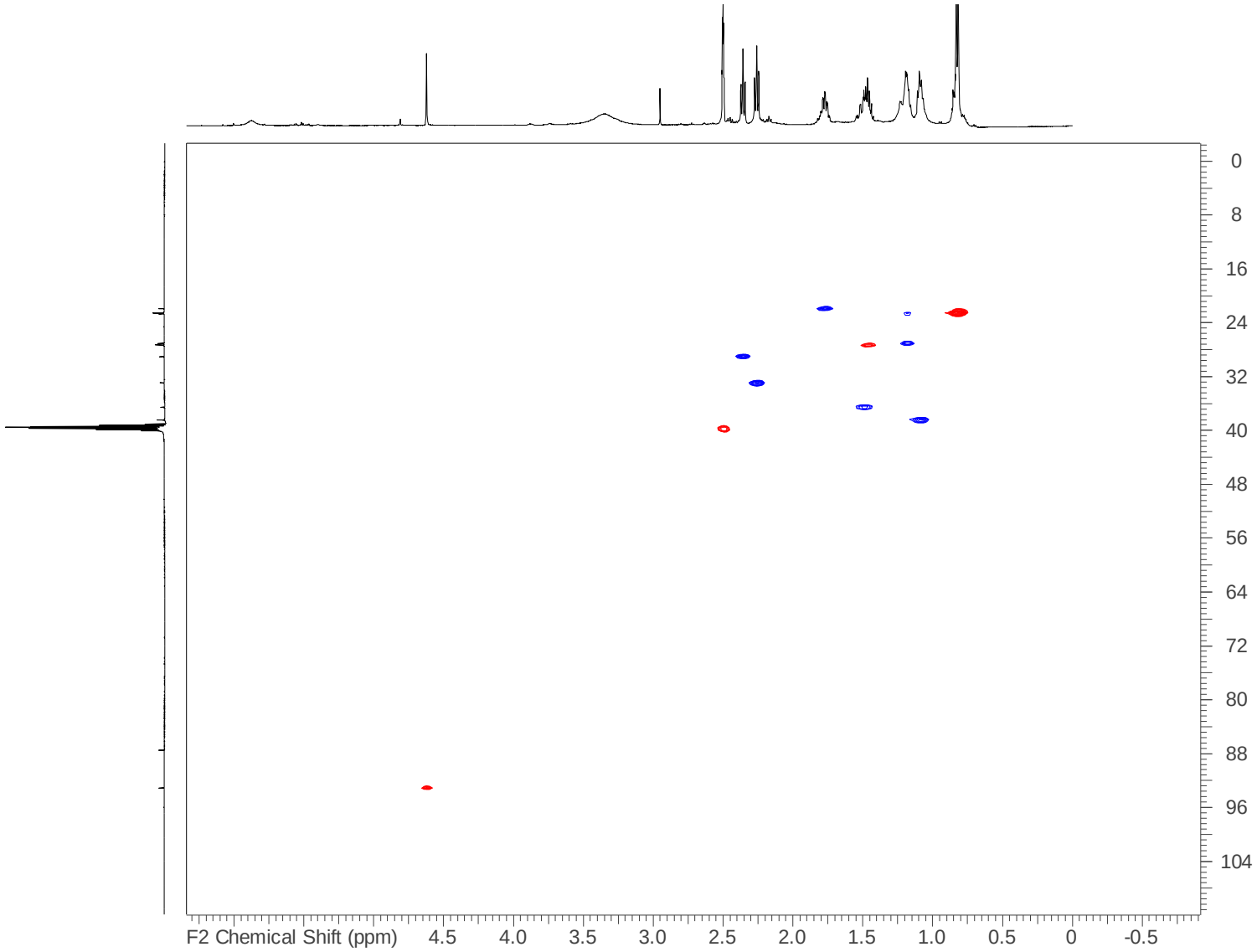

Figure S59. HSQC spectrum of myxofacycline G acquired in DMSO d6 at 500/125 MHz.

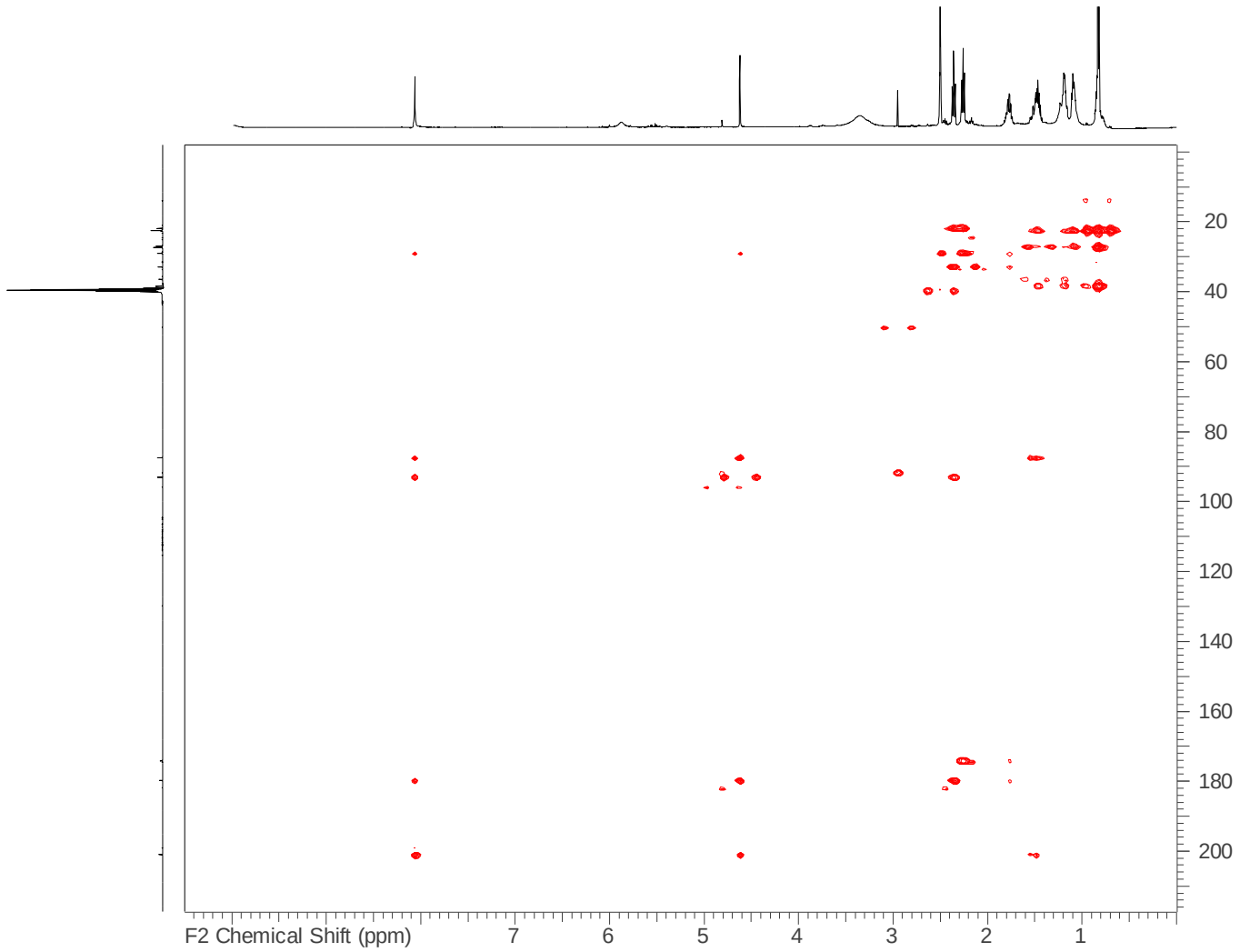

Figure S60. HMBC spectrum of myxofacycline G acquired in DMSO d6 at 500/125 MHz.

3. References

[1] R. C. Edgar, *Nucleic Acids Res.* **2004**, *32*, 1792.

[2] R. D. Finn, P. Coggill, R. Y. Eberhardt, S. R. Eddy, J. Mistry, A. L. Mitchell, S. C. Potter, M. Punta, M. Qureshi, A. Sangrador-Vegas et al., *Nucleic Acids Res.* **2016**, *44*, D279-285.

[3] L. A. Kelley, S. Mezulis, C. M. Yates, M. N. Wass, M. J. E. Sternberg, *Nat. Protoc.* **2015**, *10*, 845.

[4] H. Irschik, W. Trowitzsch-Kienast, K. Gerth, G. Höfle, H. Reichenbach, *J. Antibiot.* **1988**, *41*, 993.

[5] M. R. Green, J. Sambrook, *Molecular cloning*. *A laboratory manual*, Cold Spring Harbor Laboratory Press, Cold Spring Harbor, N.Y., **2012**.

[6] H. Sucipto, D. Pogorevc, E. Luxenburger, S. C. Wenzel, R. Müller, *Metab. Eng.* **2017**, *44*, 160.

[7] D. Pogorevc, F. Panter, C. Schillinger, R. Jansen, S. C. Wenzel, R. Müller, *Metab. Eng.* **2019**, *55*, 201.

[8] F. Panter, D. Krug, S. Baumann, R. Müller, *Chem. Sci.* **2018**, *9*, 4898.

[9] H. Wang, Z. Li, R. Jia, Y. Hou, J. Yin, X. Bian, A. Li, R. Muller, A. F. Stewart, J. Fu et al., *Nat. Protoc.* **2016**, *11*, 1175.

[10] E. J. Rubin, B. J. Akerley, V. N. Novik, D. J. Lampe, R. N. Husson, J. J. Mekalanos, *Proc. Natl. Acad. Sci. USA* **1999**, *96*, 1645.

[11] J. J. Hug, F. Panter, D. Krug, R. Müller, *J. Ind. Microbiol. Biotechnol.* **2019**, *46*, 319.

[12] R. Garcia, R. Müller in *The Prokaryotes*. *Deltaproteobacteria and Epsilonproteobacteria* (Eds.: E. Rosenberg, E. F. DeLong, S. Lory, E. Stackebrandt, F. Thompson), Springer Berlin Heidelberg, Berlin, Heidelberg, s.l., **2014**, pp. 191–212.

[13] Y. Zhang, F. Buchholz, J. P. Muyrers, F. A. Stewart, *Nat. Genet.* **1998**, *20*, 123.

[14] Pinto, D. C. G. A., C. M. M. Santos, A.M.S. Silva in *Recent research developments in heterocyclic chemistry 2007*, pp. 397–475.

[15] K. A. Thorn, *PLoS ONE* **2019**, *14*, e0224112.

[16] T. R. Hoye, C. S. Jeffrey, F. Shao, *Nat. Protoc.* **2007**, *2*, 2451.

[17] P. G. Livingstone, O. Ingleby, S. Girdwood, A. R. Cookson, R. M. Morphew, D. E. Whitworth, *Appl. Environ. Microbiol.* **2019**.

[18] H. Albataineh, M. Duke, S. K. Misra, J. S. Sharp, D. C. Stevens, *bioRxiv* **2019**, *65*.

[19] D. C. Cantu, Y. Chen, P. J. Reilly, *Protein Sci.* **2010**, *19*, 1281.

[20] a) X. Chen, T. A. Kohl, C. Rückert, D. A. Rodionov, L.-H. Li, J.-Y. Ding, J. Kalinowski, S.-J. Liu, *Appl. Environ. Microbiol.* **2012**, *78*, 5796; b) A. Ferrández, B. Miñambres, B. García, E. R. Olivera, J. M. Luengo, J. L. García, E. Díaz, *J. Biol. Chem.* **1998**, *273*, 25974.

[21] M. L. Heathcote, J. Staunton, P. F. Leadlay, *Chem. Biol.* **2001**, *8*, 207.

[22] D. L. Ollis, E. Cheah, M. Cygler, B. Dijkstra, F. Frolow, S. M. Franken, M. Harel, S. J. Remington, I. Silman, J. Schrag et al., *Protein Eng.* **1992**, *5*, 197.

[23] S. C. Dillon, A. Bateman, *BMC bioinformatics* **2004**, *5*, 109.

[24] Z. Zhang, R. Zhou, J. M. Sauder, P. J. Tonge, S. K. Burley, S. Swaminathan, *J. Mol. Biol.* **2011**, *406*, 313.

[25] L. Clark, D. Leatherby, E. Krilich, A. J. Ropelewski, J. Perozich, *PLoS ONE* **2018**, *13*, e0203218.

[26] A. T. Keating-Clay, *Nat. Prod. Rep.* **2012**, *29*, 1050.

[27] F. Hemmerling, K. E. Lebe, J. Wunderlich, F. Hahn, *ChemBioChem* **2018**.

[28] P. M. Marchetti, van Kelly, J. P. Simpson, M. Ward, D. J. Campopiano, *Org. Biomol. Chem.* **2018**, *16*, 2735.

[29] K. Voráčová, J. Hájek, J. Mareš, P. Urajová, M. Kuzma, J. Cheel, A. Villunger, A. Kapuscik, M. Bally, P. Novák et al., *PLoS ONE* **2017**, *12*, e0172850.

[30] Y. Inahashi, T. Shiraishi, A. Také, A. Matsumoto, Y. Takahashi, S. Ōmura, T. Kuzuyama, T. Nakashima, *J Antibiot* **2018**, *71*, 749.

[31] S. Puehringer, M. Metlitzky, R. Schwarzenbacher, *BMC Biochem.* **2008**, *9*, 8.

[32] C. Rausch, I. Hoof, T. Weber, W. Wohlleben, D. H. Huson, *BMC Evol. Biol.* **2007**, *7*, 78.

[33] D. Pogorevc, Y. Tang, M. Hoffmann, G. Zipf, H. S. Bernauer, A. Popoff, H. Steinmetz, S. C. Wenzel, *ACS Synth. Biol.* **2019**, *8*, 1121.

[34] T. Duerfahrt, K. Eppelmann, R. Müller, M. A. Marahiel, *Chem. Biol.* **2004**, *11*, 261.

[35] J. J. Hug, R. Müller in *Comprehensive Natural Products III* (Eds.: H.-W. (B.) Liu, T. P. Begley), Elsevier, Oxford, **2020**, pp. 149–216.

[36] V. Y. Alekseyev, C. W. Liu, D. E. Cane, J. D. Puglisi, C. Khosla, *Protein Sci.* **2007**, *16*, 2093.

[37] T. Stachelhaus, H. D. Mootz, M. A. Marahiel, *Chem. Biol.* **1999**, *6*, 493.

[38] a) F. Panter, D. Krug, R. Müller, *ACS Chem. Biol.* **2019**, *14*, 88; b) J. J. Hug, F. Panter, D. Krug, R. Müller, *J. Ind. Microbiol. Biotechnol.* **2019**, *46*, 319.

[39] A. A. Iniesta, F. García-Heras, J. Abellón-Ruiz, A. Gallego-García, M. Elías-Arnanz, *J. Bacteriol.* **2012**, *194*, 5875.

[40] K. Kashefi, P. L. Hartzell, *Mol. Microbiol.* **1995**, *15*, 483.

[41] J. Wild, Z. Hradecna, W. Szybalski, *Genome Res.* **2002**, *12*, 1434.